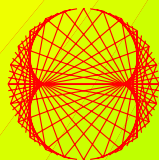


2008, VOLUME 4

PROGRESS IN PHYSICS

“All scientists shall have the right to present their scientific research results, in whole or in part, at relevant scientific conferences, and to publish the same in printed scientific journals, electronic archives, and any other media.” — Declaration of Academic Freedom, Article 8



ISSN 1555-5534

PROGRESS IN PHYSICS

A quarterly issue scientific journal, registered with the Library of Congress (DC, USA). This journal is peer reviewed and included in the abstracting and indexing coverage of: Mathematical Reviews and MathSciNet (AMS, USA), DOAJ of Lund University (Sweden), Zentralblatt MATH (Germany), Scientific Commons of the University of St. Gallen (Switzerland), Open-J-Gate (India), Referativnyi Zhurnal VINITI (Russia), etc.

To order printed issues of this journal, contact the Editors. Electronic version of this journal can be downloaded free of charge:

<http://www.ptep-online.com>
<http://www.geocities.com/ptep-online>

Editorial Board

Dmitri Rabounski (Editor-in-Chief)
rabounski@ptep-online.com

Florentin Smarandache
smarand@unm.edu

Larissa Borissova
borissova@ptep-online.com

Stephen J. Crothers
crothers@ptep-online.com

Postal address

Chair of the Department
of Mathematics and Science,
University of New Mexico,
200 College Road,
Gallup, NM 87301, USA

Copyright © *Progress in Physics*, 2007

All rights reserved. The authors of the articles do hereby grant *Progress in Physics* non-exclusive, worldwide, royalty-free license to publish and distribute the articles in accordance with the Budapest Open Initiative: this means that electronic copying, distribution and printing of both full-size version of the journal and the individual papers published therein for non-commercial, academic or individual use can be made by any user without permission or charge. The authors of the articles published in *Progress in Physics* retain their rights to use this journal as a whole or any part of it in any other publications and in any way they see fit. Any part of *Progress in Physics* howsoever used in other publications must include an appropriate citation of this journal.

This journal is powered by \LaTeX

A variety of books can be downloaded free from the Digital Library of Science:
<http://www.gallup.unm.edu/~smarandache>

ISSN: 1555-5534 (print)
ISSN: 1555-5615 (online)

Standard Address Number: 297-5092
Printed in the United States of America

OCTOBER 2008

VOLUME 4

CONTENTS

P. Wagnener A Unified Theory of Interaction: Gravitation and Electrodynamics	3
E. Goldfain and F. Smarandache On Emergent Physics, “Unparticles” and Exotic “Unmatter” States	10
M. Harney and I. I. Haranas The Dark Energy Problem	16
R. T. Cahill Unravelling Lorentz Covariance and the Spacetime Formalism	19
Xiao-Song Wang Derivation of the Newton’s Law of Gravitation Based on a Fluid Mechanical Singularity Model of Particles	25
G. I. Garas’ko A Method of Successive Approximations in the Framework of the Geometrized Lagrange Formalism	31
Huy Khanh Hoang Instant Interpretation of Quantum Mechanics	37
I. A. Abdallah, A. F. Hassan, and I. M. Tayel Thermoelastic Property of a Semi-Infinite Medium Induced by a Homogeneously Illuminating Laser Radiation	44
S. M. Diab and S. A. Eid Nature of the Excited States of the Even-Even $^{98-108}\text{Ru}$ Isotopes	51

Information for Authors and Subscribers

Progress in Physics has been created for publications on advanced studies in theoretical and experimental physics, including related themes from mathematics and astronomy. All submitted papers should be professional, in good English, containing a brief review of a problem and obtained results.

All submissions should be designed in \LaTeX format using *Progress in Physics* template. This template can be downloaded from *Progress in Physics* home page <http://www.ptep-online.com>. Abstract and the necessary information about author(s) should be included into the papers. To submit a paper, mail the file(s) to the Editor-in-Chief.

All submitted papers should be as brief as possible. We usually accept brief papers, no larger than 8–10 typeset journal pages. Short articles are preferable. Large papers can be considered in exceptional cases to the section *Special Reports* intended for such publications in the journal. Letters related to the publications in the journal or to the events among the science community can be applied to the section *Letters to Progress in Physics*.

All that has been accepted for the online issue of *Progress in Physics* is printed in the paper version of the journal. To order printed issues, contact the Editors.

This journal is non-commercial, academic edition. It is printed from private donations. (Look for the current author fee in the online version of the journal.)

A Unified Theory of Interaction: Gravitation and Electrodynamics

Pieter Wagener

Department of Physics, Nelson Mandela Metropolitan University, Port Elizabeth, South Africa

E-mail: Pieter.Wagener@nmmu.ac.za

A theory is proposed from which the basic equations of gravitation and electromagnetism are derived from a single Lagrangian. The total energy of an atom can be expressed in a power series of the fine structure constant, α . Specific selections of these terms yield the relativistic correction to the Bohr values of the hydrogen spectrum and the Sommerfeld-Dirac equation for the fine structure spectrum of the hydrogen atom. Expressions for the classical electron radius and some of the Large Number Coincidences are derived. A Lorentz-type force equation is derived for both gravitation and electrodynamics. Electron spin is shown to be an effect of fourth order in α .

1 Introduction

In a previous article [2] in this journal we presented a classical Lagrangian characterizing the *dynamics* of gravitational interaction,

$$L = -m_0(c^2 + v^2) \exp R/r, \quad (1)$$

where we denote:

m_0 = *gravitational rest mass* of a test body moving at velocity \mathbf{v} in the vicinity of a massive, central body of mass M ,

γ = $1/\sqrt{1 - v^2/c^2}$,

R = $2GM/c^2$ is the Schwarzschild radius of the central body.

The following conservation equations follow:

$$E = mc^2 e^{R/r} = \text{total energy} = \text{constant}, \quad (2)$$

$$\mathbf{L} = e^{R/r} \mathbf{M} = \text{constant}, \quad (3)$$

$$\begin{aligned} L_z &= M_z e^{R/r} = e^{R/r} m_0 r^2 \sin^2 \theta \dot{\phi} \\ &= z \text{ component of } \mathbf{L} = \text{constant}, \end{aligned} \quad (4)$$

where $m = m_0/\gamma^2$ and

$$\mathbf{M} = (\mathbf{r} \times m_0 \mathbf{v}) \quad (5)$$

is the total angular momentum of the test body.

It was shown that the tests for perihelion precession and the bending of light by a massive body are satisfied by the equations of motion derived from the conservation equations.

The *kinematics* of the system is determined by assuming the local and instantaneous validity of special relativity (SR). This leads to an expression for gravitational redshift:

$$\nu = \nu_0 e^{-R/2r}, \quad (\nu_0 = \text{constant}), \quad (6)$$

which agrees with observation.

Electrodynamics is described by the theory of special relativity. If the motion of a particle is dynamically determined

by the above Lagrangian, then a description of the kinematics of its motion in terms of special relativity should yield equations of motion analogous to those of electrodynamics. This, in principle, should allow the simultaneous manifestation of gravitation and electrodynamics in one model of interaction.

We follow this approach and show, amongst others, that electrical charge arises from a mathematical necessity for bound motion. Other expressions, such as the classical electron radius and expressions of the Large Number Hypothesis follow.

The total energy for the hydrogen atom can be expressed in terms of a power series of the fine structure constant, α . Summing the first four terms yields the Sommerfeld-Dirac expression for the total energy. For higher order terms the finite radius of the nucleus must be taken into account. This introduces a factor analogous to “electron spin”.

Details of all calculations are given in the PhD thesis of the author [1].

2 Gravitation and Special Relativity

Einstein’s title of his 1905 paper, *Zur Elektrodynamik bewegter Körper* indicates that electrodynamics and SR are interrelated, with SR giving an explanation for certain properties of electrodynamics. Red-shift is such a property, combining both gravitation and electromagnetism in a single formulation, and should provide us with a dynamical link between these two phenomena. To do this, we substitute the photoelectric effect,

$$h\nu = \tilde{m}c^2, \quad (7)$$

where $\tilde{m} = \gamma\tilde{m}_0$ and \tilde{m}_0 is the *electromagnetic rest mass* of a particle, into (6). This gives

$$\left. \begin{aligned} E &= \tilde{m}c^2 e^{R/2r} = \tilde{m}_0c^2 \frac{e^{R/2r}}{\sqrt{1 - v^2/c^2}} = \tilde{E} e^{R/2r} \\ &= \tilde{m}_0c^2 + \tilde{m}_0v^2/2 + \tilde{m}_0Rc^2/2r + \\ &\quad + \tilde{m}_0Rv^2/4r + \dots \end{aligned} \right\}, \quad (8)$$

where E is another constant of energy and $\tilde{E} = \tilde{m}c^2$ is the total energy of the theory of special relativity.

Let us compare this expansion with the expansion of (2) for the gravitational energy,

$$\frac{m_0c^2 - E}{2} = \frac{m_0v^2}{2} - \frac{GMm_0}{r} + \frac{m_0v^2R}{2r} - \frac{m_0c^2R^2}{4r^2} + \frac{m_0v^2R^2}{4r^2} + \dots \quad (9)$$

The negative sign of the second right hand term in (9) ensures attractive, or bound, motion under gravitation. In order for the motion determined by (8) to be bounded, the third right hand term must similarly be negative and inversely proportional to r . To ensure this we let

$$\tilde{m}_0c^2 = -e^2/r_e, \quad (10)$$

where e^2 is an arbitrary constant and

$$r_e = R/2. \quad (11)$$

Eq.(8) can then be rewritten as

$$E = \tilde{m}c^2 e^{r_e/r}. \quad (12)$$

As we shall see for the hydrogen atom, e represents the electron charge, r_e represents the classical electron radius and (11) yields some of the numbers of Dirac's Large Number Hypothesis.

The choice of a positive sign in (10) gives repulsive motion. Such a freedom of choice is not possible for the gravitational energy of (9).

2.1 Hamiltonian formulation

Confirmation of the above conclusions can be found by examining the predictions for the hydrogen spectrum. We follow a classical approach based on the principles of action variables [3].

Using the identity $\gamma^2 = 1 + \gamma^2 v^2/c^2$ to separate the kinetic and potential energies in (8), a corresponding Lagrangian can be found:

$$L = -\tilde{m}_0c^2 \sqrt{1 - v^2/c^2} \exp(r_e/r). \quad (13)$$

We obtain the conjugate momenta:

$$p_r = \tilde{m}v \exp(r_e/r), \quad (14)$$

$$p_\theta = \tilde{m}r^2 \dot{\theta} \exp(r_e/r), \quad (15)$$

$$p_\phi = \tilde{m}r^2 \sin^2\theta \dot{\phi} \exp(r_e/r). \quad (16)$$

The associated Hamiltonian can be derived from the formula $H = \sum \dot{q}_i p_i - L$ as follows

$$H = [\tilde{m}_0^2 c^4 \exp(r_e/r) + c^2(p_r^2 + p_\theta^2/r^2 + p_\phi^2/r^2 \sin^2\theta)]^{1/2}. \quad (17)$$

From the canonical equations

$$\dot{p}_i = \frac{\partial H}{\partial q_i}, \quad (18)$$

we find the following conservation equations:

$$L^2 \equiv M^2 \exp(2r_e/r) = p_\theta^2 + p_\phi^2/\sin^2\theta, \quad (19)$$

$$L_z \equiv M_z \exp(r_e/r) = p_\phi, \quad (20)$$

where L^2 and L_z are constants and

$$\mathbf{M} = (\mathbf{r} \times \tilde{m}\mathbf{v}), \quad (21)$$

is the total angular momentum of the orbiting particle.

It should be noted that (12), (19), (20) and (21) have respectively the same forms as for the gravitational equations (2), (3), (4), (5), but with $m = m_0/\gamma^2$ replaced by $\tilde{m} = \gamma\tilde{m}_0$ and R by $r_e = R/2$.

3 The hydrogen spectrum

In order to determine an expression for the energy levels of the H-atom, two different approaches can be followed: (i) Analogously to the Wilson-Sommerfeld model, one can apply the procedures of action angle variables, or (ii) perturbation theory, where the contribution of each energy term is evaluated separately.

To generalize our discussion we shall, where appropriate, use a general potential $\Phi = Rc^2/2r = r_e c^2/r$.

3.1 Method of action angle variables

The theory of action angle variables originated in the description of periodic motion in planetary mechanics [4, Ch.9]. From that theory Wilson and Sommerfeld postulated the quantum condition:

For any physical system in which the coordinates are periodic functions of time, there exists a quantum condition for each coordinate. These quantum conditions are

$$J_i = \oint p_i dq_i = n_i h, \quad (22)$$

where q_i is one of the coordinates, p_i is the momentum associated with that coordinate, n_i is a quantum number which takes on integral values, and the integral is taken over one period of the coordinate q_i .

Applying these quantization rules to the conjugate momenta of (14), (15) and (16) gives [3]

$$L_z = M_z \exp(r_e/r) = n_\phi \hbar, \quad (23)$$

$$L = M \exp(r_e/r) = (n_\theta + n_\phi) \hbar = k \hbar, \quad (24)$$

$$\oint [E^2/c^2 - \tilde{m}_0^2 c^2 \exp(r_e/r) - k^2 \hbar^2/r^2]^{1/2} dr = n_r \hbar, \quad (25)$$

where n_θ, n_ϕ, k and n_r have the values 0, 1, 2, ...

To determine the atomic spectrum we need to evaluate the integral of (25). Because of the finite radius of the nucleus we choose an arbitrary effective nuclear radius of gr_e . The potential term in the exponentials is then written as

$$\exp\left(\frac{2\Phi}{c^2}\right) = \exp\left(\frac{2r_e}{r - gr_e}\right), \quad (26)$$

so that

$$\begin{aligned} \exp(2\Phi/c^2) &= \\ &= 1 + 2\frac{r_e}{r} + 2\frac{r_e^2}{r^2}(g+1) + 3\frac{r_e^3}{r^3}g(g+1) + \dots \end{aligned} \quad (27)$$

For convenience we also define a parameter f such that

$$f = 2(g+1). \quad (28)$$

We shall subsequently see that the value of g , or f , is related to the concept of electron spin.

Approximating (27) to second order in r_e/r , substituting this approximation in (25) and integrating gives

$$E_m^2 = 1 - \frac{\alpha^2}{\left[n - k + \sqrt{k^2 + f\alpha^2}\right]^2}, \quad (29)$$

where $E_m = E/\tilde{m}_0c^2$, $n = n_r + k$ and $\alpha = e^2/\hbar c$ is the fine structure constant. This expression is simplified by expanding to fourth order in α :

$$E_m \cong 1 - \frac{\alpha^2}{2n^2} \left[1 + \frac{\alpha^2}{n} \left(\frac{1}{4n} - \frac{f}{k} \right) \right]. \quad (30)$$

The corresponding Sommerfeld/Dirac expressions are respectively

$$E_m^2 = \left(1 + \frac{\alpha^2}{\left[n - k + \sqrt{k^2 - \alpha^2}\right]^2} \right)^{-1} \quad (31)$$

and

$$E_m \cong 1 - \frac{\alpha^2}{2n^2} \left[1 + \frac{\alpha^2}{n} \left(\frac{1}{k} - \frac{3}{4n} \right) \right], \quad (32)$$

where $k = j + \frac{1}{2}$ for the Dirac expression, and $j = \frac{1}{2}, \frac{3}{2}, \frac{5}{2}, \dots, \frac{(n-1)}{2}$.

The difference between the energy given by our model E_W , as given by (30), and that of the Sommerfeld-Dirac model, E_D , as given by (32), is

$$(E_D - E_W)/\tilde{m}_0c^2 = \frac{\alpha^4}{2n^3} \left[\frac{1}{k}(f+1) - \frac{1}{n} \right]. \quad (33)$$

We shall show below that this difference corresponds to the energy associated with the "spin-orbit" interaction of our model.

4 Perturbation method

We use this method as applied by Born and others [3, Ch. 4].

To apply the perturbation method we need to express the energy \tilde{E} in terms of the momentum:

$$E = (p^2c^2 + \tilde{m}_0^2c^4)^{1/2} \exp(\Phi/c^2), \quad (34)$$

where $\mathbf{p} = \tilde{m}\mathbf{v}$. Again, taking the finite radius of the nucleus into account, we choose for the potential,

$$\exp(\Phi/c^2) = \exp(r_e/(r - gr_e)), \quad (35)$$

so that the potential term can be written as

$$\exp(\Phi/c^2) = 1 + \frac{r_e}{r} + w\frac{r_e^2}{r^2} + \left(w^2 - \frac{1}{4}\right)\frac{r_e^3}{r^3} + \dots, \quad (36)$$

where

$$w = (g + 1/2) = (f - 1)/2. \quad (37)$$

With this form for the potential, and using $\tilde{m}_0c^2r_e = -e^2$, (34) can be expanded as

$$\begin{aligned} E &= \underbrace{\tilde{m}_0c^2}_{E_0} + \underbrace{\frac{p^2}{2\tilde{m}_0}}_{E_1} - \underbrace{\frac{e^2}{r}}_{E_2} - \underbrace{\frac{p^4}{8\tilde{m}_0^3c^2}}_{E_2} + \underbrace{\frac{p^2r_e}{2\tilde{m}_0r}}_{E_3} \\ &+ \underbrace{w\frac{r_e^2\tilde{m}_0c^2}{r^2}}_{E_4} + \underbrace{w\frac{p^2r_e^2}{2\tilde{m}_0r^2}}_{E_5} - \underbrace{\frac{p^4r_e}{8\tilde{m}_0^3c^2r}}_{E_6} + \\ &+ \underbrace{\tilde{m}_0c^2\left(w^2 - \frac{1}{4}\right)\frac{r_e^3}{r^3}}_{E_7} + \dots \end{aligned} \quad (38)$$

Applying the unperturbed Bohr theory to each braced term, we find the following quantized expressions:

4.1 E_0 : rest mass energy

The first term on the right is the rest mass energy, which we denote by E_0 :

$$E_0 = \tilde{m}_0c^2. \quad (39)$$

4.2 E_1 : Bohr energy

The next two terms represent the unperturbed Coulomb energy of the hydrogen atom, which we indicate by E_1 :

$$E_1 = p^2/2\tilde{m}_0 - e^2/r. \quad (40)$$

According to the method of the Bohr theory,

$$E_1 = -R_e/n^2, \quad n = 1, 2, \dots \quad (41)$$

where

$$\left. \begin{aligned} R_e &= R_y\hbar c = e^2/2a_0 = \alpha^2\tilde{m}_0c^2/2 \\ a_0 &= \text{Bohr radius} = \hbar^2/\tilde{m}_0e^2 \\ R_y &= \text{Rydberg constant} = 2\pi^2e^4\tilde{m}_0/ch^3 = \alpha/4\pi a_0 \end{aligned} \right\}. \quad (42)$$

4.3 E_2 : relativistic correction

The third term is denoted by E_2 . It can be shown that [1]

$$E_2 = -p^4/8\tilde{m}_0^3c^2, \quad (43)$$

$$= -\frac{\alpha^2 R_e}{n^3} \left[\frac{1}{k} - \frac{3}{4n} \right]. \quad (44)$$

This is the ‘‘relativistic correction’’ of the Bohr-Sommerfeld model [3, §33]. This energy term is similar to that contained in the Dirac expression of (32). The sum of E_0 , E_1 and E_2 gives an expression identical to that of Sommerfeld and similar to that of Dirac.

It is well-known that Sommerfeld’s result was fortuitous as the effect of spin-orbit coupling was ignored in his model. This effect is incorporated in the Dirac model. In our model we shall see below that E_3 is an orbit-interaction term and that E_4 is related to ‘electron spin’. These two terms, missing in the Sommerfeld model, can now be added to $E_0 + E_1 + E_2$ of the Sommerfeld energy expression.

4.4 E_3 : orbital magnetic energy

We denote the fourth term by E_3 :

$$E_3 = p^2 r_e / 2\tilde{m}_0 r. \quad (45)$$

Applying the unperturbed Bohr theory, we find from (40):

$$\begin{aligned} E_3 &= (E_1 + e^2/r)r_e/r \\ &= r_e(E_1/r + e^2/r^2). \end{aligned} \quad (46)$$

Using (41) and the average values [3, p144],

$$\overline{1/r} = 1/n^2 a_0, \quad (47)$$

$$\overline{1/r^2} = 1/a_0^2 n^3 k, \quad k = 1, 2, \dots, n \quad (48)$$

as well as

$$r_e/a_0 = a^2, \quad (49)$$

we get

$$E_3 = \frac{\alpha^2 R_e}{n^3} \left(\frac{2}{k} - \frac{1}{n} \right) = \frac{\alpha^4 \tilde{m}_0 c^2}{2n^3} \left(\frac{2}{k} - \frac{1}{n} \right). \quad (50)$$

The physical interpretation of E_3 is that it is the energy due to the magnetic interaction of an electron moving in orbit about a proton. This can be seen as follows.

Substituting $\mathbf{p} = \tilde{m}\mathbf{v}$ and $r_e = -e^2/\tilde{m}_0 c^2$ into (45) gives

$$\begin{aligned} E_3 &= -\frac{e^2 v^2}{2rc^2} \left(\frac{\tilde{m}}{\tilde{m}_0} \right)^2 \\ &\approx -\frac{e^2 v^2}{2rc^2} \quad \text{in the non-relativistic limit.} \end{aligned} \quad (51)$$

It corresponds to the classical form of the magnetic energy due to orbital motion, as given by (70) below:

4.5 E_4 : ‘‘electron spin’’

$$\begin{aligned} E_4 &= w r_e^2 \tilde{m}_0 c^2 / r^2, \\ &= w e^4 / \tilde{m}_0 c^2 r^2. \end{aligned} \quad (52)$$

Applying (48) gives

$$E_4 = \frac{w 2\alpha^2 R_e}{n^3 k} = w \alpha^4 \tilde{m}_0 c^2 \frac{1}{n^3 k}. \quad (53)$$

We consider the significance of the factor w . We note that the potential energy expression (36) can be truncated after the quadratic term in r_e/r by letting $w^2 - \frac{1}{4} = 0$. As such, truncation can be considered as the limit to the resolution of the apparatus used for spectral observation. With this condition, we find that

$$w = \pm \frac{1}{2} \quad (54)$$

gives the spectrum due to all interactions up to second degree in r/r_e . Therefore, from (42) and (53):

$$E_4 = \pm \frac{1}{2} \frac{e^8 \tilde{m}_0}{\hbar^4 c^2} \frac{1}{n^3 k}. \quad (55)$$

The above expression for E_4 corresponds to the quantum mechanical result for the energy due to electron spin. Except for the quantum numbers, Eisberg and Resnick [6, Example 8–3] find a similar result for the energy due to spin-orbit interaction.

The equivalence of (55) to the result of Eisberg and Resnick also confirms the implicit value $g_s = 2$ in E_4 .

In this study E_4 corresponds to the energy due to quantum mechanical spin only. Combining E_3 and E_4 gives the corresponding total spin-orbit energy.

For $k = 1$ the expression for E_4 is equal to the Darwin term of the Dirac theory. In the Dirac theory the Darwin term has to be introduced separately for $\ell = 0$ states, whereas in our model E_4 already provides for $\ell = 0$ through the degeneracy ($\ell = 0, 1$) associated with the $k = 1$ level.

In summary, ‘electron spin’ represents a second order contribution r_e^2/r^2 to the total energy of the atom.

The above reasoning also applies to higher orders of approximation. Expanding (35) to fourth degree in r_e/r gives:

$$\begin{aligned} \exp(\Phi/c^2) &= 1 + \frac{r_e}{r} + \frac{r_e^2}{r^2} w + \frac{r_e^3}{r^3} (w^2 - \frac{1}{2}) + \\ &+ \frac{r_e^4}{r^4} \left(w^2 - \frac{1}{4} \right) w + \dots \end{aligned} \quad (56)$$

The coefficient of r_e^4/r^4 is zero if $(w^2 - \frac{1}{4})w = 0$, or

$$w = \frac{1}{2}, -\frac{1}{2}, 0. \quad (57)$$

A next higher resolution to r_e^3/r^3 therefore introduces an additional value of $w = 0$, giving a triplet symmetrical about this value.

For a comprehensive survey of the conceptual developments surrounding electron spin we refer to the text by Tomonaga [7].

4.6 E_5 : radiative reaction

$$E_5 = w \frac{p^2 r_e^2}{2\tilde{m}_0 r^2} \quad (58)$$

$$= \pm \frac{1}{2} \alpha^4 R_e \left[\frac{1}{n^5 k} - \frac{2}{n^3 k^3} \right]. \quad (59)$$

Substituting $\mathbf{p} = \tilde{m}\mathbf{v}$ in (58) gives

$$E_5 = \pm \frac{1}{2} \frac{v^2 e^4}{2\tilde{m}_0 c^4 r^2} \left(\frac{\tilde{m}}{\tilde{m}_0} \right)^2. \quad (60)$$

In the non-relativistic limit, $\tilde{m} \approx \tilde{m}_0$, the above term corresponds to the last RHS term of (69), i.e. the classical energy resulting from radiative reaction. Its value is too small ($\sim 10^{-8}$ eV) to affect the values of the fine-spectrum.

4.7 Summary

$$\begin{aligned} E_0 &= m_0 c^2 & : & \text{rest mass energy,} \\ E_1 &= -\frac{R_e}{n^2} & : & \text{Bohr energy,} \\ E_2 &= -\frac{\alpha^2 R_e}{n^3} \left[\frac{1}{k} - \frac{3}{4n} \right] & : & \text{relativistic correction,} \\ E_3 &= \frac{\alpha^2 R_e}{n^3} \left[\frac{2}{k} - \frac{1}{n} \right] & : & \text{orbital magnetic energy,} \\ E_4 &= w \frac{2\alpha^2 R_e}{n^3 k} & : & \text{electron spin energy,} \\ E_5 &= w \alpha^4 R_e \left[\frac{1}{n^5 k} - \frac{2}{n^3 k^3} \right] & : & \text{Radiative reaction,} \end{aligned}$$

where $w = \pm \frac{1}{2}$.

The sum of the energy terms $\sum E_i = E_0 + E_1 + E_2 + E_3 + E_4 + E_5$ is:

$$\sum E_i / \tilde{m}_0 c^2 = 1 - \frac{\alpha^2}{2n^2} \left[1 - \frac{\alpha^2}{n} \left(\frac{f}{k} - \frac{1}{4n} \right) \right], \quad (61)$$

which, as expected, is the same as (30).

Each term in (38) can be related to a standard electrodynamic effect. It is significant that although (38) does not explicitly contain any vector quantities, such as the vector potential \mathbf{A} , this potential is implicit, as shown in the discussion of E_3 and the comparison with (69).

An explanation for the difference (33) between the spectrum of the proposed model and that of Dirac-Sommerfeld can be seen as follows:

Consider the sum

$$E_3 + E_4 = \frac{\alpha^2 R_e}{n^3} \left[\frac{2}{k} (w + 1) - \frac{1}{n} \right] \quad (62)$$

or, since $w = (f - 1)/2$,

$$E_3 + E_4 = \frac{\alpha^2 R_e}{n^3} \left[\frac{1}{k} (f + 1) - \frac{1}{n} \right]. \quad (63)$$

The above equation corresponds to (33), the difference between the Sommerfeld-Dirac expression and that of our model. The expression (30) therefore already incorporates the spin-orbit interaction.

The energy $E_3 + E_4$ therefore represents a perturbation to the Sommerfeld-Dirac values. The only candidate for this perturbation is the Lamb-shift. For the $(n, k) = (2, 1)$ level and for $w = -0.5$ the value of $E_3 + E_4$ is $4.5283178 e-5$ eV. The Lamb-shift for this level is $4.3738019 e-6$ eV, which is an order 10 smaller. It would be overly ambitious to find the observed Lamb-shift from the present simple model. At this degree of spectral resolution one would have to look at a modification of the effective nuclear radius to $r - a_1 r_e - a_2 r_e^2 - \dots$

4.8 Comparison with classical electromagnetic energy

In order to compare the results of this study with those of conventional electromagnetic theory, we give a brief summary of the energy relations of classical electrodynamic theory.

The Hamiltonian describing the interaction of an electron with fields \mathbf{H} and \mathbf{E} is given by [8, p. 124]

$$H_{\text{classical}} = e\Phi + \left(\mathbf{p} - \frac{e}{c}\mathbf{A} \right)^2 / 2\tilde{m}, \quad (64)$$

where Φ and \mathbf{A} are respectively the electrostatic and vector potentials of the system.

It is important to note that \mathbf{A} and Φ do not merely represent the external fields in which the particle moves, but also the particle's own fields. This implies that the force of radiative reaction is automatically included.

The corresponding classical Lagrangian is

$$L_{\text{classical}} = \frac{p^2}{2\tilde{m}} - e\Phi + \frac{e}{c}\mathbf{A} \cdot \mathbf{v}. \quad (65)$$

For an electron moving under the influence of a magnetic field,

$$\mathbf{H} = e(\mathbf{v} \times \mathbf{r})/cr^3, \quad (66)$$

a vector potential \mathbf{A} can be found as

$$\mathbf{A} = \frac{1}{2}(\mathbf{H} \times \mathbf{r}) = e\mathbf{v}/2cr. \quad (67)$$

Substituting this expression for \mathbf{A} and using $\mathbf{p} = \tilde{m}\mathbf{v}$, yields

$$\left(\mathbf{p} - \frac{e}{c}\mathbf{A} \right)^2 = p^2 - \frac{e^2 v^2 \tilde{m}}{c^2 r} + \frac{e^4 v^2}{4c^4 r^2}. \quad (68)$$

Since the Hamiltonian of (64) does not contain t explicitly, we may equate it to the total energy. Consequently, substituting (68), and $e\Phi = -e^2/r$, in (64) gives the classical

energy

$$E_{\text{classical}} = -\frac{e^2}{r} + \frac{p^2}{2\tilde{m}} - \frac{e^2 v^2}{2c^2 r} + \frac{e^4 v^2}{8\tilde{m}c^4 r^2}. \quad (69)$$

The third RHS term is the magnetic energy due to the orbital motion of the electron:

$$E_{\text{orbital}} = \boldsymbol{\mu}_\ell \cdot \mathbf{H} = -\frac{g_\ell e^2 v^2}{2rc^2}, \quad (70)$$

where $\boldsymbol{\mu}_\ell$ = magnetic moment, g_ℓ = Landé g factor = 1, and \mathbf{M} and \mathbf{H} are parallel to one another. This energy corresponds to that of E_3 above.

The fourth RHS term of (69) represents radiative reaction, which corresponds to our E_5 as given by (60).

The standard relativistic Hamiltonian is given by:

$$H_{\text{relativistic}} = [(\mathbf{p} - q\mathbf{A}/c)^2 c^2 + \tilde{m}_0^2 c^4]^{\frac{1}{2}} + q\Phi. \quad (71)$$

The Hamiltonians of (64) and (71) must be compared to ours of (17).

It is well-known that the Bohr model for the atom fails because of radiative reaction; in our model this loss is compensated for by the additional and associated potential term, E_4 . This term can also be interpreted as a modification of Coulomb's law. It is significant that this energy term can also be interpreted as arising from electron spin.

It is also significant that the Sommerfeld relativistic correction term, E_2 , does not appear in either (69) or (71).

We can consider the electromagnetic energy arising from the Hamiltonians of (64) and (71) as approximations to that of our Hamiltonian of (17).

We also note that the energy derived from the Hamiltonian of (64), which is normally derived from a Lagrangian containing the vector potential \mathbf{A} , appears as an approximation to our model, which does not explicitly contain a vector potential. A vector potential arises in our theory because of the variation of mass according to (12).

5 The large number coincidences

Dirac postulated that the large dimensionless ratios ($\sim 10^{40}$) of certain universal constants underlie a fundamental relationship between them. A theoretical explanation for these ratios has not yet been found, but it became known as Dirac's Large Number Hypothesis (LNH). [9] Some of these relations are derivable from (11).

Taking R as the Schwarzschild radius of the proton, $R_p = 2GM_p/c^2$, we rewrite (11) as

$$\begin{aligned} -\frac{e^2}{\tilde{m}_0 c^2} &= \frac{GM_p}{c^2} \\ \text{or } -\frac{e^2}{GM_p \tilde{m}_0} &= 1. \end{aligned} \quad (72)$$

Defining the relationship between the *gravitational mass* M_p and the *electromagnetic rest mass* \tilde{m}_{0p} of the proton as

$$M_p = N_D \tilde{m}_{0p}, \quad (73)$$

where N_D is a dimensionless number, we can write (72) as

$$-\frac{e^2}{G \tilde{M}_{0p} \tilde{m}_0} = N_D, \quad (74)$$

which, if the absolute value is taken, is the basic relationship of the LNH.

6 Lorentz force

The force equation for a particle, mass \tilde{m} and velocity \mathbf{v} is found by applying the Euler-Lagrange equations to (13). This gives

$$\dot{\mathbf{p}} = \hat{\mathbf{r}} \frac{\tilde{m} r_e c^2}{r^2} + \frac{\tilde{m} r_e}{r^3} \mathbf{v} \times (\mathbf{v} \times \mathbf{r}). \quad (75)$$

Defining

$$\mathbf{E} = \hat{\mathbf{r}} \frac{r_e c^2}{r^2}, \quad (76)$$

$$\mathbf{H} = \frac{r_e \mathbf{v} \times \mathbf{r}}{r^3}, \quad (77)$$

we can write (75) as

$$\text{Electromagnetic } \dot{\mathbf{p}} = \tilde{m} [\mathbf{E} + \mathbf{v} \times \mathbf{H}]. \quad (78)$$

For $v \ll c$, $\tilde{m} r_e c^2 \rightarrow \tilde{m}_0 r_e c^2 = e^2$ and then (75) approaches the classical Lorentz form.

7 Unifying gravitation and electromagnetism

Equation (16) of reference [1] can be combined with (78) in one formulation:

$$\dot{\mathbf{p}} = \tilde{m} [k\mathbf{E} + \mathbf{v} \times \mathbf{H}], \quad (79)$$

where for

$$\begin{aligned} \text{Gravitation} &: k = -1, \\ \text{Electromagnetism} &: k = 1. \end{aligned}$$

The same equation gives either planetary or atomic motion, where the vectors \mathbf{E} and \mathbf{H} are respectively given by

$$\mathbf{E} = \hat{\mathbf{r}} \frac{GM}{r^2} = \hat{\mathbf{r}} \frac{r_e c^2}{r^2}, \quad (80)$$

$$\mathbf{H} = \frac{GM(\mathbf{v} \times \mathbf{r})}{c^2 r^3} = \frac{r_e \mathbf{v} \times \mathbf{r}}{r^3}. \quad (81)$$

8 Summary

<u>Gravitation</u>	<u>Electromagnetism</u>
$R = 2GM/c^2$	$r_e = R/2$
m_0	$\tilde{m}_0 = m_0/N$
$L = -m_0(c^2 + v^2)e^{R/r}$	$L = -(\tilde{m}_0 c^2 / \gamma) e^{r_e/r}$
$E = mc^2 e^{R/r}$	$E = \tilde{m} c^2 e^{r_e/r}$
$m = m_0 / \gamma^2$	$\tilde{m} = \gamma \tilde{m}_0$
$L^2 = M^2 e^{2R/r} = \text{constant}$	$L^2 = M^2 e^{2r_e/r} = \text{constant}$
$L_z = M_z e^{R/r} = \text{constant}$	$L_z = M_z e^{r_e/r} = \text{constant}$
$\mathbf{M} = (\mathbf{r} \times m_0 \mathbf{v})$	$\mathbf{M} = (\mathbf{r} \times \tilde{m}_0 \mathbf{v})$
$\dot{\mathbf{p}} = m\mathbf{E} + m_0 \mathbf{v} \times \mathbf{H}$	$\dot{\mathbf{p}} = \tilde{m}[\mathbf{E} + \mathbf{v} \times \mathbf{H}]$
$\mathbf{p} = m_0 \mathbf{v}$	$\mathbf{p} = \tilde{m} \mathbf{v}$
$\mathbf{E} = -\hat{\mathbf{r}} GM/r^2$	$\mathbf{E} = \hat{\mathbf{r}} r_e c^2 / r^2$
$\mathbf{H} = GM(\mathbf{v} \times \mathbf{r})/r^3 c^2$	$\mathbf{H} = r_e(\mathbf{v} \times \mathbf{r})/r^3$

9 Nuclear force

In a subsequent article we shall show that equations for the nuclear force, such as the Yukawa potential, can be derived by considering the forms of both the energy equations (2) and (8) at $r \approx R/2 = r_e$.

Submitted on May 25, 2008

Accepted on June 03, 2008

References

1. Wagener P.C. Principles of a theory of general interaction. PhD thesis, University of South Africa, 1987. An updated version is to be published as a book during 2008.
2. Wagener P.C. A classical model of gravitation. *Progress in Physics*, 2008, v. 3, 21–23.
3. Born M. The mechanics of the atom. Frederick Ungar Publ. Co., New York, 1960.
4. Goldstein H. Classical Mechanics. Addison-Wesley, Reading, Mass., 1958.
5. Eisberg R.M. Fundamentals of modern physics. John Wiley, New York, 1961.
6. Eisberg R. and Resnick R. Quantum physics of atoms, molecules, solids, nuclei and particles. John Wiley, New York, 1985.
7. Sin-Itiro Tomonaga. The story of spin. Univ Chicago Press, 1997.
8. Grandy Jr. W.T. Introduction to electrodynamics and radiation. Academic Press, New York, 1970.
9. Harrison E.R. *Physics Today*, December 30, 1972.

On Emergent Physics, “Unparticles” and Exotic “Unmatter” States

Ervin Goldfain* and Florentin Smarandache†

* *Photonics CoE, Welch Allyn Inc., Skaneateles Falls, NY 13153, USA*

E-mail: ervingoldfain@gmail.com

† *Chair of Math & Sc. Depart., University of New Mexico, Gallup, NM 87301, USA*

E-mail: smarand@unm.edu

Emergent physics refers to the formation and evolution of collective patterns in systems that are nonlinear and out-of-equilibrium. This type of large-scale behavior often develops as a result of simple interactions at the component level and involves a dynamic interplay between order and randomness. On account of its universality, there are credible hints that emergence may play a leading role in the Tera-ElectronVolt (TeV) sector of particle physics. Following this path, we examine the possibility of hypothetical high-energy states that have fractional number of quanta per state and consist of arbitrary mixtures of particles and antiparticles. These states are similar to “un-particles”, massless fields of non-integral scaling dimensions that were recently conjectured to emerge in the TeV sector of particle physics. They are also linked to “unmatter”, exotic clusters of matter and antimatter introduced few years ago in the context of Neutrosophy.

1 Introduction

Quantum Field Theory (QFT) is a framework whose methods and ideas have found numerous applications in various domains, from particle physics and condensed matter to cosmology, statistical physics and critical phenomena [1, 2]. As successful synthesis of Quantum Mechanics and Special Relativity, QFT represents a collection of *equilibrium* field theories and forms the foundation for the Standard Model (SM), a body of knowledge that describes the behavior of all known particles and their interactions, except gravity. Many broken symmetries in QFT, such as violation of parity and CP invariance, are linked to either the electroweak interaction or the physics beyond SM [3–5]. This observation suggests that unitary evolution postulated by QFT no longer holds near or above the energy scale of electroweak interaction ($\approx 300\text{GeV}$) [6,7]. It also suggests that progress on the theoretical front requires a framework that can properly handle *non-unitary evolution* of phenomena beyond SM. We believe that fractional dynamics naturally fits this description. It operates with derivatives of non-integer order called *fractal operators* and is suitable for analyzing many complex processes with long-range interactions [6–9]. Building on the current understanding of fractal operators, we take the dimensional parameter of the regularization program $\varepsilon = 4 - d$ to represent the order of fractional differentiation in physical space-time (alternatively, $\varepsilon = 1 - d$ in one-dimensional space) [10, 11]. It can be shown that ε is related to the reciprocal of the cutoff scale $\varepsilon \approx (\mu_0/\Lambda)$, where μ_0 stands for a finite and arbitrary reference mass and Λ is the cutoff energy scale. Under these circumstances, ε may be thought as an infinitesimal parameter that can be continuously tuned and drives the departure from equilibrium. The approach to scale invariance demands that the choice of this parameter is completely arbitrary, as

long as $\varepsilon \ll 1$. Full scale invariance and equilibrium field theory are asymptotically recovered in the limit of physical space-time ($d = 4$) as $\varepsilon \rightarrow 0$ or $\Lambda \rightarrow \infty$ [11, 12].

2 Definitions

We use below the Riemann-Liouville definition for the one-dimensional left and right fractal operators [13]. Consider for simplicity a space-independent scalar field $\varphi(t)$. Taking the time coordinate to be the representative variable, one writes

$${}_0D_L^\alpha \varphi(t) = \frac{1}{\Gamma(1-\alpha)} \frac{d}{dt} \int_0^t (t-\tau)^{-\alpha} \varphi(\tau) d\tau, \quad (1)$$

$${}_0D_R^\alpha \varphi(t) = \frac{1}{\Gamma(1-\alpha)} \left(-\frac{d}{dt}\right) \int_t^0 (\tau-t)^{-\alpha} \varphi(\tau) d\tau. \quad (2)$$

Here, fractional dimension $0 < \alpha < 1$ denotes the order of fractional differentiation. In general, it can be shown that α is linearly dependent on the dimensionality of the space-time support [8]. By definition, α assumes a continuous spectrum of values on fractal supports [11].

3 Fractional dynamics and ‘unparticle’ physics

The classical Lagrangian for the free scalar field theory in 3+1 dimensions reads [1–2, 14]

$$L = \partial^\mu \varphi \partial_\mu \varphi - m^2 \varphi^2, \quad (3)$$

and yields the following expression for the field momentum

$$\pi = \frac{\partial L}{\partial \left(\frac{\partial \varphi}{\partial t}\right)} = \frac{\partial \varphi}{\partial t}. \quad (4)$$

It is known that the standard technique of canonical quantization promotes a classical field theory to a quantum field theory by converting the field and momentum variables into operators. To gain full physical insight with minimal complications in formalism, we work below in 0+1 dimensions. Ignoring the left/right labels for the time being, we define the field and momentum operators as

$$\varphi \rightarrow \hat{\varphi} = \varphi, \tag{5}$$

$$\pi \rightarrow \hat{\pi}^\alpha = -i \frac{\partial^\alpha}{\partial |\varphi|^\alpha} \equiv -iD^\alpha. \tag{6}$$

Without the loss of generality, we set $m = 1$ in (3). The Hamiltonian becomes

$$H \rightarrow \hat{H}^\alpha = -\frac{1}{2} D^{2\alpha} + \frac{1}{2} \varphi^2 = \frac{1}{2} (\hat{\pi}^{2\alpha} + \varphi^2). \tag{7}$$

By analogy with the standard treatment of harmonic oscillator in quantum mechanics, it is convenient to work with the destruction and creation operators defined through [1–2, 14]

$$\hat{a}^\alpha \doteq \frac{1}{\sqrt{2}} [\hat{\varphi} + i\hat{\pi}^\alpha], \tag{8}$$

$$\hat{a}^{+\alpha} \doteq \frac{1}{\sqrt{2}} [\hat{\varphi} - i\hat{\pi}^\alpha]. \tag{9}$$

Straightforward algebra shows that these operators satisfy the following commutation rules

$$[\hat{a}, \hat{a}] = [\hat{a}^{+\alpha}, \hat{a}^{+\alpha}] = 0, \tag{10}$$

$$[\hat{a}^{+\alpha}, \hat{a}^\alpha] = i [\hat{\varphi}, \hat{\pi}^\alpha] = -\alpha \hat{\pi}^{(\alpha-1)}. \tag{11}$$

The second relation of these leads to

$$\hat{H}^\alpha = \hat{a}^{+\alpha} \hat{a}^\alpha + \frac{1}{2} \alpha \hat{\pi}^{(\alpha-1)}. \tag{12}$$

In the limit $\alpha = 1$ we recover the quantum mechanics of the harmonic oscillator, namely

$$\hat{H} = \hat{a}^+ \hat{a} + \frac{1}{2}. \tag{13}$$

It was shown in [6] that the fractional Hamiltonian (12) leads to a continuous spectrum of states having non-integer numbers of quanta per state. These unusual flavors of particles and antiparticles emerging as fractional objects were named “*complexons*”. Similar conclusions have recently surfaced in a number of papers where the possibility of a scale-invariant “hidden” sector of particle physics extending beyond SM has been investigated. A direct consequence of this setting is a continuous spectrum of massless fields having non-integral scaling dimensions called “un-particles”. The reader is directed to [15–21] for an in-depth discussion of “un-particle” physics.

4 Mixing properties of fractal operators

Left and right fractal operators (L/R) are natural analogues of chiral components associated with the structure of quantum fields [8, 9]. The goal of this section is to show that there is an inherent mixing of (L/R) operators induced by the fractional dynamics, as described below. An equivalent representation of (1) is given by

$${}_0D_L^\alpha \varphi(t) = \frac{1}{\Gamma(1-\alpha)} \left(-\frac{d}{dt}\right) \int_t^0 [-(\tau-t)]^{-\alpha} \varphi(\tau) d\tau, \tag{14}$$

or

$$\begin{aligned} {}_0D_L^\alpha \varphi(t) &= \frac{(-1)^{-\alpha}}{\Gamma(1-\alpha)} \left(-\frac{d}{dt}\right) \int_t^0 (\tau-t)^{-\alpha} \varphi(\tau) d\tau = \\ &= (-1)^{-\alpha} {}_0D_R^\alpha \varphi(t), \end{aligned} \tag{15}$$

$${}_0D_R^\alpha = (-1)^\alpha {}_0D_L^\alpha = \exp(i\pi\alpha) {}_0D_L^\alpha. \tag{16}$$

Starting from (2) instead, we find

$${}_0D_L^\alpha = (-1)^\alpha {}_0D_R^\alpha = \exp(i\pi\alpha) {}_0D_R^\alpha. \tag{17}$$

Consider now the one-dimensional case $d = 1$, take $\alpha = \varepsilon = 1 - d$ and recall that continuous tuning of ε does not impact the physics as a consequence of scale invariance. Let us iterate (16) and (17) a finite number of times ($n \geq 1$) under the assumption that $n\varepsilon \ll 1$. It follows that the fractal operator of any infinitesimal order may be only defined up to an arbitrary dimensional factor $\exp(i\pi n\varepsilon) \approx 1 + (i\pi n\varepsilon) = 1 - i\tilde{\varepsilon}$, that is,

$${}_0D_{L,R}^\varepsilon \varphi(t) \approx [{}_0D_{L,R}^0 - i\tilde{\varepsilon}] \varphi(t) \tag{18}$$

or

$$i{}_0D_{L,R}^\varepsilon \varphi(t) = [i{}_0D_{L,R}^0 + \tilde{\varepsilon}] \varphi(t), \tag{19}$$

where

$$\lim_{\varepsilon \rightarrow 0} D_{L,R}^\varepsilon \varphi(t) = \varphi(t). \tag{20}$$

Relations (18–20) indicate that fractional dimension $\tilde{\varepsilon}$ induces: (a) a new type of mixing between chiral components of the field and (b) an ambiguity in the very definition of the field, fundamentally different from measurement uncertainties associated with Heisenberg principle. Both effects are *irreversible* (since fractional dynamics describes irreversible processes) and of *topological nature* (being based on the concept of continuous dimension). They do not have a counterpart in conventional QFT.

5 Emergence of “unmatter” states

Using the operator language of QFT and taking into account (6), (18) can be presented as

$$\hat{\pi}^\varepsilon \varphi(t) = \hat{\pi}^\varepsilon \varphi(t) - \tilde{\varepsilon} \hat{\varphi}(t). \tag{21}$$

Relation (21) shows that the fractional momentum operator $\hat{\pi}^\varepsilon$ and the field operator $\hat{\varphi}(t) = \varphi(t)$ are no longer independent entities but linearly coupled through fractional dimension $\tilde{\varepsilon}$. From (11) it follows that the destruction and creation operators are also coupled to each other. As a result, particles and antiparticles can no longer exist as linearly independent objects. Because $\tilde{\varepsilon}$ is continuous, they emerge as an *infinite spectrum of mixed states*. This surprising finding is counterintuitive as it does not have an equivalent in conventional QFT. Moreover, arbitrary mixtures of particles and antiparticles may be regarded as a manifestation of “unmatter”, a concept launched in the context of Neutrosophic Logic [22–24].

6 Definition of unmatter

In short, unmatter is formed by matter and antimatter that bind together [23, 24].

The building blocks (most elementary particles known today) are 6 quarks and 6 leptons; their 12 antiparticles also exist.

Then *unmatter* will be formed by at least a building block and at least an antibuilding block which can bind together.

Let’s start from neutrosophy [22], which is a generalization of dialectics, i.e. not only the opposites are combined but also the neutralities. Why? Because when an idea is launched, a category of people will accept it, others will reject it, and a third one will ignore it (don’t care). But the dynamics between these three categories changes, so somebody accepting it might later reject or ignore it, or an ignorant will accept it or reject it, and so on. Similarly the dynamicity of $\langle A \rangle$, $\langle \text{anti}A \rangle$, $\langle \text{neut}A \rangle$, where $\langle \text{neut}A \rangle$ means neither $\langle A \rangle$ nor $\langle \text{anti}A \rangle$, but in between (neutral). Neutrosophy considers a kind not of di-alectics but tri-alectics (based on three components: $\langle A \rangle$, $\langle \text{anti}A \rangle$, $\langle \text{neut}A \rangle$).

Hence unmatter is a kind of intermediary (not referring to the charge) between matter and antimatter, i.e. neither one, nor the other.

Neutrosophic Logic (NL) is a generalization of fuzzy logic (especially of intuitionistic fuzzy logic) in which a proposition has a degree of truth, a degree of falsity, and a degree of neutrality (neither true nor false); in the normalized NL the sum of these degrees is 1.

7 Exotic atom

If in an atom we substitute one or more particles by other particles of the same charge (constituents) we obtain an exotic atom whose particles are held together due to the electric charge. For example, we can substitute in an ordinary atom one or more electrons by other negative particles (say π^- , anti-Rho meson, D^- , D_s^- , muon, tau, Ω^- , Δ^- , etc., generally clusters of quarks and antiquarks whose total charge is negative), or the positively charged nucleus replaced by other

positive particle (say clusters of quarks and antiquarks whose total charge is positive, etc.).

8 Unmatter atom

It is possible to define the unmatter in a more general way, using the exotic atom.

The classical unmatter atoms were formed by particles like (a) electrons, protons, and antineutrons, or (b) antielectrons, antiprotons, and neutrons.

In a more general definition, an unmatter atom is a system of particles as above, or such that one or more particles are replaced by other particles of the same charge.

Other categories would be (c) a matter atom with where one or more (but not all) of the electrons and/or protons are replaced by antimatter particles of the same corresponding charges, and (d) an antimatter atom such that one or more (but not all) of the antielectrons and/or antiprotons are replaced by matter particles of the same corresponding charges.

In a more composed system we can substitute a particle by an unmatter particle and form an unmatter atom.

Of course, not all of these combinations are stable, semi-stable, or quasi-stable, especially when their time to bind together might be longer than their lifespan.

9 Examples of unmatter

During 1970–1975 numerous pure experimental verifications were obtained proving that “atom-like” systems built on nucleons (protons and neutrons) and anti-nucleons (anti-protons and anti-neutrons) are real. Such “atoms”, where nucleon and anti-nucleon are moving at the opposite sides of the same orbit around the common centre of mass, are very unstable, their life span is no more than 10^{-20} sec. Then nucleon and anti-nucleon annihilate into gamma-quanta and more light particles (pions) which can not be connected with one another, see [6, 7, 8]. The experiments were done in mainly Brookhaven National Laboratory (USA) and, partially, CERN (Switzerland), where “proton–anti-proton” and “anti-proton–neutron” atoms were observed, called them $\bar{p}p$ and $\bar{p}n$ respectively.

After the experiments were done, the life span of such “atoms” was calculated in theoretical way in Chapiro’s works [9, 10, 11]. His main idea was that nuclear forces, acting between nucleon and anti-nucleon, can keep them far way from each other, hindering their annihilation. For instance, a proton and anti-proton are located at the opposite sides in the same orbit and they are moved around the orbit centre. If the diameter of their orbit is much more than the diameter of “annihilation area”, they are kept out of annihilation. But because the orbit, according to Quantum Mechanics, is an actual cloud spreading far around the average radius, at any radius between the proton and the anti-proton there is a probability

that they can meet one another at the annihilation distance. Therefore nucleon—anti-nucleon system annihilates in any case, this system is unstable by definition having life span no more than 10^{-20} sec.

Unfortunately, the researchers limited the research to the consideration of $\bar{p}p$ and $\bar{p}n$ nuclei only. The reason was that they, in the absence of a theory, considered $\bar{p}p$ and $\bar{p}n$ “atoms” as only a rare exception, which gives no classes of matter.

The unmatter does exist, for example some mesons and antimessons, through for a trifling of a second lifetime, so the pions are unmatter (which have the composition $u\bar{d}$ and $d\bar{u}$, where by u we mean anti-up quark, d = down quark, and analogously u = up quark and \bar{d} = anti-down quark, while by \bar{u} means anti, the kaon K^+ ($u\bar{s}$), K^- ($\bar{u}s$), Φ ($s\bar{s}$), D^+ ($c\bar{d}$), D^0 ($c\bar{u}$), D_s^+ ($c\bar{s}$), J/Ψ ($c\bar{c}$), B^- ($b\bar{u}$), B^0 ($d\bar{b}$), B_s^0 ($s\bar{b}$), $Upsilon$ ($b\bar{b}$), where c = charm quark, s = strange quark, b = bottom quark, etc. are unmatter too.

Also, the pentaquark Theta-plus (Θ^+), of charge $+1$, $uudd\bar{s}$ (i.e. two quarks up, two quarks down, and one anti-strange quark), at a mass of 1.54 GeV and a narrow width of 22 MeV, is unmatter, observed in 2003 at the Jefferson Lab in Newport News, Virginia, in the experiments that involved multi-GeV photons impacting a deuterium target. Similar pentaquark evidence was obtained by Takashi Nakano of Osaka University in 2002, by researchers at the ELSA accelerator in Bonn in 1997–1998, and by researchers at ITEP in Moscow in 1986.

Besides Theta-plus, evidence has been found in one experiment [25] for other pentaquarks, Ξ_5^- ($ddssu\bar{u}$) and Ξ_5^+ ($uusd\bar{s}$).

D. S. Carman [26] has reviewed the positive and null evidence for these pentaquarks and their existence is still under investigation.

In order for the paper to be self-contained let’s recall that the *pionium* is formed by a π^+ and π^- mesons, the *positronium* is formed by an antielectron (positron) and an electron in a semi-stable arrangement, the *protonium* is formed by a proton and an antiproton also semi-stable, the *antiprotonic helium* is formed by an antiproton and electron together with the helium nucleus (semi-stable), and *muonium* is formed by a positive muon and an electron.

Also, the *mesonic atom* is an ordinary atom with one or more of its electrons replaced by negative mesons.

The *strange matter* is a ultra-dense matter formed by a big number of strange quarks bounded together with an electron atmosphere (this strange matter is hypothetical).

From the exotic atom, the pionium, positronium, protonium, antiprotonic helium, and muonium are unmatter.

The mesonic atom is unmatter if the electron(s) are replaced by negatively-charged antimessons.

Also we can define a mesonic antiatom as an ordinary antiatomic nucleus with one or more of its antielectrons replaced by positively-charged mesons. Hence, this mesonic

antiatom is unmatter if the antielectron(s) are replaced by positively-charged mesons.

The strange matter can be unmatter if these exist at least an antiquark together with so many quarks in the nucleus. Also, we can define the strange antimatter as formed by a large number of antiquarks bound together with an antielectron around them. Similarly, the strange antimatter can be unmatter if there exists at least one quark together with so many antiquarks in its nucleus.

The bosons and antibosons help in the decay of unmatter. There are 13+1 (Higgs boson) known bosons and 14 antibosons in present.

10 Chromodynamics formula

In order to save the colorless combinations prevailed in the Theory of Quantum Chromodynamics (QCD) of quarks and antiquarks in their combinations when binding, we devise the following formula:

$$Q - A \in \pm M3, \tag{22}$$

where $M3$ means multiple of three, i.e. $\pm M3 = \{3 \cdot k | k \in \mathbb{Z}\} = \{\dots, -12, -9, -6, -3, 0, 3, 6, 9, 12, \dots\}$, and Q = number of quarks, A = number of antiquarks.

But (22) is equivalent to:

$$Q \equiv A \pmod{3} \tag{23}$$

(Q is congruent to A modulo 3).

To justify this formula we mention that 3 quarks form a colorless combination, and any multiple of three ($M3$) combination of quarks too, i.e. 6, 9, 12, etc. quarks. In a similar way, 3 antiquarks form a colorless combination, and any multiple of three ($M3$) combination of antiquarks too, i.e. 6, 9, 12, etc. antiquarks. Hence, when we have hybrid combinations of quarks and antiquarks, a quark and an antiquark will annihilate their colors and, therefore, what’s left should be a multiple of three number of quarks (in the case when the number of quarks is bigger, and the difference in the formula is positive), or a multiple of three number of antiquarks (in the case when the number of antiquarks is bigger, and the difference in the formula is negative).

11 Quantum chromodynamics unmatter formula

In order to save the colorless combinations prevailed in the Theory of Quantum Chromodynamics (QCD) of quarks and antiquarks in their combinations when binding, we devise the following formula:

$$Q - A \in \pm M3, \tag{24}$$

where $M3$ means multiple of three, i.e. $\pm M3 = \{3 \cdot k | k \in \mathbb{Z}\} = \{\dots, -12, -9, -6, -3, 0, 3, 6, 9, 12, \dots\}$, and Q = number of quarks, A = number of antiquarks, with $Q \geq 1$ and $A \geq 1$.

But (24) is equivalent to:

$$\mathbf{Q} \equiv \mathbf{A} \pmod{3} \quad (25)$$

(\mathbf{Q} is congruent to \mathbf{A} modulo 3), and also $\mathbf{Q} \geq 1$ and $\mathbf{A} \geq 1$.

12 Quark-antiquark combinations

Let's note by $q = \text{quark} \in \{\text{Up, Down, Top, Bottom, Strange, Charm}\}$, and by $a = \text{antiquark} \in \{\text{Up, Down, Top, Bottom, Strange, Charm}\}$.

Hence, for combinations of n quarks and antiquarks, $n \geq 2$, prevailing the colorless, we have the following possibilities:

- if $n = 2$, we have: qa (biquark — for example the mesons and antimesons);
- if $n = 3$, we have qqq, aaa (triquark — for example the baryons and antibaryons);
- if $n = 4$, we have $qqaa$ (tetraquark);
- if $n = 5$, we have $qqqqa, aaaaq$ (pentaquark);
- if $n = 6$, we have $qqqaaa, qqqqq, aaaaa$ (hexaquark);
- if $n = 7$, we have $qqqqaa, qqaaaa$ (septiquark);
- if $n = 8$, we have $qqqqaaa, qqqqqaa, qqaaaaa$ (octoquark);
- if $n = 9$, we have $qqqqqqq, qqqqqaa, qqaaaaa, aaaaaaa$ (nonaquark);
- if $n = 10$, obtain $qqqqaaaa, qqqqqaa, qqaaaaa$ (decaquark);
- etc.

13 Unmatter combinations

From the above general case we extract the unmatter combinations:

- For combinations of 2 we have: qa (unmatter biquark), (mesons and antimons); the number of all possible unmatter combinations will be $6 \cdot 6 = 36$, but not all of them will bind together.

It is possible to combine an entity with its mirror opposite and still bound them, such as: $u\bar{u}, d\bar{d}, s\bar{s}, c\bar{c}, b\bar{b}$ which form mesons.

It is possible to combine, unmatter + unmatter = unmatter, as in $u\bar{d} + u\bar{s} = u\bar{d}\bar{s}$ (of course if they bind together);

- For combinations of 3 (unmatter triquark) we can not form unmatter since the colorless can not hold.
- For combinations of 4 we have: $qqaa$ (unmatter tetraquark); the number of all possible unmatter combinations will be $6^2 \cdot 6^2 = 1,296$, but not all of them will bind together;

- For combinations of 5 we have: $qqqqa, or aaaaq$ (unmatter pentaquarks); the number of all possible unmatter combinations will be $6^4 \cdot 6 + 6^4 \cdot 6 = 15,552$, but not all of them will bind together;

- For combinations of 6 we have: $qqqaaa$ (unmatter hexaquarks); the number of all possible unmatter combinations will be $6^3 \cdot 6^3 = 46,656$, but not all of them will bind together;

- For combinations of 7 we have: $qqqqaa, qqaaaa$ (unmatter septiquarks); the number of all possible unmatter combinations will be $6^5 \cdot 6^2 + 6^2 \cdot 6^5 = 559,872$, but not all of them will bind together;

- For combinations of 8 we have: $qqqqaaa, qqqqqqa, qaaaaaa$ (unmatter octoquarks); the number of all possible unmatter combinations will be $6^4 \cdot 6^4 + 6^7 \cdot 6^1 + 6^1 \cdot 6^7 = 5,038,848$, but not all of them will bind together;

- For combinations of 9 we have: $qqqqqaaa, qqaaaaa$ (unmatter nonaquarks); the number of all possible unmatter combinations will be $6^6 \cdot 6^3 + 6^3 \cdot 6^6 = 2 \cdot 6^9 = 20,155,392$, but not all of them will bind together;

- For combinations of 10: $qqqqqqaa, qqqqqaaa, qaaaaaaa$ (unmatter decaquarks); the number of all possible unmatter combinations will be $3 \cdot 6^{10} = 181,398,528$, but not all of them will bind together;

— etc.

I wonder if it is possible to make infinitely many combinations of quarks/antiquarks and leptons/antileptons. . . Unmatter can combine with matter and/or antimatter and the result may be any of these three.

Some unmatter could be in the strong force, hence part of hadrons.

14 Unmatter charge

The charge of unmatter may be positive as in the pentaquark Theta-plus, 0 (as in positronium), or negative as in anti-Rho meson, i.e. $u^{\bar{d}}$, (M. Jordan).

15 Containment

I think for the containment of antimatter and unmatter it would be possible to use electromagnetic fields (a container whose walls are electromagnetic fields). But its duration is unknown.

16 Summary and conclusions

It is apparent from these considerations that, in general, both "unmatter" and "unparticles" are non-trivial states that may become possible under conditions that substantially deviate from our current laboratory settings. Unmatter can be thought

as *arbitrary* clusters of ordinary matter and antimatter, unparticles contain *fractional numbers of quanta* per state and carry *arbitrary spin* [6]. They both display a much richer dynamics than conventional SM doublets, for example mesons (quark-antiquark states) or lepton pairs (electron-electron antineutrino). Due to their unusual properties, “unmatter” and “unparticles” are presumed to be highly unstable and may lead to a wide range of symmetry breaking scenarios. In particular, they may violate well established conservation principles such as electric charge, weak isospin and color. Future observational evidence and analytic studies are needed to confirm, expand or falsify these tentative findings.

Submitted on June 26, 2008 / Accepted on July 19, 2008

References

1. Weinberg S. The quantum theory of fields. Volume 1: foundations. Cambridge University Press, London, 1995.
2. Zinn-Justin J. Quantum field theory and critical phenomena. Oxford University Press, Oxford, 2002.
3. Hagiwara K. et al. *Phys. Rev. D*, 2002, v. 66, 010001-1; Nir Y. CP violation and beyond the Standard Model. XXVII SLAC Summer Institute, 1999; Rogalyov R.N. arXiv: hep-ph/0204099.
4. Bigi I.I. and Sanda A.I. CP violation. Cambridge University Press, 2000; Yao W.M. et al. *Journal of Phys. G*, 2006, v. 33(1).
5. Donoghue J.F. et al.. Dynamics of the Standard Model. Cambridge University Press, 1996.
6. Goldfain E. *Chaos, Solitons and Fractals*, 2006, v. 28(4), 913.
7. Goldfain E. *Intern. Journal of Nonlinear Sciences and Numerical Simulation*, 2005, v. 6(3), 223.
8. Goldfain E. *Comm. in Nonlinear Science and Numer. Simulation*, 2008, v. 13, 666.
9. Goldfain E. *Comm. in Nonlinear Science and Numer. Simulation*, 2008, v. 13, 1397.
10. Ballhausen H. et al. *Phys. Lett. B*, 2004, v. 582, 144.
11. Goldfain E. *Chaos, Solitons and Fractals*, 2008, v. 38(4), 928.
12. Goldfain E. *Intern. Journal of Nonlinear Science*, 2007, v. 3(3), 170.
13. Samko S.G. et al. Fractional integrals and derivatives. Theory and applications. Gordon and Breach, New York, 1993.
14. Ryder L. Quantum field theory. Cambridge University Press, 1996.
15. Georgi H. *Phys. Rev. Lett.*, 2007, v. 98, 221601.
16. Georgi H. *Phys. Lett. B*, 2007, v. 650, 275.
17. Cheung K. et al. *Phys. Rev. D*, 2007, v. 76, 055003.
18. Bander M. et al. *Phys. Rev. D*, 2007, v. 76, 115002.
19. Zwicky R. *Phys. Rev. D*, 2008, v. 77, 036004.
20. Kikuchi T. et al. *Phys. Rev. D*, 2008, v. 77, 094012.
21. Goldfain E. A brief note on “un-particle” physics. *Progress in Physics*, 2008, v. 28, v. 3, 93.
22. Smarandache F. A unifying field in logics, neutrosophic logic. Neutrosophy, neutrosophic set, neutrosophic probability. Am. Res. Press, 1998.
23. Smarandache F. Matter, antimatter, and unmatter. CDS-CERN, EXT-2005-142, 2004; *Bulletin of Pure and Applied Sciences*, 2004, v. 23D, no. 2, 173–177.
24. Smarandache F. Verifying unmatter by experiments, more types of unmatter, and a quantum chromodynamics formula. *Progress in Physics*, 2005, v. 2, 113–116; *Infinite Energy*, 2006, v. 12, no. 67, 36–39.
25. Chubb S. Breaking through editorial. *Infinite Energy*, 2005, v. 11, no. 62, 6–7.
26. Carman D.S. Experimental evidence for the pentaquark. *Euro Phys. A*, 2005, v. 24, 15–20.
27. Gray L., Hagerty P., and Kalogeropoulos T.E. Evidence for the existence of a narrow p-barn bound state. *Phys. Rev. Lett.*, 1971, v. 26, 1491–1494.
28. Carrol A.S., Chiang I.-H., Kucia T.F., Li K.K., Mazur P.O., Michael D.N., Mockett P., Rahm D.C., and Rubinstein R. Observation of structure in p-bar p and p-bar d total cross sections below 1.1 GeV/c. *Phys. Rev. Lett.*, 1974, v. 32, 247–250.
29. Kalogeropoulos T.E., Vayaki A., Grammatikakis G., Tsilimigras T., and Simopoulou E. Observation of excessive and direct gamma production in p-bar d annihilations at rest. *Phys. Rev. Lett.*, 1974, v. 33, 1635–1637.
30. Chapiro I.S. *Physics-Uspekhi (Uspekhi Fizicheskikh Nauk)*, 1973, v. 109, 431.
31. Bogdanova L.N., Dalkarov O.D., and Chapiro I.S. Quasinuclear systems of nucleons and antinucleons. *Annals of Physics*, 1974, v. 84, 261–284.
32. Chapiro I.S. New “nuclei” built on nucleons and anti-nucleons. *Nature-USSR*, 1975, no. 12, 68–73.
33. Barmin V.V. et al. (DIANA Collaboration). *Phys. Atom. Nucl.*, 2003, v. 66, 1715.
34. Ostrick M. (SAPHIR Collaboration). *Pentaquark 2003 Workshop*, Newport News, VA, Nov. 6–8, 2003.
35. Smith T.P. Hidden worlds, hunting for quarks in ordinary matter. Princeton University Press, 2003.
36. Wang M.J. (CDF Collaboration). In: *Quarks and Nuclear Physics 2004*, Bloomington, IN, May 23–28, 2004.

The Dark Energy Problem

Michael Harney* and Ioannis Iraklis Haranas†

*841 North 700 West, Pleasant Grove, Utah, 84062, USA

E-mail: michael.harney@signaldisplay.com

†Department of Physics and Astronomy, York University, 314A Petrie Building,
North York, Ontario, M3J-1P3, Canada

E-mail: ioannis@yorku.ca

The proposal for dark energy based on Type Ia Supernovae redshift is examined. It is found that the linear and non-Linear portions in the Hubble Redshift are easily explained by the use of the Hubble Sphere model, where two interacting Hubble spheres sharing a common mass-energy density result in a decrease in energy as a function of distance from the object being viewed. Interpreting the non-linear portion of the redshift curve as a decrease in interacting volume between neighboring Hubble Spheres removes the need for a dark energy.

1 Introduction

The discovery in 1998 of fainter than expected Type Ia supernova resulted in the hypothesis of an apparent acceleration in our expanding universe [1]. Type Ia supernovas have a previously determined standard-candle distance which has shown to be the same as their redshift distance for low z values. However, their fainter brightness at far distances indicate that they are further away than expected when compared with their redshift distance. This lead to the conclusion that the standard candle distance is correct but that there is an apparent acceleration in the expansion of the universe occurring in the range where the Type Ia supernovas were measured. This explanation was designed the preserve the linearity of Hubble's Law while explaining the further distance of the Type Ia supernova. The existence of dark energy, a repulsive gravitational field that is a manifestation of the cosmological constant, was theorized as the likely cause of the acceleration [2]. Experimentalists are now embarking on the task of proving the existence of dark energy with little examination or critical analysis of the cause and effect of the initial observations. We can show that the observed effects of the Type Ia supernova redshift are explainable by another phenomena which satisfies known laws of physics.

2 Assumptions

We begin by making the following assumptions:

Assumption 1: *The gravitational and electromagnetic force ranges are not infinite.*

Although there is as of yet no widely accepted model of unifying the gravitational and electromagnetic (QED) forces, they both follow an inverse-square law and have similar divergence properties so we assume they are fairly equivalent in nature but by no means infinite in range. We assume the gravitational and electromagnetic force ranges have a steep

decline in effect similar to the profile for the strong nuclear force but at a range $= 10^{26}$ meters $= R_u/2$ which BB theorists currently estimate as the radius of the Universe. We will call the sphere that is centered around our point of observation on Earth as our Hubble sphere, and it encompasses what we see out to the radius $R_u/2$ which we assume as the limit of the gravitational and electromagnetic forces. Likewise, objects at a distant d from us on Earth also have a Hubble sphere that is centered on their point of observation.

Assumption 2: *The Universe is bigger than the Hubble sphere and is perhaps infinite.*

When we refer to the Universe we are referring to all space including what lies beyond our Hubble sphere, which we cannot view because light is infinitely redshifted at the boundary of our sphere due to the steep decay of the gravitational and EM forces at a distance $R_u/2$. We currently accept that a decrease in energy between two points can cause a redshift in photons. This explanation should be adequate for the purposes of our discussion on how the apparent redshift-acceleration may be the cause of two overlapping Hubble spheres, each with their own center of observation. This explanation also answers Olber's Paradox in which an infinite Universe would contain so many stars that the darkness of night would be overwhelmed with starlight. The answer to the paradox is that there is no starlight that can reach us beyond our Hubble sphere radius because of the limit of the electromagnetic force range.

Assumption 3: *If one views an object at a distance d from Earth, the light from that object is affected by the mass-energy density of our local Hubble sphere interacting with the mass-energy density of the distant object's Hubble sphere.*

The intersecting volumes of two neighboring Hubble spheres correspond to a common mass-energy density between the spheres that decreases as the distance between the centers of the spheres increases, resulting in less common volume.

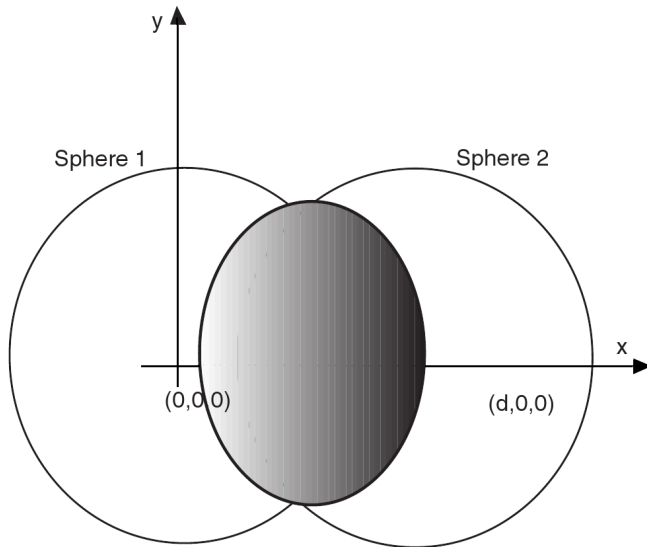


Fig. 1: Hubble sphere's 1 and 2 intersect sharing a volume (shaded gray).

The decrease in common mass-energy density between the spheres results in a redshift of photons emitted from the center of either Hubble sphere to the center of the other Hubble sphere. Regardless of which direction we look, we always see a redshift because there is matter all around the outside of our Hubble sphere that gravitationally attracts the matter inside our Hubble sphere. The Hubble sphere by this account is a three-dimensional Euclidean sphere, which is assumed to have a constant mass-energy density.

3 The common energy of Hubble spheres

If we examine Figure 1, we see the intersection of two Hubble spheres with their centers separated by a distance d . The shaded gray area is the intersecting volume, which also represents common mass-energy between the spheres. The center of sphere 1 can be imagined as our viewpoint from Earth and the center of sphere 2 can be the distant object we are viewing.

From Figure 1 we can find the ratio of intersecting volume between the spheres to the volume in our sphere as:

$$\frac{Volume_{common}}{Volume_{local}} = \frac{\pi(16R_u^3 - 12dR_u^2 + d^3)}{\frac{4}{3}\pi R_u^3} = \frac{3}{48} \left(\frac{d^3}{R_u^3} - 12 \frac{d}{R_u} + 16 \right), \quad (1)$$

where $Volume_{common}$ is the intersecting volume between the spheres and $Volume_{local}$ is the volume of our own sphere.

If we assume homogenous mass-energy throughout both spheres, then the ratio of common mass-energy between the spheres to the energy in our own sphere is proportional to the

ratio of the intersecting volume between the spheres to our sphere's volume. We also know that the mass-energy in a given sphere is proportional to the $h\nu$, so we arrive at:

$$\frac{\nu_2}{\nu_1} = \frac{Volume_{common}}{Volume_{local}} = \frac{3}{48} \left(\frac{d^3}{R_u^3} - 12 \frac{d}{R_u} + 16 \right) = 1 - \frac{3d}{4R_u} + \frac{d^3}{16R_u^3}, \quad (2)$$

The change in frequency $\Delta\nu/\nu_1 = (\nu_2 - \nu_1)/\nu_1$ is the similar to the measured value of z with respect to wavelength λ large, but we now look at it with respect to ν and $\Delta\nu/\nu$ is found to be:

$$\frac{\Delta\nu}{\nu} = -\frac{3d}{4R_u} + \frac{d^3}{16R_u^3}. \quad (3)$$

From (3) we see that the energy viewed from our observation point decreases with the distance d to the object (which is also the distance between the centers of the spheres), and is essentially linear for $d \ll R_u$ where R_u is the radius of each Hubble sphere. This linear decrease in energy is interpreted as an increase in redshift or a linear increase in velocity with distance by Big Bang (BB) theorists and amounts to the linear portion of Hubble's Law. For situations where d gets close to R_u there is a slight increase in energy resulting from the d^3 term in (3), suggesting to the BB theorist that the object being viewed is decelerating and is closer to us than would be expected from the previously linear Hubble slope when $d \ll R_u$.

Instead of accepting a non-linearity in the Hubble curve, BB theorists believe that the curve is still linear and that the shorter distance computed at larger d based on measured wavelength is still correct. The fainter-than-expected brightness of the Type Ia supernova is then a result of an apparent acceleration in the object due to some unknown "dark energy" with a negative gravitational force. In reality, the Hubble Law coincides fairly well with standard candle observations until d approaches R_u , where it then becomes non-linear and produces a result that mimics acceleration of the viewed object, if one still believes that Hubble's Law is linear. The d^3 term in (3) results in an apparent acceleration of the object viewed at larger distances and in fact this acceleration is not a real but instead is a non-linearity in Hubble's Law.

4 Conclusions

The results of the analysis of intersecting Hubble spheres shows that a linear redshift results by assuming that the gravitational and electromagnetic forces have a finite range, R_u . The linear relationship for smaller d explains Hubble's Law without requiring an expansion of the Universe or our own Hubble sphere. The derivation also explains the apparent acceleration of objects as our distance d to them approaches R_u . Therefore, a simpler explanation of a non-expanding Universe exists which to current knowledge is at least the size

of $2R_u$ and possibly much bigger. The Cosmic Microwave Background Radiation (CMBR) has been shown by others to be a result of absorption and scattering of the intergalactic medium [3]. The additional production of Helium and other element ratios is easily found by allowing the Universe as much time as it needs to produce these results in stellar cores. The proposed explanation is a far simpler one than the requirement to balance photon to proton ratios in the theorized early Universe of the Big Bang, with the added concern of an inflationary period to allow smoothness in the CMBR.

Submitted on April 08, 2008

Accepted on June 28, 2008

References

1. Goldhaber G. and Perlmutter S. A study of 42 type Ia supernovae and a resulting measurement of $\Omega(M)$ and $\Omega(\Lambda)$. *Physics-Reports Review Section of Physics Letters*, 1998, v. 307(1-4), 325-331.
2. Peebles P.J.E. and Ratra B. The cosmological constant and Dark Energy. *Reviews of Modern Physics*, 2003, v. 75, 559-606.
3. Lerner Eric J. Radio absorption by the intergalactic medium. *Astrophys. Journal*, 1990, v. 361, 63-68.

Unravelling Lorentz Covariance and the Spacetime Formalism

Reginald T. Cahill

School of Chemistry, Physics and Earth Sciences, Flinders University, Adelaide 5001, Australia

E-mail: Reg.Cahill@flinders.edu.au

We report the discovery of an exact mapping from Galilean time and space coordinates to Minkowski spacetime coordinates, showing that Lorentz covariance and the spacetime construct are consistent with the existence of a dynamical 3-space, and “absolute motion”. We illustrate this mapping first with the standard theory of sound, as vibrations of a medium, which itself may be undergoing fluid motion, and which is covariant under Galilean coordinate transformations. By introducing a different non-physical class of space and time coordinates it may be cast into a form that is covariant under “Lorentz transformations” wherein the speed of sound is now the “invariant speed”. If this latter formalism were taken as fundamental and complete we would be led to the introduction of a pseudo-Riemannian “spacetime” description of sound, with a metric characterised by an “invariant speed of sound”. This analysis is an allegory for the development of 20th century physics, but where the Lorentz covariant Maxwell equations were constructed first, and the Galilean form was later constructed by Hertz, but ignored. It is shown that the Lorentz covariance of the Maxwell equations only occurs because of the use of non-physical space and time coordinates. The use of this class of coordinates has confounded 20th century physics, and resulted in the existence of a “flowing” dynamical 3-space being overlooked. The discovery of the dynamics of this 3-space has led to the derivation of an extended gravity theory as a quantum effect, and confirmed by numerous experiments and observations.

1 Introduction

It is commonly argued that the manifest success of Lorentz covariance and the spacetime formalism in Special Relativity (SR) is inconsistent with the anisotropy of the speed of light, and indeed the existence of absolute motion, that is, a detectable motion relative to an actual dynamical 3-space, despite the repeated experimental detection of such effects over, as we now understand, more than 120 years. This apparent incompatibility between a preferred frame, *viz* a dynamical 3-space, and the spacetime formalism is explicitly resolved by the discovery of an exact mapping from Galilean time and space coordinates to Minkowski spacetime coordinates*, showing that Lorentz covariance and the spacetime construct are indeed consistent with Galilean covariance, but that they suppress any account of an underlying dynamical 3-space.

In the neo-Galilean formalism, known also as the Lorentzian interpretation of SR, length contraction and clock effects are real effects experienced by objects and clocks in motion relative to an actual 3-space, whereas in the Minkowski-Einstein spacetime formalism these effects are transferred to the metric of the mathematical spacetime, and then appear to be merely perspective effects for different observers. Experiments, however, have shown that the Galilean space and time coordinates competently describe reality, whereas the Minkowski-Einstein spacetime construct is merely a mathe-

matical artifact, and that various observable phenomena cannot be described by that formalism. We thus arrive at the dramatic conclusion that the neo-Galilean formalism is the valid description of reality, and that it is a superior more encompassing formalism than the Minkowski-Einstein formalism in terms of both mathematical clarity and ontology.

Physics arrived at the Minkowski-Einstein formalism because of two very significant accidents of history, first that Maxwell’s unification of electric and magnetic phenomena failed to build in the possibility of an actual 3-space, for which the speed of light is only c relative to that space, and not relative to observers in general, and 2nd that the first critical test of the Maxwell EM unification by Michelson using interferometry actually suffered a fundamental design flaw, causing the instrument to be almost 2000 times less sensitive than Michelson had assumed. A related issue is that the Newtonian theory of gravity used an acceleration field for the description of gravitational phenomena, when a velocity field description would have immediately led to a richer description, and for which notions such as “dark matter” and “dark energy” are not needed.

We illustrate the properties of this new mapping first with the standard theory of sound, as vibrations of a medium which itself may be undergoing fluid motion, and which is covariant under Galilean coordinate transformations, which relate the observations by different observers who may be in motion wrt the fluid and wrt one another. Here we show that by introducing a different non-physical class of space and time co-

*See [1] and Damour [2] for discussion of Minkowski’s work.

ordinates, essentially the Minkowski coordinates, the sound vibration dynamics may be cast into a form that is covariant under “Lorentz transformations”, wherein the speed of sound is now the invariant speed. If this latter formalism were taken as fundamental and complete we would be lead to the introduction of a pseudo-Riemannian “spacetime” formalism for sound with a metric characterised by the invariant speed of sound, and where “sound cones” would play a critical role.

This analysis is an allegory for the development of 20th century physics, but where the Lorentz covariant Maxwell equations were constructed first, and the Galilean form was later suggested by Hertz, but ignored. It is shown that the Lorentz covariance of the Maxwell equations only occurs because of the use of degenerate non-physical space and time coordinates. The conclusion is that Lorentz covariance and the spacetime formalism are artifacts of the use of peculiar non-physical space and time coordinates. The use of this class of coordinates has confounded 20th century physics, and lead to the existence of a “flowing” dynamical 3-space being overlooked. The dynamics of this 3-space, when coupled to the new Schrödinger and Dirac equations, has lead to the derivation of an extended gravity theory confirmed by numerous experiments and observations. This analysis also shows that Lorentz symmetry is consistent with the existence of a preferred frame, namely that defined by the dynamical 3-space. This dynamical 3-space has been repeatedly detected over more than 120 years of experiments, but has always been denied because of the obvious success of the Lorentz covariant formalism, where there the Lorentz transformations are characterised by the so-called invariant speed of light. Einstein’s fundamental principle that ‘the speed of light is invariant’ is not literally true, it is only valid if one uses the non-physical space and time coordinates.

As with sound waves, the non-invariance or speed anisotropy of the actual speed of light in vacuum is relatively easy to measure, and is also relatively large, being approximately 1 part in 1000 when measured on earth, with the direction of the “flowing space” known since the 1925/26 experiment by Miller [3]. Successful direct and sufficiently accurate measurements of the one-way speed of light have never been made simply because the speed of light is so fast that accurate timing for laboratory-sized speed measurements are not possible. For that reason indirect measurements have always been used. One of the first was the Michelson interferometer. However a subtlety always arises for indirect measurements — namely that the anisotropy of the speed of light also affects the operation of the experimental apparatus in ways that have not always been apparent. The Michelson interferometer, for example, has a major design flaw that renders it nearly 2000 times less sensitive than believed by Michelson, who used Newtonian physics in calibrating his instrument. It was only in 2002 [5, 6] that the correct calibration of the Michelson interferometer was derived, and analysis of the non-null fringe shift data from that Michelson-Morley 1887 experiment was

analysed and shown to reveal a “flowing space” with a speed in excess of 300km/s. The 2002 analysis [5, 6] showed that the presence of a gas in the Michelson interferometer was a key component of its operation — for in vacuum mode the instrument is totally defective as a detector of light speed anisotropy. This is merely because different unrelated effects just happen to cancel when the Michelson interferometer is used in vacuum mode — a simple design flaw that at least Michelson could not have known about. It so happens that having a gas in the light paths causes this cancellation to be incomplete. The sensitivity of the instrument varies as $n - 1$, where n is the refractive index. For gases this calibration factor is very small — for air at STP $n - 1 = 0.00029$, whereas Michelson, using Newtonian physics, used a calibration coefficient of value 1. However if we use optical fibers in place of air $n - 1 \approx 0.5$, and the detector is some 2000 times more sensitive, and the use of such detectors has lead to the detailed characterisation of turbulence in the 3-space flow — essentially gravitational waves*.

There are now four different experimental techniques for detecting light speed anisotropy: (1) gas-mode Michelson interferometer [3, 4, 7–10], (2) one-way RF speed in coaxial cables [11–13], (3) optical fiber interferometer [14, 15], and (4) doppler-shift effects in earth-flyby of spacecraft [16]. These consistent light-speed anisotropy experiments reveal earth rotation and orbit effects, and sub-mHz gravitational waves. The detection of gravitational wave effects, it now turns out, dates back to the pioneering work of Michelson and Morley in 1887 [4], as discussed in [20], and detected again by Miller [3] also using a gas-mode Michelson interferometer, and by Torr and Kolen [11], DeWitte [12] and Cahill [13] using RF waves in coaxial cables, and by Cahill [14] and Cahill and Stokes [15] using an optical-fiber interferometer design, and also present in the spacecraft flyby doppler shifts [16].

2 Sound wave Galilean covariant formalism

Let us first use the example of sound waves to discuss the mapping from Galilean space and time coordinates to Minkowski-Einstein spacetime coordinates — as in this case the underlying physics is well understood. The standard formulation for sound waves in a moving fluid is

$$\left(\frac{\partial}{\partial t} + \mathbf{v}(\mathbf{r}, t) \cdot \nabla \right)^2 \phi(\mathbf{r}, t) = c^2 \nabla^2 \phi(\mathbf{r}, t), \quad (1)$$

where $\nabla = \left\{ \frac{\partial}{\partial x}, \frac{\partial}{\partial y}, \frac{\partial}{\partial z} \right\}$. The physical time coordinate t and Euclidean space coordinates $\mathbf{r} = \{x, y, z\}$ are used by

*The design flaw of the vacuum-mode Michelson interferometer has been repeated in the large and expensive terrestrial gravitational wave detectors such as LIGO, and also in the vacuum-mode resonant cavity interferometers [17]. These cavity experiments are based on two mistaken notions: (i) that a breakdown of Lorentz symmetry is related to the existence of a preferred frame, and (ii) that vacuum-mode Michelson interferometers can detect a light speed anisotropy associated with such a preferred frame.

an observer O to label the readings of a clock and the location in space where the “wind” or “fluid flow” has velocity $\mathbf{v}(\mathbf{r}, t)$, and small pressure variations $\phi(\mathbf{r}, t)$, relative to the background pressure. Clearly the “fluid flow” and “pressure fluctuations” are different aspects of the same underlying phenomena — namely the dynamics of some macroscopic system of atoms and/or molecules, but separated into very low frequency effects, — the flow, and high frequency effects, — the sound waves. The dynamics for the flow velocity $\mathbf{v}(\mathbf{r}, t)$ is not discussed here. As well the symbol c is the speed of sound waves relative to the fluid. In (1) the coordinates $\{t, x, y, z\}$ ensure that the dynamical flow \mathbf{v} is correctly related to the pressure fluctuation ϕ , at the same time and space. Whenever we separate some unified phenomenon into two or more related phenomena we must introduce a “coordinate system” that keeps track of the connection. To demonstrate this we find plane-wave solutions of (1) for the case where the fluid flow velocity is time and space independent, *viz* uniform,

$$\phi(\mathbf{r}, t) = A \sin(\mathbf{k} \cdot \mathbf{r} - \omega t), \quad (2)$$

$$\omega(\mathbf{k}, \mathbf{v}) = c|\vec{\mathbf{k}}| + \mathbf{v} \cdot \mathbf{k}. \quad (3)$$

The sound wave group velocity is then

$$\mathbf{v}_g = \vec{\nabla}_k \omega(\mathbf{k}, \mathbf{v}) = c\hat{\mathbf{k}} + \mathbf{v}, \quad (4)$$

and we see that the wave has velocity \mathbf{v}_g relative to the observer, with the fluid flowing at velocity \mathbf{v} also relative to the observer, and so the speed of sound is c in direction $\hat{\mathbf{k}}$ relative to the fluid itself. This corresponds to a well known effect, namely that sound travels slower up-wind than down-wind. This “sound speed anisotropy” effect can be measured by means of one-way sound travel times, or indirectly by means of doppler shifts for sound waves reflected from a distant object separated by a known distance from the observer.

Next consider two observers, O and O' , in relative motion. Then the physical time and space coordinates of each are related by the Galilean transformation

$$\begin{aligned} t' &= t, \\ x' &= x - Vt, \quad y' = y, \quad z' = z. \end{aligned} \quad (5)$$

We have taken the simplest case where V is the relative speed of the two observers in their common x directions. Then the derivatives are related by

$$\begin{aligned} \frac{\partial}{\partial t} &= \frac{\partial}{\partial t'} - V \frac{\partial}{\partial x}, \\ \frac{\partial}{\partial x} &= \frac{\partial}{\partial x'}, \quad \frac{\partial}{\partial y} = \frac{\partial}{\partial y'}, \quad \frac{\partial}{\partial z} = \frac{\partial}{\partial z'}. \end{aligned} \quad (6)$$

Then (1) becomes for the 2nd observer, with $v' = v - V$,

$$\left(\frac{\partial}{\partial t'} + \mathbf{v}'(\mathbf{r}', t') \cdot \nabla' \right)^2 \phi'(\mathbf{r}', t') = c^2 \nabla'^2 \phi'(\mathbf{r}', t'). \quad (7)$$

For sound waves $\phi'(\mathbf{r}', t') = \phi(\mathbf{r}, t)$. If the flow velocity $\mathbf{v}(\mathbf{r}, t)$ is not uniform then we obtain refraction effects for the

sound waves. Only for an observer at rest in a time independent and uniform fluid does v' disappear from (7).

3 Sound wave Lorentz covariant formalism

The above Galilean formalism for sound waves is well known and uses physically sensible choices for the time and space coordinates. Of course we could choose to use spherical or cylindrical space coordinates if we so desired. This would cause no confusion. However we could also choose to use a new class of time and space coordinates, indicated by upper-case symbols T, X, Y, Z , that mixes the above time and space coordinates. One such new class of coordinates is

$$\begin{aligned} T &= \gamma(v) \left(\left(1 - \frac{v^2}{c^2} \right) t + \frac{vx}{c^2} \right), \\ X &= \gamma(v)x; \quad Y = y; \quad Z = z, \end{aligned} \quad (8)$$

where $\gamma(v) = 1/\sqrt{1 - v^2/c^2}$. Note that this is not a Lorentz transformation. The transformations for the derivatives are then found to be

$$\begin{aligned} \frac{\partial}{\partial t} &= \gamma(v) \left(1 - \frac{v^2}{c^2} \right) \frac{\partial}{\partial T}, \\ \frac{\partial}{\partial x} &= \gamma(v) \left(\frac{v}{c^2} \frac{\partial}{\partial T} + \frac{\partial}{\partial X} \right), \quad \frac{\partial}{\partial y} = \frac{\partial}{\partial Y}, \quad \frac{\partial}{\partial z} = \frac{\partial}{\partial Z}. \end{aligned} \quad (9)$$

We define $\bar{\nabla} = \left\{ \frac{\partial}{\partial X}, \frac{\partial}{\partial Y}, \frac{\partial}{\partial Z} \right\}$. Then (1) becomes, for uniform v ,

$$\left(\frac{\partial}{\partial T} \right)^2 \bar{\phi}(\mathbf{R}, T) = c^2 \bar{\nabla}^2 \bar{\phi}(\mathbf{R}, T), \quad (10)$$

with $\mathbf{R} = \{X, Y, Z\}$ and $\bar{\phi}(\mathbf{R}, T) = \phi(\mathbf{r}, t)$. This is a remarkable result. In the new class of coordinates the dynamical equation no longer contains the flow velocity \mathbf{v} — it has been mapped out of the dynamics. Eqn.(10) is now covariant under Lorentz transformations*,

$$\begin{aligned} T' &= \gamma(V) \left(T + \frac{VX}{c^2} \right), \\ X' &= \gamma(V)(X - VT), \quad Y' = Y, \quad Z' = Z, \end{aligned} \quad (11)$$

where we have taken the simplest case, and where V is a measure of the relative speed of the two observers in their common X directions.

There is now no reference to the underlying flowing fluid system — for an observer using this class of space and time coordinates the speed of sound relative to the observer is always c and so invariant — there will be no sound speed anisotropy. We could also introduce a “spacetime” construct with pseudo-Riemannian metric $ds^2 = c^2 dT^2 - d\mathbf{R}^2$,

*Lorentz did not construct the “Lorentz transformation” — and this nomenclature is very misleading as Lorentz held to a different interpretation of the so-called relativistic effects.

and sound cones along which $ds^2 = 0$. As well pairs of spacetime events could be classified into either time-like or space-like, with the time ordering of spacelike events not being uniquely defined.

However this sound-speed invariance is purely an artifact of the non-physical space and time coordinates introduced in (8). The non-physical nature of this inferred “invariance” would have been easily exposed by doing measurements of the speed of sound in different directions. However in a bizarre imaginary world the Lorentz-covariant sound formalism could have been discovered first, and the spacetime formalism might have been developed and become an entrenched belief system. If later experiments had revealed that the speed of sound was actually anisotropic then the experimentalist involved might have been applauded, or, even more bizarrely, their discoveries denied and suppressed, and further experiments stopped by various means. The overwhelming evidence is that this bizarre possibility is precisely what happened for electromagnetics, for Maxwell essentially introduced the Lorentz covariant electromagnetism formalism, and experiments that detected the light speed anisotropy.

4 Dynamical 3-space theory

Here we briefly review the dynamics of the 3-space that is the analogue of the “flowing fluid” in the sound allegory. For zero vorticity we have [19–21]

$$\begin{aligned} \nabla \cdot \left(\frac{\partial \mathbf{v}}{\partial t} + (\mathbf{v} \cdot \nabla) \mathbf{v} \right) + \frac{\alpha}{8} ((\text{tr} D)^2 - \text{tr}(D^2)) &= -4\pi G\rho, \\ \nabla \times \mathbf{v} &= \mathbf{0}, \quad D_{ij} = \frac{1}{2} \left(\frac{\partial v_i}{\partial x_j} + \frac{\partial v_j}{\partial x_i} \right), \end{aligned} \quad (12)$$

where $\rho(\mathbf{r}, t)$ is the matter and EM energy densities expressed as an effective matter density. Experiment and astrophysical data has shown that $\alpha \approx 1/137$ is the fine structure constant to within observational errors [19–22]. For a quantum system with mass m the Schrödinger equation must be generalised [22] with the new terms required to maintain that the motion is intrinsically wrt to the 3-space and that the time evolution is unitary

$$\begin{aligned} i\hbar \frac{\partial \psi(\mathbf{r}, t)}{\partial t} &= \\ &= -\frac{\hbar^2}{2m} \nabla^2 \psi(\mathbf{r}, t) - i\hbar \left(\mathbf{v} \cdot \nabla + \frac{1}{2} \nabla \cdot \mathbf{v} \right) \psi(\mathbf{r}, t). \end{aligned} \quad (13)$$

The space and time coordinates $\{t, x, y, z\}$ in (12) and (13) ensure that the separation of a deeper and unified process into different classes of phenomena — here a dynamical 3-space and a quantum system, is properly tracked and connected. As well the same coordinates may be used by an observer to also track the different phenomena. However it is important to realise that these coordinates have no ontological significance — they are not real. Nevertheless it is imperative not to use a degenerate system of coordinates that suppresses

the description of actual phenomena. The velocities \mathbf{v} have no ontological or absolute meaning relative to this coordinate system — that is in fact how one arrives at the form in (12), and so the “flow” is always relative to the internal dynamics of the 3-space. So now this is different to the example of sound waves.

A wave packet propagation analysis gives the acceleration induced by wave refraction to be [22]

$$\mathbf{g} = \frac{\partial \mathbf{v}}{\partial t} + (\mathbf{v} \cdot \nabla) \mathbf{v} + (\nabla \times \mathbf{v}) \times \mathbf{v}_R, \quad (14)$$

$$\mathbf{v}_R(\mathbf{r}_0(t), t) = \mathbf{v}_0(t) - \mathbf{v}(\mathbf{r}_0(t), t), \quad (15)$$

is the velocity of the wave packet relative to the 3-space, where \mathbf{v}_0 and \mathbf{r}_0 are the velocity and position relative to the observer, and the last term in (14) generates the Lense-Thirring effect as a vorticity driven effect. Together (12) and (14) amount to the derivation of gravity as a quantum effect, explaining both the equivalence principle (\mathbf{g} in (14) is independent of m) and the Lense-Thirring effect. Overall we see, on ignoring vorticity effects, that

$$\nabla \cdot \mathbf{g} = -4\pi G\rho - \frac{\alpha}{8} ((\text{tr} D)^2 - \text{tr}(D^2)), \quad (16)$$

which is Newtonian gravity but with the extra dynamical term whose strength is given by α . This new dynamical effect explains the spiral galaxy flat rotation curves (and so doing away with the need for “dark matter”), the bore hole g anomalies, the black hole “mass spectrum”. Eqn.(12), even when $\rho = 0$, has an expanding universe Hubble solution that fits the recent supernovae data in a parameter-free manner without requiring “dark matter” nor “dark energy”, and without the accelerating expansion artifact [21]. However (16) cannot be entirely expressed in terms of \mathbf{g} because the fundamental dynamical variable is \mathbf{v} . The role of (16) is to reveal that if we analyse gravitational phenomena we will usually find that the matter density ρ is insufficient to account for the observed \mathbf{g} . Until recently this failure of Newtonian gravity has been explained away as being caused by some unknown and undetected “dark matter” density. Eqn.(16) shows that to the contrary it is a dynamical property of 3-space itself.

Another common misunderstanding is that the success of the Dirac equation implies that a preferred frame cannot exist. This belief is again easily demolished. The generalised Dirac equation which uses the Galilean class of space-time coordinates is

$$i\hbar \frac{\partial \psi}{\partial t} = -i\hbar \left(c\vec{\alpha} \cdot \nabla + \mathbf{v} \cdot \nabla + \frac{1}{2} \nabla \cdot \mathbf{v} \right) \psi + \beta mc^2 \psi, \quad (17)$$

where $\vec{\alpha}$ and β are the usual Dirac matrices. This equation shows that the Dirac spinor propagates wrt to the 3-space, and that there are dynamical effects associated with that that are not in the generalised Schrödinger equation (13). As shown elsewhere (17) gives rise to relativistic gravitational effects*, that go beyond those in (14).

*Meaning when an object has speed comparable to c wrt the 3-space.

5 Galilean covariant electromagnetic theory

Hertz in 1890 [18] noted that Maxwell had overlooked the velocity field that accompanies time derivatives, as in (1), and presented an improved formalism, and the minimal source-free form is

$$\begin{aligned} \mu \left(\frac{\partial}{\partial t} + \mathbf{v} \cdot \nabla \right) \mathbf{H} &= -\nabla \times \mathbf{E}, \\ \epsilon \left(\frac{\partial}{\partial t} + \mathbf{v} \cdot \nabla \right) \mathbf{E} &= +\nabla \times \mathbf{H}, \\ \nabla \cdot \mathbf{H} &= \mathbf{0}, \quad \nabla \cdot \mathbf{E} = \mathbf{0}, \end{aligned} \quad (18)$$

with $\mathbf{v}(\mathbf{r}, t)$ being the dynamical 3-space velocity field as measured* by some observer using time and space coordinates $\{t, x, y, z\}$, although Hertz did not consider a time and space dependent \mathbf{v} . Again for uniform and time-independent \mathbf{v} (18) has plane wave solutions

$$\mathbf{E}(\mathbf{r}, t) = \mathbf{E}_0 e^{i(\mathbf{k} \cdot \mathbf{r} - \omega t)}, \quad \mathbf{H}(\mathbf{r}, t) = \mathbf{H}_0 e^{i(\mathbf{k} \cdot \mathbf{r} - \omega t)}, \quad (19)$$

$$\omega(\mathbf{k}, \mathbf{v}) = c|\vec{\mathbf{k}}| + \mathbf{v} \cdot \mathbf{k}, \quad \text{where } c = 1/\sqrt{\mu\epsilon}. \quad (20)$$

Then the EM group velocity is

$$\mathbf{v}_{EM} = \vec{\nabla}_{\mathbf{k}} \omega(\mathbf{k}, \mathbf{v}) = c\hat{\mathbf{k}} + \mathbf{v}. \quad (21)$$

So, like the analogy of sound, the velocity of EM radiation \mathbf{v}_{EM} has magnitude c only with respect to the 3-space, and in general not with respect to the observer if the observer is moving through that 3-space, as experiment has indicated again and again, as discussed above. Eqns.(18) give, for uniform \mathbf{v} ,

$$\begin{aligned} \left(\frac{\partial}{\partial t} + \mathbf{v} \cdot \nabla \right)^2 \mathbf{E} &= c^2 \nabla^2 \mathbf{E}, \\ \left(\frac{\partial}{\partial t} + \mathbf{v} \cdot \nabla \right)^2 \mathbf{H} &= c^2 \nabla^2 \mathbf{H}. \end{aligned} \quad (22)$$

on using the identity $\nabla \times (\nabla \times \mathbf{E}) = -\nabla^2 \mathbf{E} + \nabla(\nabla \cdot \mathbf{E})$ and $\nabla \cdot \mathbf{E} = 0$, and similarly for the \mathbf{H} field. Transforming to the Minkowski-Einstein T, X, Y, Z coordinates using (8) and (9) we obtain the form of the source-free “standard” Maxwell equations

$$\frac{\partial^2 \mathbf{E}}{\partial T^2} = c^2 \nabla^2 \mathbf{E}, \quad \frac{\partial^2 \mathbf{H}}{\partial T^2} = c^2 \nabla^2 \mathbf{H}, \quad (23)$$

which is again covariant under Lorentz transformation (11). It is important to emphasize that the transformation from the Galilean covariant Hertz-Maxwell equations (18) to the Lorentz covariant Maxwell equations (23) is *exact*. It is usually argued that the Galilean transformations (5) are the non-relativistic limit of the Lorentz transformations (11). While this is technically so, as seen by taking the limit $v/c \rightarrow 0$, this

*Earth based light speed anisotropy experiments show that v has value $\approx 420 \pm 30$ km/s in a known direction [20], and is not to be confused with the CMB velocity.

misses the key point that they are related by the new mapping in (8). Also we note that for the Galilean space-time class the speed of light is anisotropic, while it is isotropic for the Minkowski-Einstein space-time class. It is only experiment that can decide which of the two classes of coordinates is the more valid space-time coordinate system. As noted above, and since 1887, experiments have detected that the speed of light is indeed anisotropic.

Again when using the Minkowski-Einstein coordinates there is now no reference to the underlying dynamical 3-space system — for an observer using this class of space and time coordinates the speed of light relative to the observer is always c and so invariant. We could then be tricked into introducing a “spacetime” construct with pseudo-Riemannian metric $ds^2 = c^2 dT^2 - d\mathbf{R}^2$, and light cones along which $ds^2 = 0$. As well pairs of spacetime events could be classified into either time-like or space-like, with the time ordering of spacelike events not being uniquely defined. This loss of the notion of simultaneity is merely a consequence of the degenerate nature of the Minkowski-Einstein spacetime coordinates. This has confounded progress in physics for more than a century.

Hence the Minkowski-Einstein space-time coordinates are degenerate in that they map out the existence of the dynamical 3-space. So the development of 20th century physics has been misled by two immensely significant “accidents”, 1st that Maxwell failed to include the velocity \mathbf{v} , and the 2nd that the Michelson interferometer in gas-mode is some 2000 times less sensitive than Michelson had assumed, and that the observed fringe shifts actually indicate a large value for v in excess of 300km/s. These two accidents stopped physics from discovering the existence of a dynamical 3-space, until recently, and that the dynamical 3-space displays wave effects. Also again this transformation between the two classes of space-time coordinates explicitly demonstrates that “Lorentz covariance” coexists with a preferred frame, contrary to the aims of the experiments in [17]. Furthermore vacuum-mode Michelson interferometers, such as the vacuum cavity resonators, cannot even detect the long-standing light speed anisotropy. We can apply the inverse mapping, from the Minkowski-Einstein class to the Galilean class of coordinates, but in doing so we have lost the value of the velocity field. In this sense the Minkowski-Einstein class is degenerate — it cannot be used to analyse light speed anisotropy experiments for example.

6 Conclusions

We have reported herein the discovery of an exact and invertible mapping from Galilean time and space coordinates to Minkowski-Einstein spacetime coordinates. This mapping removes the effects of the velocity of the dynamical 3-space relative to an observer, and so in this sense the Minkowski-Einstein coordinates are degenerate — they stop the usual

Special Relativity formalism from being able to say anything about the existence of a preferred frame, a real 3-space, and from describing experiments that have detected light speed anisotropy. The Minkowski-Einstein formalism has nevertheless been very successful in describing other effects. The spacetime formalism, with its spacetime metric and Lorentz covariance, is really an artifact of the degenerate Minkowski-Einstein coordinates, and we have shown how one may unravel these mathematical artifacts, and display the underlying dynamics. The new mapping shows that relativistic effects are caused by motion relative to an actual 3-space — and which has been observed for more than 120 years. This was Lorentz's proposition. The belief that spacetime actually described reality has led to numerous misconceptions about the nature of space and time. These are distinct phenomena, and are not fused into some 4-dimensional entity. Indeed time is now seen to have a cosmic significance, and that all observers can measure that time — for by measuring their local absolute speed relative to their local 3-space they can correct the ticking rate of their clocks to remove the local time dilation effect, and so arrive at a measure of the ticking rate of cosmic time*. This changes completely how we might consider modelling deeper reality — one such proposition is *Process Physics* [19–21].

The Special Relativity formalism asserts that only relative descriptions of phenomena between two or more observers have any meaning. In fact we now understand that all effects are dynamically and observationally relative to an ontologically real, that is, detectable dynamical 3-space. Ironically this situation has always been known as an “absolute effect”. The most extraordinary outcome of recent discoveries is that a dynamical 3-space exists, and that from the beginning of Physics this has been missed — that a most fundamental aspect of reality has been completely overlooked.

Submitted on July 10, 2008 / Accepted on August 06, 2008

References

- Minkowski H. *Raum und Zeit. Physikalische Zeitschrift*, 1909, 10, 104–115. English translation in *The Principle of Relativity* by Lorentz H.A., Einstein A., Minkowski H. and Weyl H., translated by Perrett W. and Jeffery G.B., Dover, New York, 1952.
- Damour T. What is missing from Minkowski's “Raum und Zeit” Lecture?. arXiv: 0807.1300.
- Miller D.C. *Rev. Mod. Phys.*, 1933, v. 5, 203–242.
- Michelson A.A. and Morley E.W. *Am. J. Sc.*, 1887, v. 34, 333–345.
- Cahill R.T. and Kitto K. Michelson-Morley experiments revisited. *Apeiron*, 2003, v. 10(2), 104–117.
- Cahill R.T. The Michelson and Morley 1887 experiment and the discovery of absolute motion. *Progress in Physics*, 2005, v. 3, 25–29.
- Illingworth K.K. *Phys. Rev.*, 1927, v. 3, 692–696.
- Joos G. *Ann. d. Physik*, 1930, v. 7, 385.
- Jaseja T.S. et al. *Phys. Rev. A*, 1964, v. 133, 1221.
- Munera H.A., et al. In *Proceedings of SPIE*, v. 6664, K1–K8, 2007, eds. Roychoudhuri C. et al.
- Torr D.G. and Kolen P. In: *Precision Measurements and Fundamental Constants*, Taylor B.N. and Phillips W.D. eds. *Natl. Bur. Stand. (U.S.), Spec. Pub.*, 1984, v. 617, 675.
- Cahill R.T. *The Roland DeWitte 1991 experiment. Progress in Physics*, 2006, v. 3, 60–65.
- Cahill R.T. A new light-speed anisotropy experiment: absolute motion and gravitational waves detected. *Progress in Physics*, 2006, v. 4, 73–92.
- Cahill R.T. Optical-fiber gravitational wave detector: dynamical 3-space turbulence detected. *Progress in Physics*, 2007, v. 4, 63–68.
- Cahill R.T. and Stokes F. Correlated detection of sub-MHz gravitational waves by two optical-fiber interferometers. *Progress in Physics*, 2008, v. 2, 103–110.
- Cahill R.T. Resolving spacecraft Earth-fly anomalies with measured light speed anisotropy. *Progress in Physics*, 2008, v. 3, 9–15.
- Braxmaier C. et al. *Phys. Rev. Lett.*, 2002, v. 88, 010401; Müller H. et al. *Phys. Rev. D*, 2003, v. 68, 116006-1-17; Müller H. et al. *Phys. Rev. D*, 2003, v. 67, 056006; Wolf P. et al. *Phys. Rev. D*, 2004, v. 70, 051902-1-4; Wolf P. et al. *Phys. Rev. Lett.*, 2003, v. 90, 060402; Lipa J.A., et al. *Phys. Rev. Lett.*, v. 90, 060403.
- Hertz H. On the fundamental equations of electromagnetics for bodies in motion. *Wiedemann's Ann.*, 1890, v. 41, 369; Electric waves, collection of scientific papers. Dover Pub., New York, 1962.
- Cahill R.T. Process physics: from information theory to quantum space and matter. Nova Science Pub., New York, 2005.
- Cahill R.T. Dynamical 3-space: a review. arXiv: 0705.4146.
- Cahill R.T. A quantum cosmology: no dark matter, dark energy nor accelerating Universe. arXiv: 0709.2909.
- Cahill R.T. Dynamical fractal 3-space and the generalised Schrödinger equation: Equivalence Principle and vorticity effects. *Progress in Physics*, 2006, v. 1, 27–34.

*Uncorrected Earth-based clocks lose approximately 0.085s per day compared to cosmic time, because $v \approx 420$ km/s.

Derivation of the Newton's Law of Gravitation Based on a Fluid Mechanical Singularity Model of Particles

Xiao-Song Wang

E-mail: wangxs1999@yahoo.com

The main purpose of this paper is to seek a mechanical interpretation of gravitational phenomena. We suppose that the universe may be filled with a kind of fluid which may be called the $\Omega(0)$ substratum. Thus, the inverse-square law of gravitation is derived by methods of hydrodynamics based on a sink flow model of particles. The first feature of this theory of gravitation is that the gravitational interactions are transmitted by a kind of fluidic medium. The second feature is the time dependence of gravitational constant G and gravitational mass. The Newton's law of gravitation is arrived if we introduce an assumption that G and the masses of particles are changing so slowly that they can be treated as constants.

1 Introduction

The Newton's law of gravitation can be written as

$$\mathbf{F}_{12} = -G \frac{m_1 m_2}{r^2} \hat{\mathbf{r}}_{21}, \quad (1)$$

where m_1 and m_2 are the masses of two particles, r is the distance between the two particles, G is the gravitational constant, \mathbf{F}_{12} is the force exerted on the particle with mass m_2 by the particle with mass m_1 , $\hat{\mathbf{r}}_{21}$ denotes the unit vector directed outward along the line from the particle with mass m_1 to the particle with mass m_2 .

The main purpose of this paper is to derive the Newton's law of gravitation by means of fluid mechanics based on sink flow model of particles.

The motive of this paper is to seek a mechanism of gravitational phenomena. The reasons why new models of gravity are interesting may be summarized as follows.

Firstly, there exists some astronomical phenomena that could not be interpreted by the present theories of gravitation, for instance, the Titius-Bode law [1]. New theories of gravity may view these problems from new angles.

Secondly, whether the gravitational constant G depends on time and space is still unknown [2–8]. It is known that the gravitational constant G is a constant in the Newton's theory of gravitation and in theory of general relativity.

Thirdly, the mechanism of the action-at-a-distance gravitation remains an unsolved problem in physics for more than 300 years [9–11]. Although theory of general relativity is a field theory of gravity [12], the concept of field is different from that of continuum mechanics [13–16] because of the absence of a continuum in theory of general relativity. Thus, theory of general relativity can only be regarded as a phenomenological theory of gravity.

Fourthly, we do not have a satisfactory quantum theory of gravity presently [17–21]. One of the challenges in theoretic-

all physics is to reconcile quantum theory and theory of general relativity [17, 22]. New theories of gravity may open new ways to solve this problem.

Fifthly, one of the puzzles in physics is the problem of dark matter and dark energy [23–31]. New theories of gravity may provide new methods to attack this problem [24, 25].

Finally, we do not have a successful unified field theory presently. Great progress has been made towards an unification of the four fundamental interactions in the universe in the 20th century. However, gravitation is still not unified successfully. New theories of gravity may shed some light on this puzzle.

To conclude, it seems that new considerations on gravitation is needed. It is worthy keeping an open mind with respect to all the theories of gravity before the above problems been solved.

Now let us briefly review the long history of mechanical interpretations of gravitational phenomena. Many philosophers and scientists, such as Laozi [32], Thales, Anaximenes, believed that everything in the universe is made of a kind of fundamental substance [9]. Descartes was the first to bring the concept of aether into science by suggesting that it has mechanical properties [9]. Since the Newton's law of gravitation was published in 1687 [33], this action-at-a-distance theory was criticized by the French Cartesian [9]. Newton admitted that his law did not touch on the mechanism of gravitation [34]. He tried to obtain a derivation of his law based on Descartes' scientific research program [33]. Newton himself even suggested an explanation of gravity based on the action of an aetherial medium pervading the space [34, 35]. Euler attempted to explain gravity based on some hypotheses of a fluidic aether [9].

In a remarkable paper published in 1905, Einstein abandoned the concept of aether [36]. However, Einstein's assertion did not cease the explorations of aether [9, 37–46]. Einstein changed his view later and introduced his new con-

cept of ether [47, 48]. I regret to admit that it is impossible for me to mention all the works related to this field in history. Adolphe Martin and Roy Keys [49–51] proposed a fluidic cosmic gas model of vacuum to explain the physical phenomena such as electromagnetism, gravitation, quantum mechanics and the structure of elementary particles.

Inspired by the aforementioned thoughts and others [52–56], we show that the Newton's law of gravitation is derived based on the assumption that all the particles are made of singularities of a kind of ideal fluid.

During the preparation of the manuscript, I noticed that John C. Taylor had proposed an idea that the inverse-square law of gravitation may be explained based on the concept of source or sink [65].

2 Forces acting on sources and sinks in ideal fluids

The purpose of this section is to calculate the forces between sources and sinks in inviscid incompressible fluids which is called ideal fluids usually.

Suppose the velocity field \mathbf{u} of an ideal fluid is irrotational, then we have [16, 54–59],

$$\mathbf{u} = \nabla \phi, \quad (2)$$

where ϕ is the velocity potential, $\nabla = \mathbf{i} \frac{\partial}{\partial x} + \mathbf{j} \frac{\partial}{\partial y} + \mathbf{k} \frac{\partial}{\partial z}$ is the Hamilton operator.

It is known that the equation of mass conservation of an ideal fluid becomes Laplace's equation [54–59],

$$\nabla^2 \phi = 0, \quad (3)$$

where ϕ is velocity potential, $\nabla^2 = \frac{\partial^2}{\partial x^2} + \frac{\partial^2}{\partial y^2} + \frac{\partial^2}{\partial z^2}$ is the Laplace operator.

Using spherical coordinates (r, θ, φ) , a general form of solution of Laplace's equation (3) can be obtained by separation of variables as [56]

$$\phi(r, \theta) = \sum_{l=0}^{\infty} \left(A_l r^l + \frac{B_l}{r^{l+1}} \right) P_l(\cos \theta), \quad (4)$$

where A_l and B_l are arbitrary constants, $P_l(x)$ are Legendre's function of the first kind which is defined as

$$P_l(x) = \frac{1}{2^l l!} \frac{d^l}{dx^l} (x^2 - 1)^l. \quad (5)$$

If there exists a velocity field which is continuous and finite at all points of the space, with the exception of individual isolated points, then these isolated points are called singularities usually.

Definition 1 Suppose there exists a singularity at point $P_0 = (x_0, y_0, z_0)$. If the velocity field of the singularity at point $P = (x, y, z)$ is

$$\mathbf{u}(x, y, z, t) = \frac{Q}{4\pi r^2} \hat{\mathbf{r}}, \quad (6)$$

where $r = \sqrt{(x - x_0)^2 + (y - y_0)^2 + (z - z_0)^2}$, $\hat{\mathbf{r}}$ denotes the unit vector directed outward along the line from the singularity to the point $P = (x, y, z)$, then we call this singularity a source if $Q > 0$ or a sink if $Q < 0$. Q is called the strength of the source or sink.

Suppose a static point source with strength Q locates at the origin $(0, 0, 0)$. In order to calculate the volume leaving the source per unit time, we may enclose the source with an arbitrary spherical surface S with radius a . A calculation shows that

$$\oint_S \mathbf{u} \cdot \mathbf{n} dS = \oint_S \frac{Q}{4\pi a^2} \hat{\mathbf{r}} \cdot \mathbf{n} dS = Q, \quad (7)$$

where \mathbf{n} denotes the unit vector directed outward along the line from the origin of the coordinates to the field point (x, y, z) . Equation (7) shows that the strength Q of a source or sink evaluates the volume of the fluid leaving or entering a control surface per unit time.

From (4), we see that the velocity potential $\phi(r, \theta)$ of a source or sink is a solution of Laplace's equation $\nabla^2 \phi = 0$.

Theorem 2 Suppose (1) there exists an ideal fluid (2) the ideal fluid is irrotational and barotropic, (3) the density ρ is homogeneous, that is $\partial \rho / \partial x = \partial \rho / \partial y = \partial \rho / \partial z = \partial \rho / \partial t = 0$, (4) there are no external body forces exerted on the fluid, (5) the fluid is unbounded and the velocity of the fluid at the infinity is approaching to zero. Suppose a source or sink is stationary and is immersed in the ideal fluid. Then, there is a force

$$\mathbf{F}_Q = -\rho Q \mathbf{u}_0 \quad (8)$$

exerted on the source by the fluid, where ρ is the density of the fluid, Q is the strength of the source or the sink, \mathbf{u}_0 is the velocity of the fluid at the location of the source induced by all means other than the source itself.

Proof Only the proof of the case of a source is needed. Let us select the coordinates that is attached to the static fluid at the infinity.

We set the origin of the coordinates at the location of the source. We surround the source by an arbitrary small spherical surface S . The surface S is centered at the origin of the coordinates with radius r . The outward unit normal to the surface S is denoted by \mathbf{n} . Let $\tau(t)$ denotes the mass system of fluid enclosed in the volume between the surface S and the source at time t . Let \mathbf{F}_Q denotes the hydrodynamic force exerted on the source by the mass system τ , then a reaction of this force must act on the the fluid enclosed in the mass system τ . Let \mathbf{F}_S denotes the hydrodynamic force exerted on the mass system τ due to the pressure distribution on the surface S , \mathbf{K} denotes momentum of the mass system τ .

As an application of the Newton's second law of motion to the mass system τ , we have

$$\frac{D\mathbf{K}}{Dt} = -\mathbf{F}_Q + \mathbf{F}_S, \quad (9)$$

where D/Dt represents the material derivative in the lagrangian system [16, 54–59]. The expressions of the momentum \mathbf{K} and the force \mathbf{F}_S are

$$\mathbf{K} = \iiint_{\tau} \rho \mathbf{u} dV, \quad \mathbf{F}_S = \oint_S (-p) \mathbf{n} dS, \quad (10)$$

where the first integral is volume integral, the second integral is surface integral, \mathbf{n} denotes the unit vector directed outward along the line from the origin of the coordinates to the field point (x, y, z) .

Since the velocity field is irrotational, we have the following relation

$$\mathbf{u} = \nabla \phi, \quad (11)$$

where ϕ is the velocity potential.

According to Ostrogradsky–Gauss theorem (see, for instance, [54–56, 58, 59]), we have

$$\iiint_{\tau} \rho \mathbf{u} dV = \iiint_{\tau} \rho \nabla \phi dV = \oint_S \rho \phi \mathbf{n} dS. \quad (12)$$

Note that the mass system τ does not include the singularity at the origin. According to Reynolds’ transport theorem [54–56, 58, 59], we have

$$\frac{D}{Dt} \iiint_{\tau} \rho \mathbf{u} dV = \frac{\partial}{\partial t} \iiint_V \rho \mathbf{u} dV + \oint_S \rho \mathbf{u} (\mathbf{u} \cdot \mathbf{n}) dS, \quad (13)$$

where V is the volume fixed in space which coincide with the mass system $\tau(t)$ at time t , that is $V = \tau(t)$.

Then, using (13), (10) and (12), we have

$$\frac{D\mathbf{K}}{Dt} = \oint_S \rho \frac{\partial \phi}{\partial t} \mathbf{n} dS + \oint_S \rho \mathbf{u} (\mathbf{u} \cdot \mathbf{n}) dS. \quad (14)$$

According to Lagrange–Cauchy integral [54–56, 58, 59], we have

$$\frac{\partial \phi}{\partial t} + \frac{(\nabla \phi)^2}{2} + \frac{p}{\rho} = f(t), \quad (15)$$

where $f(t)$ is an arbitrary function of time t . Since the velocity \mathbf{u} of the fluid at the infinity is approaching to zero, and noticing (4), $\phi(t)$ must be of the following form

$$\phi(r, \theta, t) = \sum_{l=0}^{\infty} \frac{B_l(t)}{r^{l+1}} P_l(\cos \theta), \quad (16)$$

where $B_l(t), l \geq 0$ are functions of time t . Thus, we have the following estimations at the infinity of the velocity field

$$\phi = O\left(\frac{1}{r}\right), \quad \frac{\partial \phi}{\partial t} = O\left(\frac{1}{r}\right), \quad r \rightarrow \infty, \quad (17)$$

where $\varphi(x) = O(\psi(x)), x \rightarrow a$ stands for $\overline{\lim}_{x \rightarrow a} |\varphi(x)| / \psi(x) = k, (0 \leq k < +\infty)$.

Applying (15) at the infinity and using (17), we have $|\mathbf{u}| \rightarrow 0, \partial \phi / \partial t \rightarrow 0$ and $p = p_{\infty}$, where p_{∞} is a constant. Thus, $f(t) = p_{\infty} / \rho$. Therefore, according to (15), we have

$$p = p_{\infty} - \rho \frac{\partial \phi}{\partial t} - \frac{\rho (\mathbf{u} \cdot \mathbf{u})}{2}. \quad (18)$$

Using (10) and (18), we have

$$\mathbf{F}_S = \oint_S \rho \frac{\partial \phi}{\partial t} \mathbf{n} dS + \oint_S \frac{\rho (\mathbf{u} \cdot \mathbf{u}) \mathbf{n}}{2} dS. \quad (19)$$

Using (9), (14), (19), we have

$$\mathbf{F}_Q = \oint_S \left[\frac{1}{2} \rho (\mathbf{u} \cdot \mathbf{u}) \mathbf{n} - \rho \mathbf{u} (\mathbf{u} \cdot \mathbf{n}) \right] dS. \quad (20)$$

Now let us calculate this velocity \mathbf{u} in order to obtain \mathbf{F}_Q . Since the velocity field induced by the source Q is (6), then according to the superposition principle of velocity field of ideal fluids, the velocity on the surface S is

$$\mathbf{u} = \frac{Q}{4\pi r^2} \mathbf{n} + \mathbf{u}_0, \quad (21)$$

where \mathbf{n} denotes the unit vector directed outward along the line from the origin of the coordinates to the field point (x, y, z) . Using (20) and (21), we have

$$\mathbf{F}_Q = \rho \oint_S \left[-\frac{Q^2}{32\pi^2 r^4} \mathbf{n} + \frac{1}{2} (\mathbf{u}_0 \cdot \mathbf{u}_0) \mathbf{n} - \frac{Q}{4\pi r^2} \mathbf{u}_0 - (\mathbf{u}_0 \cdot \mathbf{n}) \mathbf{u}_0 \right] dS. \quad (22)$$

Since the radius r can be arbitrarily small, the velocity \mathbf{u}_0 can be treated as a constant in the integral of (22). Thus, (22) turns out to be

$$\mathbf{F}_Q = -\rho \oint_S \frac{Q}{4\pi r^2} \mathbf{u}_0 dS. \quad (23)$$

Since again \mathbf{u}_0 can be treated as a constant, (23) turns out to be (8). This completes the proof. \square

Remark Lagally [52], Landweber and Yih [53, 54], Faber [55] and Currie [56] obtained the same result of Theorem 2 for the special case where the velocity field is steady.

Theorem 2 only considers the situation that the sources or sinks are at rest. Now let us consider the case that the sources or sinks are moving in the fluid.

Theorem 3 Suppose the presuppositions (1), (2), (3), (4) and (5) in Theorem 2 are valid and a source or a sink is moving in the fluid with a velocity \mathbf{v}_s , then there is a force

$$\mathbf{F}_Q = -\rho Q (\mathbf{u}_f - \mathbf{v}_s) \quad (24)$$

is exerted on the source by the fluid, where ρ is the density of the fluid, Q is the strength of the source or the sink, \mathbf{u}_f is the

velocity of the fluid at the location of the source induced by all means other than the source itself.

Proof The velocity of the fluid relative to the source at the location of the source is $\mathbf{u}_f - \mathbf{v}_s$. Let us select the coordinates that is attached to the source and set the origin of the coordinates at the location of the source. Then (24) can be arrived following the same procedures in the proof of Theorem 2. \square

Applying Theorem 3 to the situation that a source or sink is exposed to the velocity field of another source or sink, we have:

Corollary 4 Suppose the presuppositions (1), (2), (3), (4) and (5) in Theorem 2 are valid and a source or a sink with strength Q_2 is exposed to the velocity field of another source or sink with strength Q_1 , then the force \mathbf{F}_{21} exerted on the singularity with strength Q_2 by the velocity field of the singularity with strength Q_1 is

$$\mathbf{F}_{21} = -\rho Q_2 \frac{Q_1}{4\pi r^2} \hat{\mathbf{r}}_{21} + \rho Q_2 \mathbf{v}_2, \quad (25)$$

where $\hat{\mathbf{r}}_{21}$ denotes the unit vector directed outward along the line from the singularity with strength Q_1 to the singularity with strength Q_2 , r is the distance between the two singularities, \mathbf{v}_2 is the velocity of the source with strength Q_2 .

3 Derivation of inverse-square-law of gravitation

Since quantum theory shows that vacuum is not empty and has physical effects, e.g., the Casimir effect [45, 60–62], it is valuable to probe vacuum by introducing the following hypotheses:

Assumption 5 Suppose the universe is filled by an ideal fluid named $\Omega(0)$ substratum; the ideal fluid fulfil the conditions (2), (3), (4), (5) in Theorem 2.

This fluid may be named $\Omega(0)$ substratum in order to distinguish with Cartesian aether. Following Einstein, Infeld and Hoffmann, who introduced the idea that particles may be looked as singularities in fields [63, 64], and noticing (25), it is nature to introduce the following:

Assumption 6 All the microscopic particles were made up of a kind of elementary sinks of $\Omega(0)$ substratum. These elementary sinks were created simultaneously. The initial masses and the strengths of the elementary sinks are the same.

We may call these elementary sinks as monads.

Suppose a particle with mass m is composed of N monads. Then, according to Assumption 6, we have:

$$m_0(t) = m_0(0) + \rho q_0 t, \quad (26)$$

$$Q = -Nq_0, \quad m(t) = Nm_0(t) = -\frac{Q}{q_0} m_0(t), \quad (27)$$

$$\frac{dm_0}{dt} = \rho q_0, \quad \frac{dm}{dt} = -\rho Q, \quad (28)$$

where $m_0(t)$ is the mass of monad at time t , $-q_0(q_0 > 0)$ is the strength of a monad, $m(t)$ is the mass of a particle at time

t , Q is the strength of the particle, N is the number of monads that make up the particle, ρ is the density of the $\Omega(0)$ substratum, $t \geq 0$.

From (28), we see that the mass m_0 of a monad is increasing since q_0 evaluates the volume of the $\Omega(0)$ substratum fluid entering the monad per unit time. From (28), we also see that the mass of a monad or a particle is increasing linearly.

Based on Assumption 5 and Assumption 6, the motion of a particle is determined by:

Theorem 7 The equation of motion of a particle is

$$m(t) \frac{d\mathbf{v}}{dt} = \frac{\rho q_0}{m_0(t)} m(t) \mathbf{u} - \frac{\rho q_0}{m_0(t)} m(t) \mathbf{v} + \mathbf{F}, \quad (29)$$

where $m_0(t)$ is the mass of monad at time t , $-q_0$ is the strength of a monad, $m(t)$ is the mass of a particle at time t , \mathbf{v} is the velocity of the particle, \mathbf{u} is the velocity of the $\Omega(0)$ substratum at the location of the particle induced by all means other than the particle itself, \mathbf{F} denotes other forces.

Proof Applying the Newton's second law and Theorem 3 to this particle, we have $m d\mathbf{v}/dt = -\rho Q (\mathbf{u} - \mathbf{v}) + \mathbf{F}$. Noticing (27), we get (29). \square

Formula (29) shows that there exists a universal damping force

$$\mathbf{F}_d = -\frac{\rho q_0}{m_0} m \mathbf{v} \quad (30)$$

exerted on each particle.

Now let us consider a system consists of two particles. Based on Assumption 6, applying Theorem 7 to this system, we have:

Corollary 8 Suppose there is a system consists of two particles and there are no other forces exerted on the particles, then the equations of motion of this system are

$$m_1 \frac{d\mathbf{v}_1}{dt} = -\frac{\rho q_0}{m_0} m_1 \mathbf{v}_1 - \frac{\rho q_0^2}{4\pi m_0^2} \frac{m_1 m_2}{r^2} \hat{\mathbf{r}}_{12} \quad (31)$$

$$m_2 \frac{d\mathbf{v}_2}{dt} = -\frac{\rho q_0}{m_0} m_2 \mathbf{v}_2 - \frac{\rho q_0^2}{4\pi m_0^2} \frac{m_1 m_2}{r^2} \hat{\mathbf{r}}_{21}, \quad (32)$$

where $m_{i=1,2}$ is the mass of the particles, $\mathbf{v}_{i=1,2}$ is the velocity of the particles, m_0 is the mass of a monad, $-q_0$ is the strength of a monad, ρ is the density of the $\Omega(0)$ substratum, $\hat{\mathbf{r}}_{12}$ denotes the unit vector directed outward along the line from the particle with mass $m_2(t)$ to the particle with mass $m_1(t)$, $\hat{\mathbf{r}}_{21}$ denotes the unit vector directed outward along the line from the particle with mass $m_1(t)$ to the particle with mass $m_2(t)$.

Ignoring the damping forces in (32), we have:

Corollary 9 Suppose (1) $\mathbf{v}_{i=1,2} \ll \mathbf{u}_{i=1,2}$, where \mathbf{v}_i is the velocity of the particle with mass m_i , \mathbf{u}_i is the velocity of the $\Omega(0)$ substratum at the location of the particle with mass m_i induced by the other particle, (2) there are no other forces exerted on the particles, then the force $\mathbf{F}_{21}(t)$ exerted on the

particle with mass $m_2(t)$ by the velocity field of $\Omega(0)$ substratum induced by the particle with mass $m_1(t)$ is

$$\mathbf{F}_{21}(t) = -G(t) \frac{m_1(t) m_2(t)}{r^2} \hat{\mathbf{r}}_{21}, \quad (33)$$

where $G = \rho q_0^2 / (4\pi m_0^2(t))$, $\hat{\mathbf{r}}_{21}$ denotes the unit vector directed outward along the line from the particle with mass $m_1(t)$ to the particle with mass $m_2(t)$, r is the distance between the two particles.

Corollary 9 is coincide with the Newton's inverse-square-law of gravitation (1) except for two differences. The first difference is that $m_{i=1,2}$ are constants in the Newton's law (1) while in (1) while in Corollary are functions of time t . The second difference is that G is a t . The second difference is that G is a constant in the Newton's

Let us now introduce an assumption that G and the masses of particles are changing so slowly relative to the time scale of human beings that they can be treated as constants approximately. Thus, the Newton's law (1) of gravitation may be considered as a result of Corollary 9 based on this assumption.

4 Superposition principle of gravitational field

The definition of gravitational field \mathbf{g} of a particle with mass m is $\mathbf{g} = \mathbf{F}/m_{test}$, where m_{test} is the mass of a test point mass, \mathbf{F} is the gravitational force exerted on the test point mass by the gravitational field of the particle with mass m . Based on Theorem 7 and Corollary 9, we have

$$\mathbf{g} = \frac{\rho q_0}{m_0} \mathbf{u}, \quad (34)$$

where ρ is the density of the $\Omega(0)$ substratum, m_0 is the mass of a monad, q_0 is the strength of a monad, \mathbf{u} is the velocity of the $\Omega(0)$ substratum at the location of the test point mass induced by the particle mass m . From (34), we see that the superposition principle of gravitational field is deduced from the superposition theorem of the velocity field of ideal fluids.

5 Time dependence of gravitational constant G and mass

According to Assumption 6 and Corollary 9, we have we have

$$G = \frac{\rho q_0^2}{4\pi m_0^2(t)}, \quad (35)$$

where $m_0(t)$ is the mass of monad at time t , $-q_0$ is the strength of a monad, ρ is the density of the $\Omega(0)$ substratum. The time dependence of gravitational mass can be seen from (35) and (28).

6 Conclusion

We suppose that the universe may be filled with a kind of fluid which may be called the $\Omega(0)$ substratum. Thus, the inverse-

square law of gravitation is derived by methods of hydrodynamics based on a sink flow model of particles. There are two features of this theory of gravitation. The first feature is that the gravitational interactions are transmitted by a kind of fluidic medium. The second feature is the time dependence of gravitational constant and gravitational mass. The Newton's law of gravitation is arrived if we introduce an assumption that G and the masses of particles are changing so slowly that they can be treated as constants. As a byproduct, it is shown that there exists a universal damping force exerted on each particle.

Acknowledgements

I am grateful to Robert L. Oldershaw for informing me his researches in the field of Self-Similar Cosmological Paradigm (SSCP) and discrete fractal cosmological models during the preparation of the manuscript. I wish to express my thanks to Dr. Roy Keys for providing me three interesting articles [49–51].

Submitted on July 24, 2008
Accepted on August 06, 2008

References

1. Nietro M. M. The Titius-Bode Law of planetary distances: its history and theory. Pergamon Press, New York, 1972.
2. Gilvarry J. J. and Muller P. M. *Phys. Rev. Lett.*, 1972, v. 28, 1665.
3. Tomaschitz R. *Astrophysics and Space Science*, 2000, v. 271, 181.
4. Gaztanaga E. et al. *Phys. Rev. D*, 2001, v. 65, 023506.
5. Copi C. J. et al. *Phys. Rev. Lett.*, 2004, v. 92, 171301.
6. Khoury J. and Weltman A. *Phys. Rev. Lett.*, 2004, v. 93, 171104.
7. Nagata R. et al. *Phys. Rev. D*, 2004, v. 69, 083512.
8. Biesiada M. and Malec B. *Mon. Not. R. Astron. Soc.*, 2004, v. 350, 644.
9. Whittaker E. A history of the theories of aether and electricity. Thomas Nelson and Sons Ltd., London, 1953.
10. Hesse M. B. Forces and fields: the concept of action at a distance in the history of physics. Thomas Nelson and Sons Ltd, London, 1961.
11. Jaakkola T. *Apeiron*, 1996, v. 3, 61.
12. Fock V. The theory of space, time and gravitation. Translated by N. Kemmer, Pergamon Press, London, 1959.
13. Truesdell C. The elements of continuum mechanics. Springer-Verlag, New York, 1966.
14. Fung Y. C. A first course in continuum mechanics. Prentice-Hall, London, 1977.
15. Eringen A. C. The elements of continuum mechanics. Robert E. Krieger Pub. Co., Huntington, 1980.
16. Landau L. D. and Lifshitz E. M. Fluid mechanics. Translated from the Russian by J.B. Sykes and W.H. Reid. Pergamon, New York, 1987.

17. Carlip S. *Rep. Prog. Phys.*, 2001, v. 64, 885.
18. Amelino-Camelia G. *Modern Phys. Lett. A*, 2002, v. 17, 899.
19. Ahluwalia D. V. *Modern Phys. Lett. A*, 2002, v. 17, 1135.
20. Mitrofanov I. G. *Nature*, 2003, v. 426, 139.
21. Christian J. *Phys. Rev. D*, 2005, v. 71, 024012 .
22. Collins J. et al. *Phys. Rev. Lett.*, 2004, v. 93, 191301.
23. Ellis J. *Philos. Trans. R. Soc. London, A*, 2003, v. 361, 2607.
24. Linder E. V. *Phys. Rev. D*, 2004, v. 70, 023511.
25. Bernardeau F. *Rep. Prog. Phys.*, 2003, v. 66, 691.
26. Bergstrom L. et al. *Phys. Rev. Lett.*, 2005, v. 94, 131301 .
27. Beacom J. F. et al. *Phys. Rev. Lett.*, 2005, v. 94, 171301.
28. Akerib D. S. et al. *Phys. Rev. Lett.*, 2006, v. 96, 011302 .
29. Feng J. L. et al. *Phys. Rev. Lett.*, 2006, v. 96, 151802.
30. P. Fayet G. S. and Hooper D. *Phys. Rev. Lett.*, 2006, v. 96, 211302 .
31. Carena M. et al. *Phys. Rev. Lett.*, 2006, v. 97, 051801.
32. Laozi Tao Te King: in seven languages. Farkas Lorinc Imre Pub., transl. Stephen Mitchell et al., 1995.
33. Newton I. *Mathematical principles of natural philosophy and the system of the world*. Univ. of Calif. Press, Berkeley, 1962.
34. Cohen I. B. *The Newtonian revolution*. Cambridge University Press, 1980.
35. Newton I. *Optics*. Bell London, 1931.
36. Einstein A. *Ann. Phys.*, 1905, v. 17, 891.
37. Vigier J. P. *Lettere al Nuovo Cimento*, 1980, v. 29, 467.
38. Barut A. *Found. Phys.*, 1988, v. 18, 95.
39. Oldershaw R. L. *Int. J. of Theor. Phys.*, 1989, v. 28, 669 .
40. Oldershaw R. L. *Int. J. of Theor. Phys.*, 1989, v. 28, 1503 .
41. Carvalho M. et al. *Found. of Phys. Lett.*, 2003, v. 16, 255.
42. Arminjon M. *Int. J. of Modern Phys. A*, 2002, v. 17, 4203.
43. Carvalho M. and Oliveira A. L. *Found. Phys. Lett.*, 2003, v. 16, 255.
44. Jacobson T. *Phys. Rev. D*, 2004, v. 70, 024003.
45. Davies P. C. W. *J. Opt. B: Quantum Semiclass. Opt.*, 2005, v. 7, S40.
46. Levin M. and Wen X.-G. *Phys. Rev. B*, 2006, v. 73, 035122.
47. Einstein A. *Aether and the theory of relativity*. 1920. Translated in *Sidelights on Relativity*, Dover, 1983.
48. Kostro L. *Einstein and the ether*. Apeiron, 2000.
49. Martin A. *Gravitation in a gaseous ether*. In: *Einstein and Poincaré: the physical vacuum*, Valeri V. Dvoeglazov ed., Apeiron, Montreal, 2005.
50. Martin A. *The electron as an extended structure in cosmic gas*. In: *What is the Electron?* Volodimir Simulik ed., Apeiron, Montreal, 2005.
51. Martin A. and Keys C. *The ether revisited*. In: *Frontiers of Fundamental Physics*, Volodimir Simulik ed., Plenum, New York, 1994.
52. Lagally M. Z. *Angew. Math. Mech.*, 1922, v. 2, 409 .
53. Landweber L. and Yih C.-S. *J. Fluid Mech.*, 1956, v. 1, 319.
54. Yih C.-S. *Fluid mechanics*. McGraw-Hill Book Company, New York, 1969.
55. Faber T. E. *Fluid dynamics for physicists*. Cambridge University Press, Cambridge, 1995.
56. Currie I. G. *Fundamental mechanics of fluids*. Cambridge University Press, 2003, 3rd ed.
57. Lamb H. *Hydrodynamics*. Cambridge University Press, 1932, 6th ed.
58. Kochin N. E. et al. *Theoretical hydrodynamics*. Translated from the fifth Russian ed., Interscience Publishers, New York, 1964.
59. Wu W.-Y. *Fluid mechanics*. Vol. 1. In Chinese, Beijing University Press, Beijing, 1982.
60. Lamoreaux S. K. *Rep. Prog. Phys.*, 2005, v. 68, 201.
61. Intravaia F. and Lambrecht A. *Phys. Rev. Lett.*, 2005, v. 94, 110404.
62. Guo J. G. and Zhao Y. P. *Journal of Microelectromechanical Systems*, 2004, v. 13, 1027.
63. Einstein A. et al. *Ann. Math.*, 1938, v. 39, 65.
64. Einstein A. and Infeld L. *Ann. Math.*, 1940, v. 41, 455.
65. Taylor John C. *Hidden unity in Nature's laws*. Appendix A. Cambridge University Press, 2001.

A Method of Successive Approximations in the Framework of the Geometrized Lagrange Formalism

Grigory I. Garas'ko

*Department of Physics, Scientific Research Institute of
Hyper Complex Systems in Geometry and Physics
Zavodskoy proezd 3, Frjazino, Moscow Region 141190, Russia*

E-mail: gri9z@mail.ru

It is shown that in the weak field approximation the new geometrical approach can lead to the linear field equations for the several independent fields. For the stronger fields and in the second order approximation the field equations become non-linear, and the fields become dependent. This breaks the superposition principle for every separate field and produces the interaction between different fields. The unification of the gravitational and electromagnetic field theories is performed in frames of the geometrical approach in the pseudo-Riemannian space and in the curved Berwald-Moor space.

1 Introduction

In paper [1] the new (geometrical) approach was suggested for the field theory. It is applicable for any Finsler space [2] for which in any point of the main space x^1, x^2, \dots, x^n the indicatrix volume $(V_{ind}(x^1, x^2, \dots, x^n))_{ev}$ can be defined, provided the tangent space is Euclidean. Then the action I for the fields present in the metric function of the Finsler space is defined within the accuracy of a constant factor as a volume of a certain n -dimensional region V :

$$I = \text{const} \cdot \int_V^{(n)} \frac{dx^1 dx^2 \dots dx^n}{(V_{ind}(x^1, x^2, \dots, x^n))_{ev}}. \quad (1)$$

Thus, the field Lagrangian is defined in the following way

$$L = \text{const} \cdot \frac{1}{(V_{ind}(x^1, x^2, \dots, x^n))_{ev}}. \quad (2)$$

In papers [3,4] the spaces conformally connected with the Minkowski space and with the Berwald-Moor space were regarded. These spaces have a single scalar field for which the field equation was written and the particular solutions were found for the spherical symmetry and for the rhombododecaedron symmetry of the space.

The present paper is a continuation of those papers dealing with the study and development of the geometric field theory.

2 Pseudo-Riemannian space with the signature (+ - - -)

Let us consider the pseudo-Riemannian space with the signature (+ - - -) and select the Minkowski metric tensor $\overset{\circ}{g}_{ij}$ in the metric tensor $g_{ij}(x)$, of this space explicitly

$$g_{ij}(x) = \overset{\circ}{g}_{ij} + h_{ij}(x). \quad (3)$$

Let us suppose that the field $h_{ij}(x)$ is weak, that is

$$|h_{ij}(x)| \ll 1. \quad (4)$$

According to [1], the Lagrangian for a pseudo-Riemannian space with the signature (+ - - -) is equal to

$$L = \sqrt{-\det(g_{ij})}. \quad (5)$$

Let us calculate the value of $[-\det(g_{ij})]$ within the accuracy of $|h_{ij}(x)|^2$:

$$-\det(g_{ij}) \simeq 1 + L_1 + L_2, \quad (6)$$

$$L_1 = \overset{\circ}{g}^{ij} h_{ij} \equiv h_{00} - h_{11} - h_{22} - h_{33}, \quad (7)$$

$$L_2 = -h_{00}(h_{11} + h_{22} + h_{33}) + h_{11}h_{22} + h_{11}h_{33} + h_{22}h_{33} - h_{12}^2 - h_{13}^2 - h_{23}^2 + h_{03}^2 + h_{02}^2 + h_{01}^2. \quad (8)$$

The last formula can be rewritten in a more convenient way

$$L_2 = - \left| \begin{array}{cc} h_{00} & h_{01} \\ h_{01} & h_{11} \end{array} \right| - \left| \begin{array}{cc} h_{00} & h_{02} \\ h_{02} & h_{22} \end{array} \right| - \left| \begin{array}{cc} h_{00} & h_{03} \\ h_{03} & h_{33} \end{array} \right| + \left| \begin{array}{cc} h_{11} & h_{12} \\ h_{12} & h_{22} \end{array} \right| + \left| \begin{array}{cc} h_{11} & h_{13} \\ h_{13} & h_{33} \end{array} \right| + \left| \begin{array}{cc} h_{22} & h_{23} \\ h_{23} & h_{33} \end{array} \right|, \quad (9)$$

then

$$L \simeq 1 + \frac{1}{2}L_1 + \frac{1}{2} \left[L_2 - \frac{1}{4}L_1^2 \right]. \quad (10)$$

To obtain the field equations in the first order approximation, one should use the Lagrangian L_1 , and to do the same in the second order approximation — the Lagrangian $(L_1 + L_2 - \frac{1}{4}L_1^2)$.

3 Scalar field

For the single scalar field $\varphi(x)$ the simplest representation of tensor $h_{ij}(x)$ has the form:

$$h_{ij}(x) \equiv h_{ij}^{(\varphi)}(x) = \pm \frac{\partial \varphi}{\partial x^i} \frac{\partial \varphi}{\partial x^j}. \quad (11)$$

That is why

$$L_\varphi = \sqrt{-\det(g_{ij})} = \sqrt{1 \pm L_1} \simeq 1 \pm \frac{1}{2} L_1 - \frac{1}{8} L_1^2, \quad (12)$$

where

$$L_1 = \left(\frac{\partial \varphi}{\partial x^0} \right)^2 - \left(\frac{\partial \varphi}{\partial x^1} \right)^2 - \left(\frac{\partial \varphi}{\partial x^2} \right)^2 - \left(\frac{\partial \varphi}{\partial x^3} \right)^2. \quad (13)$$

In the first order approximation, we can use the Lagrangian L_1 to obtain the following field equation

$$\frac{\partial^2 \varphi}{\partial x^0 \partial x^0} - \frac{\partial^2 \varphi}{\partial x^1 \partial x^1} - \frac{\partial^2 \varphi}{\partial x^2 \partial x^2} - \frac{\partial^2 \varphi}{\partial x^3 \partial x^3} = 0, \quad (14)$$

which presents the wave equation. The stationary field that depends only on the radius

$$r = \sqrt{(x^1)^2 + (x^2)^2 + (x^3)^2}, \quad (15)$$

will satisfy the equation

$$\frac{d}{dr} \left(r^2 \frac{d\varphi}{dr} \right) = 0, \quad (16)$$

the integration of which gives

$$\frac{d\varphi}{dr} = -C_1 \frac{1}{r^2} \Rightarrow \varphi(r) = C_0 + C_1 \frac{1}{r}. \quad (17)$$

In the second order approximation one should use the Lagrangian $(L_1 - \frac{1}{4} L_1^2)$ to obtain the field equation in the second order approximation

$$\overset{\circ}{g}{}^{ij} \frac{\partial}{\partial x^i} \left[\left(\pm 1 - \frac{1}{2} L_1 \right) \frac{\partial \varphi}{\partial x^j} \right] = 0; \quad (18)$$

this equation is already non-linear.

The strict field equation for the tensor $h_{ij}(x)$ (11) is

$$\overset{\circ}{g}{}^{ij} \frac{\partial}{\partial x^i} \left(\frac{\frac{\partial \varphi}{\partial x^j}}{\sqrt{1 \pm L_1}} \right) = 0, \quad (19)$$

then the stationary field depending only on the radius must satisfy the equation

$$\frac{d}{dr} \left(r^2 \frac{\frac{d\varphi}{dr}}{\sqrt{1 \mp \left(\frac{d\varphi}{dr} \right)^2}} \right) = 0. \quad (20)$$

Integrating it, we get

$$\begin{aligned} \frac{d\varphi}{dr} &= -\frac{C_1}{\sqrt{r^4 \pm C_1^2}} \Rightarrow \\ \Rightarrow \varphi(r) &= C_0 + \int_r^\infty \frac{C_1}{\sqrt{r^4 \pm C_1^2}} dr. \end{aligned} \quad (21)$$

The field with the upper sign and the field with the lower sign differ qualitatively: the upper sign “+” in Eq. (11) gives a finite field with no singularity in the whole space, the lower sign “-” in Eq. (11) gives a field defined everywhere but for the spherical region

$$0 \leq r \leq \sqrt{|C_1|}, \quad (22)$$

in which there is no field, while

$$r > \sqrt{|C_1|}, r \rightarrow \sqrt{|C_1|} \Rightarrow \frac{d\varphi}{dr} \rightarrow -C_1 \cdot \infty. \quad (23)$$

At the same time in the infinity ($r \rightarrow \infty$) both solutions $\varphi_\pm(r)$ behave as the solution of the wave equation Eq. (17).

If we know the Lagrangian, we can write the energy-momentum tensor T_j^i for the these solutions and calculate the energy of the system derived by the light speed c :

$$P_0 = \text{const} \int^{(3)} T_0^0 dV. \quad (24)$$

To obtain the stationary spherically symmetric solutions, we get

$$T_0^0 = -\frac{r^2}{\sqrt{r^4 \pm C_1^2}}, \quad (25)$$

that is why for both upper and lower signs $P_0 \rightarrow \infty$.

The metric tensor of Eq. (3,11) is the simplest way to “insert” the gravity field into the Minkowski space — the initial flat space containing no fields. Adding several such terms as in Eq. (11) to the metric tensor, we can describe more and more complicated fields by tensor $h_{ij} = h_{ij}^{(grav)}$.

4 Covariant vector field

To construct the twice covariant symmetric tensor $h_{ij}(x)$ with the help of a covariant field $A_i(x)$ not using the connection objects, pay attention to the fact that the alternated partial derivative of a tensor is a tensor too

$$F_{ij} = \frac{\partial A_j}{\partial x^i} - \frac{\partial A_i}{\partial x^j}, \quad (26)$$

but a skew-symmetric one. Let us construct the symmetric tensor on the base of tensor F_{ij} . To do this, first, form a scalar

$$\begin{aligned} L_A &= \overset{\circ}{g}{}^{ij} \overset{\circ}{g}{}^{km} F_{ik} F_{jm} = \\ &= 2 \overset{\circ}{g}{}^{ij} \overset{\circ}{g}{}^{km} \left(\frac{\partial A_k}{\partial x^i} \frac{\partial A_m}{\partial x^j} - \frac{\partial A_k}{\partial x^i} \frac{\partial A_j}{\partial x^m} \right), \end{aligned} \quad (27)$$

which gives the following expressions for two symmetric tensors

$$h_{ij}^{(1)} = \overset{\circ}{g}{}^{km} \left(2 \frac{\partial A_k}{\partial x^i} \frac{\partial A_m}{\partial x^j} - \frac{\partial A_k}{\partial x^i} \frac{\partial A_j}{\partial x^m} - \frac{\partial A_k}{\partial x^j} \frac{\partial A_i}{\partial x^m} \right), \quad (28)$$

$$h_{ij}^{(2)} = \overset{\circ}{g}{}^{km} \left(2 \frac{\partial A_i}{\partial x^k} \frac{\partial A_j}{\partial x^m} - \frac{\partial A_i}{\partial x^k} \frac{\partial A_m}{\partial x^j} - \frac{\partial A_j}{\partial x^k} \frac{\partial A_m}{\partial x^i} \right). \quad (29)$$

Notice, that not only F_{ij} and L_A but also the tensors $h_{ij}^{(1)}$, $h_{ij}^{(2)}$ are gradient invariant, that is they don't change with transformations

$$A_i \rightarrow A_i + \frac{\partial f(x)}{\partial x^i}, \quad (30)$$

where $f(x)$ is an arbitrary scalar function.

Let

$$h_{ij} \equiv h_{ij}^{(A_k)} = \chi(x) h_{ij}^{(1)} + [1 - \chi(x)] h_{ij}^{(2)}, \quad (31)$$

where $\chi(x)$ is some scalar function. Then in the first order approximation we get

$$L_1 = 2 \overset{\circ}{g}{}^{ij} \overset{\circ}{g}{}^{km} \left(\frac{A_k}{\partial x^i} \frac{\partial A_j}{\partial x^m} \right) \equiv L_A, \quad (32)$$

and the first order approximation for the field $A_i(x)$ gives Maxwell equations

$$\overset{\circ}{g}{}^{ij} \frac{\partial^2}{\partial x^i \partial x^j} A_k - \frac{\partial}{\partial x^k} \left(\overset{\circ}{g}{}^{ij} \frac{\partial A_j}{\partial x^i} \right) = 0. \quad (33)$$

For Lorentz gauge

$$\overset{\circ}{g}{}^{ij} \frac{\partial A_j}{\partial x^i} = 0, \quad (34)$$

the equations Eqs. (33) take the form

$$\square A_k = 0. \quad (35)$$

It is possible that Eq. (31) is not the most general form for tensor h_{ij} which in the first order approximation gives the field equations coinciding with Maxwell equations.

To obtain Maxwell equations not for the free field but for the field with sources $j_i(x)$, one should add to $h_{ij}^{(A_k)}$ Eq. (31) the following tensor

$$h_{ij}^{(j_k)} = \left(\frac{16\pi}{c} \right) \cdot \frac{1}{2} (A_i j_j + A_j j_i). \quad (36)$$

This means that the metric tensor Eq. (3) with tensor

$$h_{ij} = h_{ij}^{(Max)} \equiv h_{ij}^{(A_k)} + h_{ij}^{(j_k)} \quad (37)$$

describes the weak electromagnetic field with source $j_k(x)$. We must bear in mind that we use the geometrical approach to the field theory, and we have to consider $j_k(x)$ to be given and not obtained from the field equations.

So, the metric tensor Eq. (3) with tensor

$$h_{ij} = \mu h_{ij}^{(A_k)} + \gamma h_{ij}^{(grav)}, \quad (38)$$

where μ, γ are the fundamental constants in frames of the unique pseudo-Riemannian geometry describes simultaneously the free electromagnetic field and the free gravitational field. To include the sources, $j_k(x)$, of the electromagnetic field, the metric tensor must either include not only $j_k(x)$ but the partial derivatives of this field too or the field $j_k(x)$ must be expressed by the other fields as shown below.

If the gravity field is "inserted" in the simplest way as shown in the previous section, then the sources of the electromagnetic field can be expressed by the scalar field as follows

$$j_i(x) = q \frac{\partial \varphi}{\partial x^i}. \quad (39)$$

In this case the first order approximation for Lorentz gauge gives

$$\square A_k = \frac{4\pi}{c} j_k, \quad (40)$$

$$\square \varphi = 0. \quad (41)$$

Since the density of the current has the form of Eq. (39), the Eq. (41) gives the continuity equation

$$\overset{\circ}{g}{}^{ij} \frac{\partial j_i}{\partial x^j} = 0. \quad (42)$$

5 Several weak fields

The transition from the weak fields to the strong fields may lead to the transition from the linear equations for the independent fields to the non-linear field equations for the mutually dependent interacting fields $\varphi(x)$ and $\psi(x)$ "including" gravity field in the Minkowski space.

Let

$$h_{ij} = \varepsilon_\varphi \frac{\partial \varphi}{\partial x^i} \frac{\partial \varphi}{\partial x^j} + \varepsilon_\psi \frac{\partial \psi}{\partial x^i} \frac{\partial \psi}{\partial x^j}, \quad (43)$$

where $\varepsilon_\varphi, \varepsilon_\psi$ are independent sign coefficients. Then the strict Lagrangian can be written as follows

$$L_{\varphi, \psi} = \sqrt{1 + L_1 + L_2}, \quad (44)$$

and

$$L_1 = \overset{\circ}{g}{}^{ij} \left(\varepsilon_\varphi \frac{\partial \varphi}{\partial x^i} \frac{\partial \varphi}{\partial x^j} + \varepsilon_\psi \frac{\partial \psi}{\partial x^i} \frac{\partial \psi}{\partial x^j} \right), \quad (45)$$

where

$$L_2 = \varepsilon_\varphi \varepsilon_\psi \left[\begin{aligned} & - \left(\frac{\partial \varphi}{\partial x^0} \frac{\partial \psi}{\partial x^1} - \frac{\partial \varphi}{\partial x^1} \frac{\partial \psi}{\partial x^0} \right)^2 - \\ & - \left(\frac{\partial \varphi}{\partial x^0} \frac{\partial \psi}{\partial x^2} - \frac{\partial \varphi}{\partial x^2} \frac{\partial \psi}{\partial x^0} \right)^2 - \\ & - \left(\frac{\partial \varphi}{\partial x^0} \frac{\partial \psi}{\partial x^3} - \frac{\partial \varphi}{\partial x^3} \frac{\partial \psi}{\partial x^0} \right)^2 + \\ & + \left(\frac{\partial \varphi}{\partial x^1} \frac{\partial \psi}{\partial x^2} - \frac{\partial \varphi}{\partial x^2} \frac{\partial \psi}{\partial x^1} \right)^2 + \\ & + \left(\frac{\partial \varphi}{\partial x^1} \frac{\partial \psi}{\partial x^3} - \frac{\partial \varphi}{\partial x^3} \frac{\partial \psi}{\partial x^1} \right)^2 + \\ & + \left(\frac{\partial \varphi}{\partial x^2} \frac{\partial \psi}{\partial x^3} - \frac{\partial \varphi}{\partial x^3} \frac{\partial \psi}{\partial x^2} \right)^2 \end{aligned} \right] \quad (46)$$

This formula, Eq. (46), can be obtained from Eq. (9) most easily, if one uses the following simplifying formula

$$\begin{aligned} \left| \begin{array}{cc} h_{ii-} & h_{i-j-} \\ h_{i-j-} & h_{jj-} \end{array} \right| &= \pm \left| \begin{array}{cc} \frac{\partial \varphi}{\partial x^i} & \frac{\partial \psi}{\partial x^i} \\ \frac{\partial \varphi}{\partial x^j} & \frac{\partial \psi}{\partial x^j} \end{array} \right|^2 = \\ &= \pm \left(\frac{\partial \varphi}{\partial x^i} \frac{\partial \psi}{\partial x^j} - \frac{\partial \varphi}{\partial x^j} \frac{\partial \psi}{\partial x^i} \right)^2. \end{aligned}$$

In the first order approximation for the Lagrangian, the expression L_1 should be used. Then the field equations give the system of two independent wave equations

$$\left. \begin{aligned} \frac{\partial^2 \varphi}{\partial x^0 \partial x^0} - \frac{\partial^2 \varphi}{\partial x^1 \partial x^1} - \frac{\partial^2 \varphi}{\partial x^2 \partial x^2} - \frac{\partial^2 \varphi}{\partial x^3 \partial x^3} &= 0 \\ \frac{\partial^2 \psi}{\partial x^0 \partial x^0} - \frac{\partial^2 \psi}{\partial x^1 \partial x^1} - \frac{\partial^2 \psi}{\partial x^2 \partial x^2} - \frac{\partial^2 \psi}{\partial x^3 \partial x^3} &= 0 \end{aligned} \right\}$$

Here the fields $\varphi(x)$ and $\psi(x)$ are independent and the superposition principle is fulfilled.

Using the strict Lagrangian for the two scalar fields Eq. (44) we get a system of two non-linear differential equations of the second order

$$\begin{aligned} \overset{\circ}{g}{}^{ij} \frac{\partial}{\partial x^i} \left[\frac{\varphi_{,j} \left(1 \pm \overset{\circ}{g}{}^{rs} \psi_{,r} \psi_{,s} \right) \mp \psi_{,j} \overset{\circ}{g}{}^{rs} \varphi_{,r} \psi_{,s}}{\sqrt{1 + L_1 + L_2}} \right] &= 0, \\ \overset{\circ}{g}{}^{ij} \frac{\partial}{\partial x^i} \left[\frac{\psi_{,j} \left(1 + \overset{\circ}{g}{}^{rs} \varphi_{,r} \varphi_{,s} \right) - \varphi_{,j} \overset{\circ}{g}{}^{rs} \varphi_{,r} \psi_{,s}}{\sqrt{1 + L_1 + L_2}} \right] &= 0, \end{aligned}$$

where comma means the partial derivative. Here the fields $\varphi(x)$, $\psi(x)$ depend on each other, and the superposition principle is not fulfilled. The transition from the last but one equations to the last equations may be regarded as the transition from the weak fields to the strong fields.

6 Non-degenerate polynumbers

Consider a certain system of the non-degenerate polynumbers P_n [5], that is n -dimensional associative commutative non-degenerated hyper complex numbers. The corresponding coordinate space x^1, x^2, \dots, x^n is a Finsler metric flat space with the length element equal to

$$ds = \sqrt[n]{\overset{\circ}{g}{}_{i_1 i_2 \dots i_n} dx^{i_1} dx^{i_2} \dots dx^{i_n}}, \quad (47)$$

where $\overset{\circ}{g}{}_{i_1 i_2 \dots i_n}$ is the metric tensor which does not depend on the point of the space. The Finsler spaces of this kind can be found in literature (e.g. [6–9]) but the fact that all the non-degenerated polynumber spaces belong to this type of Finsler spaces was established beginning from the papers [10, 11] and the subsequent papers of the same authors, especially in [5].

The components of the generalized momentum in geometry corresponding to Eq. (47) can be found by the formulas

$$p_i = \frac{\overset{\circ}{g}{}_{i j_2 \dots j_n} dx^{j_2} \dots dx^{j_n}}{\left(\overset{\circ}{g}{}_{i_1 i_2 \dots i_n} dx^{i_1} dx^{i_2} \dots dx^{i_n} \right)^{\frac{n-1}{n}}}. \quad (48)$$

The tangent equation of the indicatrix in the space of the non-degenerated polynumbers P_n can be always written [5] as follows

$$\overset{\circ}{g}{}^{i_1 i_2 \dots i_n} p_{i_1} p_{i_2} \dots p_{i_n} - \mu^n = 0, \quad (49)$$

where μ is a constant. There always can be found such a basis (and even several such bases) and such a $\mu > 0$ that

$$\left(\overset{\circ}{g}{}^{i_1 i_2 \dots i_n} \right) = \left(\overset{\circ}{g}{}_{i_1 i_2 \dots i_n} \right). \quad (50)$$

Let us pass to a new Finsler geometry on the base of the space of non-degenerated polynumbers P_n . This new geometry is not flat, but its difference from the initial geometry is infinitely small, and the length element in this new geometry is

$$ds = \sqrt[n]{\left[\overset{\circ}{g}{}_{i_1 i_2 \dots i_n} + \varepsilon h_{i_1 i_2 \dots i_n}(x) \right] dx^{i_1} dx^{i_2} \dots dx^{i_n}}, \quad (51)$$

where ε is an infinitely small value. If in the initial space the volume element was defined by the formula

$$dV = dx^{i_1} dx^{i_2} \dots dx^{i_n}, \quad (52)$$

in the new space within the accuracy of ε in the first power we have

$$dV_h \simeq \left[1 + \varepsilon \cdot C_0 \overset{\circ}{g}{}^{i_1 i_2 \dots i_n} h_{i_1 i_2 \dots i_n}(x) \right] dx^{i_1} dx^{i_2} \dots dx^{i_n}.$$

That is according to [1], the Lagrangian of the weak field in the space with the length element Eq. (51) in the first order

approximation is

$$L_1 = \overset{\circ}{g}{}^{i_1 i_2 \dots i_n} h_{i_1 i_2 \dots i_n}(x). \quad (53)$$

This expression generalizes formula Eq. (7).

7 Hyper complex space H_4

In the physical (“orthonormal” [5]) basis in which every point of the space is characterized by the four real coordinates x^0, x^1, x^2, x^3 the fourth power of the length element ds_{H_4} is defined by the formula

$$\begin{aligned} (ds_{H_4})^4 &\equiv \overset{\circ}{g}{}_{ijkl} dx^0 dx^1 dx^2 dx^3 = \\ &= (dx^0 + dx^1 + dx^2 + dx^3)(dx^0 + dx^1 - dx^2 - dx^3) \times \\ &\times (dx^0 - dx^1 + dx^2 - dx^3)(dx^0 - dx^1 - dx^2 + dx^3) = \\ &= (dx^0)^4 + (dx^1)^4 + (dx^2)^4 + (dx^3)^4 + 8dx^0 dx^1 dx^2 dx^3 - \\ &- 2(dx^0)^2 (dx^1)^2 - 2(dx^0)^2 (dx^2)^2 - 2(dx^0)^2 (dx^3)^2 - \\ &- 2(dx^1)^2 (dx^2)^2 - 2(dx^1)^2 (dx^3)^2 - 2(dx^2)^2 (dx^3)^2. \end{aligned} \quad (54)$$

Let us compare the fourth power of the length element ds_{H_4} in the space of polynumbers H_4 with the fourth power of the length element $ds_{M_{in}}$ in the Minkowski space

$$\begin{aligned} (ds_{M_{in}})^4 &= (dx^0)^4 + (dx^1)^4 + (dx^2)^4 + (dx^3)^4 - \\ &- 2(dx^0)^2 (dx^1)^2 - 2(dx^0)^2 (dx^2)^2 - 2(dx^0)^2 (dx^3)^2 - \\ &+ 2(dx^1)^2 (dx^2)^2 + 2(dx^1)^2 (dx^3)^2 + 2(dx^2)^2 (dx^3)^2. \end{aligned} \quad (55)$$

This means

$$\begin{aligned} (ds_{H_4})^4 &= (ds_{M_{in}})^4 + 8dx^0 dx^1 dx^2 dx^3 - \\ &- 4(dx^1)^2 (dx^2)^2 - 4(dx^1)^2 (dx^3)^2 - 4(dx^2)^2 (dx^3)^2, \end{aligned} \quad (56)$$

and in the covariant notation we have

$$\begin{aligned} (ds_{H_4})^4 &= \left(\overset{\circ}{g}{}_{ij} \overset{\circ}{g}{}_{kl} + \frac{1}{3} \overset{\circ}{g}'{}_{ijkl} - \overset{\circ}{G}{}_{ijkl} \right) \times \\ &\times dx^i dx^j dx^k dx^l, \end{aligned} \quad (57)$$

where

$$\overset{\circ}{g}'{}_{ijkl} = \begin{cases} 1, & \text{if } i, j, k, l \text{ are all different} \\ 0, & \text{else} \end{cases} \quad (58)$$

$$\overset{\circ}{G}{}_{ijkl} = \begin{cases} 1, & \text{if } i, j, k, l \neq 0 \text{ and } i = j \neq k = l, \\ & \text{or } i = k \neq j = l, \\ & \text{or } i = l \neq j = k \\ 0, & \text{else} \end{cases} \quad (59)$$

The tangent equation of the indicatrix in the H_4 space can be written in the physical basis as in [5]:

$$\begin{aligned} (p_0 + p_1 + p_2 + p_3)(p_0 + p_1 - p_2 - p_3) \times \\ \times (p_0 - p_1 + p_2 - p_3)(p_0 - p_1 - p_2 + p_3) - 1 = 0, \end{aligned} \quad (60)$$

where p_i are the generalized momenta

$$p_i = \frac{\partial ds_{H_4}}{\partial (dx^i)}. \quad (61)$$

Comparing formula Eq. (60) with formula Eq. (61), we have

$$\overset{\circ}{g}{}^{ijkl} p_i p_j p_k p_l - 1 = 0. \quad (62)$$

Here

$$\overset{\circ}{g}{}^{ijkl} = \overset{\circ}{g}{}^{ij} \overset{\circ}{g}{}^{kl} + \frac{1}{3} \overset{\circ}{g}'{}^{ijkl} - \overset{\circ}{G}{}^{ijkl}, \quad (63)$$

and

$$\left. \begin{aligned} \left(\overset{\circ}{g}{}^{ijkl} \right) &= \left(\overset{\circ}{g}{}_{ijkl} \right) \\ \left(\overset{\circ}{g}'{}^{ijkl} \right) &= \left(\overset{\circ}{g}'{}_{ijkl} \right) \\ \left(\overset{\circ}{G}{}^{ijkl} \right) &= \left(\overset{\circ}{G}{}_{ijkl} \right) \end{aligned} \right\}. \quad (64)$$

To get the Lagrangian for the weak field in the first order approximation, we have to get tensor h_{ijkl} in Eq. (53). In the simplified version it could be splitted into two additive parts: gravitational part and electromagnetic part. The gravitational part can be constructed analogously to Sections 3 and 5 with regard to the possibility to use the two-index number tensors, since now tensors $\overset{\circ}{g}{}^{ijkl}, h_{ijkl}$ have four indices. The construction of the electromagnetic part should be regarded in more detail.

Since we would like to preserve the gradient invariance of the Lagrangian and to get Maxwell equations for the free field in the H_4 space, let us write the electromagnetic part of tensor h_{ijkl} in the following way

$$h_{ijkl}^{A_k} = \chi(x) h_{ijkl}^{(1)} + [1 - \chi(x)] h_{ijkl}^{(2)}, \quad (65)$$

where the tensors $h_{ijkl}^{(1)}, h_{ijkl}^{(2)}$ are the tensors present in the round brackets in the r.h.s. of formulas Eqs. (28,29). Then

$$\begin{aligned} L_A &= \overset{\circ}{g}{}^{ijkl} h_{ijkl}^{A_k} \equiv \\ &\equiv \overset{\circ}{g}{}^{ij} \overset{\circ}{g}{}^{km} \left(\frac{\partial A_k}{\partial x^i} \frac{\partial A_m}{\partial x^j} - \frac{\partial A_k}{\partial x^i} \frac{\partial A_j}{\partial x^m} \right). \end{aligned} \quad (66)$$

To obtain Maxwell equations not for the free field but for the field with a source $j_i(x)$, one should add to the tensor $h_{ijkl}^{(A_k)}$ Eq. (65) the following tensor

$$h_{ijkl}^{(j_k)} = \left(\frac{8}{3\pi} \right) \left(2A_i j_j \overset{\circ}{g}{}_{kl} - A_i \overset{\circ}{g}{}_{jk} j_l - j_i \overset{\circ}{g}{}_{jk} A_l \right),$$

symmetrized in all indices, that is tensor

$$h_{ijkl} = h_{ijkl}^{M_{ax}} \equiv h_{ijkl}^{(A_k)} + h_{ijkl}^{(j_k)}$$

describes the weak electromagnetic field with the sources $j_i(x)$, where

$$j_i = \sum_b q_{(a)} \frac{\partial \psi_{(b)}}{\partial x^i}, \quad (67)$$

and $\psi_{(b)}$ are the scalar components of the gravitational field.

To obtain the unified theory for the gravitational and electromagnetic fields one should take the linear combination of tensor $h_{ijkl}^{(Max)}$ corresponding to the electromagnetic field in the first order approximation, and tensor $h_{ijkl}^{(grav)}$ corresponding to the gravitational field in the first order approximation

$$h_{ijkl} = \mu h_{ijkl}^{(Max)} + \gamma h_{ijkl}^{(grav)}, \quad (68)$$

where μ, γ are constants. Tensor $h_{ijkl}^{(grav)}$ may be, for example, constructed in the following way

$$h_{ijkl}^{grav} = \sum_{a=1}^N \varepsilon_{(a)} \frac{\partial \varphi_{(a)}}{\partial x^i} \frac{\partial \varphi_{(a)}}{\partial x^j} \frac{\partial \varphi_{(a)}}{\partial x^k} \frac{\partial \varphi_{(a)}}{\partial x^l} + \sum_{b=1}^M \varepsilon_{(b)} \frac{\partial \psi_{(b)}}{\partial x^i} \frac{\partial \psi_{(b)}}{\partial x^j} \overset{\circ}{g}_{kl}, \quad (69)$$

where $\varepsilon_{(a)}, \varepsilon_{(b)}$ are the sign coefficients, and $\varphi_{(a)}, \psi_{(b)}$ are the scalar fields. The whole number of scalar fields is equal to $(N + M)$.

8 Conclusion

In this paper it was shown that the geometrical approach [1] to the field theory in which there usually appear the non-linear and non-splitting field equations could give a system of independent linear equations for the weak fields in the first order approximation. When the fields become stronger the superposition principle (linearity) breaks, the equations become non-linear and the fields start to interact with each other. We may think that these changes of the equations that take place when we pass from the weak fields to the strong fields are due to the two mechanisms: first is the qualitative change of the field equations for the free fields in the first order approximation; second is the appearance of the additional field sources, that is the generation of the field by the other fields.

In frames of the geometrical approach to the field theory [1] the unification of the electromagnetic and gravitational fields is performed both for the four-dimensional pseudo-Riemannian space with metric tensor $g_{ij}(x)$ and for the four-dimensional curved Berwald-Moor space with metric tensor $g_{ijkl}(x)$.

Acknowledgements

This work was supported in part by the Russian Foundation for Basic Research under grant $RFB R - 07 - 01 - 91681 - RA_a$ and by the Non-Commercial Foundation for Finsler Geometry Research.

Submitted on August 03, 2008 / Accepted on August 11, 2008

References

1. Garas'ko G.I. Field theory and Finsler spaces. *Hyper Complex Numbers in Geometry and Physics*, 2006, v. 3 (2), 6–20.
2. Rashevsky P.K. Geometrical theory of equations with partial derivatives. OGIZ, Moscow-Leningrad, 1947.
3. Garas'ko G.I. Particular stationary solution of the field equation for the space conformally connected with Minkowski space. *Hyper Complex Numbers in Geometry and Physics*, 2007, v. 4 (1), 26–37.
4. Garas'ko G.I. The space conformally connected with Berwald-Moor space. *Hyper Complex Numbers in Geometry and Physics*, 2007, v. 4 (1), 38–51.
5. Pavlov D.G., Garas'ko G.I. Geometry of the non-degenerated polynumbers. *Hyper Complex Numbers in Geometry and Physics*, 2007, v. 4 (1), 3–25.
6. Matsumoto M., Numata S. On Finsler spaces with 1-form metric. *Tensor*, 1978, v. 32, 161–169.
7. Matsumoto M., Numata S. On Finsler spaces with 1-form metric II. Berwald — Moor's metric $L = (y^1 y^2 \dots y^n)^{\frac{1}{n}}$. *Tensor*, 1978, v. 32, 275–277.
8. Matsumoto M., Numata S. On Finsler spaces with a cubic metric. *Tensor*, 1979, v. 33, 153–162.
9. Shimada H. On Finsler spaces with the metric L of m -th root metric. *Tensor*, 1979, v. 33, 365–372.
10. Pavlov D.G. Generalized axioms of the scalar product. *Hyper Complex Numbers in Geometry and Physics*, 2004, v. 1 (1), 6–20.
11. Garas'ko G.I. Generalized analytical functions of the polynumber variable. *Hyper Complex Numbers in Geometry and Physics*, 2004, v. 1 (1), 75–88.

Instant Interpretation of Quantum Mechanics

Huy Khanh Hoang

E-mail: hoang.huy.khanh@gmail.com

We suggest a new interpretation of Quantum Mechanics, in which the system state vectors are identified with q-instants — new elements of reality that are similar to time instants but can be overlapped with each other. We show that this new interpretation provides a simple and objective solution to the measurement problem, while preserving the general validity of the Schrodinger equation as well as the superposition principle in Quantum Mechanics.

1 Introduction

In spite of the extraordinary practical successes of Quantum Mechanics, the foundations of the theory contain unresolved problems, of which the most commonly cited is the measurement problem. In standard Quantum Mechanics, the quantum state evolves according to the Schrodinger equation into a linear superposition of different states, but the actual measurements always find the physical system in a single state, with some probability given by Quantum Mechanics. To bridge this gap between theory and observed reality, different interpretations of Quantum Mechanics have been suggested, ranging from the conventional Copenhagen interpretation to Hidden-variables and Many-worlds interpretations.

The Copenhagen interpretation of Quantum Mechanics proposed a process of *collapse* which is responsible for the reduction of the superposition into a single state. This postulate of wavefunction collapse was widely regarded as artificial, ad-hoc and does not represent a satisfactory solution to the measurement problem. Hidden-variable theories are proposed as alternative interpretations in which the behavior of measurement could be understood by the assumptions on the existence of inaccessible local variables with definite values which determine the measurement outcome. However, Bell's celebrated inequality [1], and the more recent GHZ argument [2], show that a Hidden-variable theory which is consistent with Quantum Mechanics would have to be non-local and therefore contradictory to Relativity. The best known of such theory is Bohmian mechanics [3, 4], to which many physicists feel that it looks contrived. It was deliberately designed to give predictions which are in all details identical to conventional Quantum Mechanics.

In Everett's *Relative State* formulation [5], also known as the Many-worlds interpretation [6], one insists on the general validity of the superposition principle. The final state after the measurement is considered to be the full superposition state, and the measurement process is interpreted as the splitting of the system + apparatus into various branches (these are often called Everett branches) only one of which we observe. All measurement outcomes in the superposition thus coexist as separate real world outcomes. This means that, in some sense,

there is a very large, perhaps infinite, number of universes. Most physicists find this extremely unattractive. Moreover, in this interpretation it is not clear how to recover the empirical quantum mechanical probabilities.

In this paper we suggest a new interpretation of Quantum Mechanics, called Instant interpretation, which can give a simple, objective solution to the measurement problem and does not have the difficulties mentioned above. It assumes, as in the Everett interpretations, the general validity of the Schrodinger equation as well as the superposition principle of Quantum Mechanics. Basically, it consists in the introduction of the concept of *q-instant* (or *quantum instant*), and the interpretation of the system state vectors as the q-instants at which the quantum system is present or occurred. The q-instant, being a new concept of instant, is an element of reality that has the same role as time instants in classical physics: quantum events take place at different q-instants similarly to that classical events take place at different time instants. However, q-instants have new properties, especially the superposition, that are fundamentally different to time instants. Mathematically, q-instants are vector-like instants, while time instants are point-like instants. The difference in behavior of quantum and classical objects is essentially due to such differences between q-instants and time instants.

A particularly intriguing consequence of the linear time evolution of the quantum system in the context of Instant interpretation is that it leads, in quantum observation, to the *apparent collapse* phenomenon, or the *apparent unique measurement outcome*, an illusion that happens to any conscious-being observer. This is the key point to resolve the measurement problem by the Instant interpretation.

The outline of the article is as follows. We start with a preliminary introduction of the concept of quantum instant in Quantum Mechanics. In Section 3, we present the Instant interpretation and the formalism of Quantum Mechanics in this interpretation, named as *Instant Quantum Mechanics*. In Section 4, we show how the new interpretation can provide a simple and objective solution to the problem of definite outcome in quantum measurement theory, i.e. the problem related to the fact that a particular experiment on a quantum system always gives a unique result. Finally, in Section 5,

we give some conclusion remarks on the instant formalism of Quantum Mechanics and the role of quantum decoherence in this new interpretation.

2 Preliminary Concept of Quantum Instant

Before introducing the concept of q-instants in Quantum Mechanics, we shall describe briefly the basic meaning and property of its closed concept — the time instant notion.

From the physical viewpoint, time is part of the fundamental structure of the universe, a dimension in which events occur. A time instant or time point in this dimension is thus considered as a *holder* for the presence of events and objects. Each of the object's presences is called an occurrence of the object. A physical object at two different instants is considered as the same object, and not as two objects. Similarly, the worlds at different instants in the past, present and future are different occurrences of a single world, not of multiple worlds. We consider this as the basic meaning of the instant notion.

One particular property of time instant is its *distinctness*: Different time instants are strictly distinguished in the sense that when a physical object is being present in a given time instant, it is not present in other time instants. In other words, due to this separateness, the object completely leaves one time instant, before it can occur in another time instant.

The notion of q-instants that we use to interpret the wave function state in Quantum Mechanics has the same basic meaning as time instants, that is, q-instants are new *holders* for the presences of a physical system.

We shall illustrate the introduction of this new concept of instant in Quantum Mechanics by means of a simple example. Let ψ be a state vector such that

$$\psi = \frac{1}{\sqrt{2}}(\psi_1 + \psi_2), \quad (1)$$

where ψ_1 and ψ_2 are two orthogonal state vectors (correspond to two eigenstates of some observable F).

What it really means a physical system in such a superposed state ψ ? It seems likely that the system is half in the state ψ_1 and half in ψ_2 , a property of quantum objects that is usually considered as weird and inexplicable (as it is typically expressed for the behavior of the particle in the two-slit experiment).

Using the concept of instants, however, we can explain the superposition in (1) as describing the occurrences of the system at two different *instants*: one associated with the state vector ψ_1 and other with ψ_2 .

Note that we do not intend to add some hidden-time τ associated with the system states by some mapping $f(\tau_i) = \psi_i$. Instead of introducing such classical extra hidden-variables that control the occurrences of the state ψ_i , we identify the state ψ_i with the *instant* itself. We then try to know what

are the properties of this new kind of instant, which we call *quantum instant* or *q-instant*.

In fact, by considering the state vectors ψ , ψ_1 and ψ_2 in the superposition (1) as q-instants, we see that the q-instant concept exhibits intriguing new properties, compared with conventional time instants: different q-instants can be superposed or overlapped, in contrast with the distinctness property mentioned above of time instants.

In our example, the q-instant ψ is a superposition of two q-instants ψ_1 and ψ_2 , it overlaps with each of these two q-instants. On the contrary, the two q-instants ψ_1 and ψ_2 are orthogonal, they are distinct and do not overlap with each other as in the case of two different time instants. The overlap of two q-instants has the consequence that when an object is being present in one instant, one of its occurrences can be found in another instant.

Mathematically, q-instants are vector-like instants, while time instants are point-like instants. In fact, due to its superposition property, quantum instant has the structure of a vector and is not represented by a point on the real line R like a time instant. The inner product of two vectors can then be used to measure the overlap of the two corresponding q-instants.

3 Formalism of Quantum Mechanics in Instant Interpretation

In the above section, we have illustrated the introduction of the notion of q-instant in Quantum Mechanics. For the sake of simplicity, we have identified the state vector of a physical object with the q-instant at which the object located. Taking into account the time dimension, we see that the state vector of a physical object evolves in time, while the q-instants are rather something independent with time. Indeed, in the Instant interpretation, we will consider that, for each physical system, besides the time dimension, there exists independently a continuum of q-instants in which the system takes its presences. Quantum events take place in time dimension as well as in the q-instant continuum. The state vector, in the Instant interpretation, is then considered as the *representation* of a q-instant at a time t . So the q-instant itself is independent with time, but its representation, i.e. the state vector, evolves in time according to the Schrodinger equation. Note that, in this sense, the q-instant corresponds to the state vector in the Heisenberg representation of Quantum Mechanics.

The axioms of Quantum Mechanics in the Instant interpretation are as follows:

- A1 Every physical system S is associated to a Hilbert space H_S and a q-instant continuum \mathbb{Q}_S in which the system takes its presences.
- A2 Each q-instant Q of the continuum \mathbb{Q}_S is described, at each time t , by a normalized vector $|\psi\rangle$ of H_S . The time evolution of the q-instant representation, i.e. the

vector $|\psi\rangle$ representing the instant Q , is governed by the Schrodinger equation:

$$i\hbar \frac{\partial |\psi(t)\rangle}{\partial t} = H |\psi(t)\rangle. \quad (2)$$

The operator H is the Hamiltonian of the system S .

A3 Let Q_1, Q_2 be two q-instants of the continuum \mathbb{Q}_S represented, at some given time, respectively by two vectors ψ_1, ψ_2 of H_S , then $|\langle\psi_1|\psi_2\rangle|^2$ is the measure of presence of q-instant Q_1 in q-instant Q_2 .

A4 Each physical observable O of the system S is represented by a self-adjointed operator in H_S . If a q-instant Q of the system S is described, at some time t , by an eigenvector $|O_n\rangle$ of an observable O then the value of the observable O of the system S at q-instant Q and time t is o_n , where o_n is the corresponding eigen-value of $|O_n\rangle$.

Quantum Mechanics based on these axioms is called *Instant Quantum Mechanics*. In the following, we will give some remarks about its axioms and the underlying concept q-instants. In particular, we will show how the notion of probability can be defined in the context of the Instant interpretation.

(R1) For each q-instant Q , we denote by $Q(t)$ the vector $|\psi\rangle$ of H_S that describes it at time t . We say that the system S at time t and q-instant Q is in the *state* ψ . Let U be the time unitary evolution of the system, then:

- at time t_0 and q-instant Q , the system is in the state $Q(t_0) \equiv |\psi_0\rangle$, and
- at time t and q-instant Q , the system is in the state $Q(t) \equiv |\psi\rangle = U(t) |\psi_0\rangle$.

Thus, according to Instant Quantum Mechanics, the state of a physical system is determined by a time instant and a q-instant. This is in contrast with standard Quantum Mechanics in which only the time t determines the *state* ψ of a physical system. In standard Quantum Mechanics, one basic axiom is that the physical system at each time t is described by a state vector ψ . This axiom seems evident, and the practical successes of Quantum Mechanics confirm it. However, as we shall show in the next sections, this is just apparently true, and the description of *state* in Instant Quantum Mechanics is not in contradiction with practical observations. While in standard Quantum Mechanics, to fix an initial system setting, we use the expression “*Suppose at time t_0 , the system S is in the state ψ* ”, in the Instant interpretation, we can equivalently express this by “*Consider the system S at time t_0 and q-instant Q such that $Q(t_0) = \psi$* ”.

(R2) Similar to the state space, the q-instant continuum \mathbb{Q}_S has also the structure of a Hilbert vector space. This structure is defined as follows.

Let, at some given time t , $|\psi\rangle, |\psi_1\rangle$ and $|\psi_2\rangle$ be the state vectors that describe respectively the q-instants Q, Q_1 and Q_2 . Then, we define:

- $Q = c_1 Q_1 + c_2 Q_2$ if $|\psi\rangle = c_1 |\psi_1\rangle + c_2 |\psi_2\rangle$,
- the inner product $\langle Q_1 | Q_2 \rangle = \langle \psi_1 | \psi_2 \rangle$.

Due to the linearity and unitarity of the time evolution of the q-instants representation, it is easy to see that the above definitions are consistent, that is, they are time-independent.

Let $|\psi\rangle = \sum_{i=1}^n c_i |\psi_i\rangle$ and $Q, Q_i, 1 \leq i \leq n$, be q-instants such that $Q(t) = |\psi\rangle, Q_i(t) = |\psi_i\rangle$, then we have the following facts:

- q-instant Q is a superposition of the q-instants Q_i :
 $Q = \sum_{i=1}^n c_i Q_i$,
- at time t and q-instant Q_i , the state of the system is $|\psi_i\rangle$, for $1 \leq i \leq n$,
- at time t and q-instant Q , the state of the system is $|\psi\rangle$.

(R3) Since q-instants are vectors, there is no order relation between them as in the case of time instants. There is thus no concept of *next* q-instant of a q-instant. If the system is being present at instant Q , it makes no sense to ask *what q-instant it will be present next?* Instead, there is a superposition between the different instants of the q-instant continuum. Between any two q-instants Q_α and Q_β there is a *weight* $w_{\alpha\beta} = |\langle Q_\alpha | Q_\beta \rangle|^2$, which is the *measure of presence or overlap* of the instant Q_α in the instant Q_β , defined in the axiom A3. If Q_α and Q_β are overlapped, i.e. $w_{\alpha\beta} \neq 0$, then when the system is present in instant Q_α , it is present also in Q_β . If $w_{\alpha\beta} = 0$, we say that the two instants Q_α and Q_β are *orthogonal*, that is, when the system is present in one instant, it is not present in the other instant.

(R4) The notion of *current instant*, having a straightforward meaning in the case of time instants, is not directly defined for the case of q-instants. It is not globally defined for the whole q-instant continuum and it makes no sense to ask *which is the current q-instant of the q-instant continuum?* In fact, in its usual sense, the *current* instant means the instant that the system is being present at and not elsewhere. This has sense only if the so-called current instant is orthogonal with all the others, a requirement which is impossible if we consider the whole q-instant continuum. The notion of *current q-instant* is thus defined *only* with respect to a *context* in which this orthogonality requirement is satisfied. We define it as follows: A context is a pair (Q, E) , where Q is a q-instant and $E = \{Q_i\}$ is an orthogonal basis. Suppose that $Q = \sum_i c_i Q_i$ is the expansion of Q in this basis. So when the system is present at instant Q , it will present also at all instants Q_i with $c_i \neq 0$. But as the instants Q_i 's of the basis E are pairwise orthogonal, there is always only one instant Q_i of E that the system is *currently* present, this Q_i is called the *current q-instant* of the context (Q, E) . As the system will present in all the above instants Q_i 's, all these instants will become the current q-instant while the system under consideration is in the context (Q, E) . The role of the current instant is thus alternatively played by each of the q-instants of E . This notion of current q-instant is therefore similar to that

of current time instant for the time dimension. However, different to the case of time instants, in which all time instants equally take the role of current instant during the flow of time, the assignment of this role in the case of q-instants is proportional to the measure of presence of each q-instant Q_i in the context q-instant Q . The measure of presence $|\langle Q|Q_i\rangle|^2$ determines therefore the *probability* that the q-instant Q_i becomes the current instant of (Q, E) . One can understand the intuition behind this probability notion by means of the following thought experiment: Imagine a person who lives in the q-instant dimension E , in which he takes a long sleep and then wakes up at some q-instant of E . Suppose that before sleeping the person does not know at which instant he will wake up. He knows it only when he wakes up and opens his eyes, at that moment he realizes that he is currently at some instant Q_i . So, before opening his eyes, the person can only predict with a certain probability which instant Q_i he is currently at. This probability for an instant Q_i is the *probability* that Q_i becomes the current instant, and it is proportional to the measure of presence of Q_i .

4 The measurement process and the apparent collapse phenomenon

In this section, we recall briefly first the standard description of the measurement process within traditional Quantum Mechanics and the problem arising from it, usually referred as *the measurement problem* in the literature. We then show how our Instant interpretation of Quantum Mechanics can give a simple and objective solution to this problem.

4.1 Measurements in traditional Quantum Mechanics — the problem of definite outcome

A standard scheme using pure Quantum Mechanics to describe the measurement process is the one devised by von Neumann (1932). In this schema, both the measured system and the apparatus are considered as quantum objects.

Let H_S be the Hilbert space of the measured system S and $\{|e_i\rangle\}$ be the eigenvectors of the operator F representing the observable to be measured. Let H_A be the Hilbert space of the apparatus A and $\{|a_i\rangle\}$ be the basis vectors of H_A , where the $|a_i\rangle$'s are assumed to correspond to macroscopically distinguishable *pointer* positions that correspond to the outcome of a measurement if S is in the state $|e_i\rangle$. The apparatus A is in the initial *ready* state $|a_0\rangle$.

The total system $S \otimes A$, assumed to be represented by the Hilbert product space $H_{SA} = H_S \otimes H_A$, evolves according to the Schrodinger equation. Let U be the time evolution of the total system from the initial state to the final state of the measuring process.

Suppose that the measured system S is initially in one of the eigenvector state $|e_i\rangle$ then $U(|e_i\rangle|a_0\rangle) = |e_i\rangle|a_i\rangle$ where $|\phi_f\rangle = |e_i\rangle|a_i\rangle$ is the final state of the total system + appara-

tus $S \otimes A$. The outcome $|a_i\rangle$ of the apparatus A can be predicted with certainty merely from the unitary dynamics.

Now, consider the case of measurement in which the system S is initially prepared not in the eigenstate $|e_i\rangle$ but in a superposition of the form $\sum_i c_i |e_i\rangle$. Due to the linearity of the Schrodinger equation, the final state $|\phi_f\rangle$ of total system is:

$$|\phi_f\rangle = U\left(\sum_i c_i |e_i\rangle |a_0\rangle\right) = \sum_i c_i |e_i\rangle |a_i\rangle. \quad (3)$$

So the final state $|\phi_f\rangle$ describes a state that does not correspond to a definite state of the apparatus. This is in contrast to what is actually perceived at the end of the measurement: in actual measurements, the observer always finds the apparatus in a definite pointer state $|a_i\rangle$, for some i , but not in a superposition of these states. The difficulty to understand this fact is typically referred to as the measurement problem in the literature.

Von Neumann's approach (like all other standard presentations of Quantum Mechanics) assumes that after the first stage of the measurement process, described as above, a second non-linear, indeterministic process takes place, the *reduction* (or *collapse*) of the wave packet, that involves $S \otimes A$ *jumping* from the entangled state $\sum_i c_i |e_i\rangle |a_i\rangle$ into the state $|e_i\rangle |a_i\rangle$ for some i . It's obvious that the wave-packet reduction postulate, abandoning the general validity of the Schrodinger equation without specifying any physical conditions under which the linear evolution fails, is *ad hoc* and does not consequently represent a satisfactory solution to the measurement problem.

In the last few decades, some important advances related to a theoretical understanding of the collapse process have been made. This new theoretical framework, called quantum decoherence, supersedes previous notions of instantaneous collapse and provides an explanation for the absence of quantum coherence after measurement [7–11]. While this theory correctly predicts the form and probability distribution of the final eigenstates, it does not explain the observation of a unique stable pointer state at the end of a measurement [12, 13].

4.2 Solution from Instant Quantum Mechanics

We will show how the Instant interpretation based on the concept of q-instants allows a simple and objective solution to the measurement problem. The above description of the measurement process can be reformulated in Instant Quantum Mechanics as follows:

According to the Instant interpretation, the combined system $S \otimes A$ takes its presences in a continuum \mathbb{Q}_{SA} of q-instants, each of which is represented at each time t by a normalized vector of the Hilbert product space $H_{SA} = H_S \otimes H_A$.

Following the remark (RI) of Section 3, the initial setting (according to standard Quantum Mechanics) in which

the combined system $S \otimes A$ is in the state

$$|\phi_0\rangle = \sum_i c_i |e_i\rangle |a_0\rangle . \quad (4)$$

is equivalent to the initial setting (according to the Instant interpretation) in which the combined system $S \otimes A$ under consideration is being present at the q-instant Q of the continuum \mathbb{Q}_{SA} such that

$$Q(t_0) = |\phi_0\rangle , \quad (5)$$

where $|\phi_0\rangle$ is defined in (4).

For each i , let Q_i be the q-instant of $S \otimes A$ such that

$$Q_i(t_0) = |\phi_i\rangle = |e_i\rangle |a_0\rangle . \quad (6)$$

The instants Q_i 's are, hence, orthogonal one with another. Following the remark (R2) of Section 3, the instant Q is spanned over this set of instants as follows:

$$Q = \sum_i c_i Q_i . \quad (7)$$

Following the axiom A3, the $|c_i|^2$ is the measure of presence of the system $S \otimes A$ in instant Q_i as long as the system is being present in instant Q .

The state vectors, representing the instants Q and Q_i 's, evolve independently in time following the Schrodinger equation. At the end of the measurement process, we have:

$$Q_i(t_f) = |e_i\rangle |a_i\rangle , \quad (8)$$

$$Q(t_f) = \sum_i c_i |e_i\rangle |a_i\rangle . \quad (9)$$

From (8), (9) we see that after measurement:

- at time t_f and q-instant Q , the state of the combined system is $\sum_i c_i |e_i\rangle |a_i\rangle$;
- at time t_f and q-instant Q_i , the state of the combined system is $|e_i\rangle |a_i\rangle$, hence the state of the apparatus is $|a_i\rangle$.

Thus, after measurement, the observer sees different outcomes $|a_i\rangle$'s, at different instants Q_i 's. So far, the description still seems to be in contrast to what is actually perceived by the observer at the end of the measurement, i.e. to the following fact:

Fact 1. The observer always sees the apparatus in one definite state $|a_i\rangle$, for some i , after the measurement.

The difficulty to explain Fact 1 is usually referred as the *problem of definite outcome* in quantum measurement theory. However, we will show that Fact 1 is intriguingly not true, it is an illusion of the observer. More precisely, we will show, according to the Instant interpretation, the following *apparent "collapse"* phenomenon (or the phenomenon of *apparent unique measurement outcome*):

Fact 2. The observer does see different measurement outcomes, but it seems to him that there is only one unique measurement outcome and the apparatus is in one definite state $|a_i\rangle$, for some i , after the measurement.

Proof. To prove this fact we will take into account the presence of the observer in the measurement process by considering him as a component of the total system. We will see that the illusion in Fact 2 comes from the property of time evolution independence of different q-instants in the measurement process and its impacts on the observer's recognition of the world.

To be consistent and objective, we will treat the observer quantum mechanically, that is, as a quantum object. We can simply write $|O_i\rangle$ to denote the state of the observer seeing the apparatus in position $|a_i\rangle$. However, to well understand the illusion, we need to consider the cognitive aspect of the observer in a little more detail. A conscious being can observe the world and use his brain cells to stock information he perceived. What make he feels that he is seeing an event, is the result of a process of recognition during which the brain cells "memorize" the event.

Let C be the set of memory cells that the observer uses in the recognition of the apparatus state, and C_i be the content of C when the observer perceives that the apparatus state is $|a_i\rangle$. This content C_i is considered as the *proof* that the observer perceives the apparatus in position $|a_i\rangle$.

Suppose that at some instant the content of the cells is C_i and the observer actually perceives that the apparatus state is $|a_i\rangle$. If the cells contents are later destroyed, not only the observer will not see the apparatus being in the state $|a_i\rangle$, but as his concerned memory data is lost, he will feel that he has never seen the apparatus being in the state $|a_i\rangle$. If, alternatively, the cell contents are changed and replaced by C_j , not only the observer will see that the apparatus is now in the state $|a_j\rangle$, but as his old data is lost, for him the apparatus have never been in the state $|a_i\rangle$.

This is what happens to the observer in the measurement process according to Instant Quantum Mechanics.

In fact, including the observer in the measurement process, the Hilbert space of the total system will be the product $H_S \otimes H_A \otimes H_O$, where H_O is the Hilbert space of the observer. We assume that H_O is spanned over the basis of state vectors $\{|O_i, C_i\rangle\}$ where the $|O_i, C_i\rangle$ describes the state of the observer seeing the apparatus in position $|a_i\rangle$ and having his memory cells contents C_i .

Initially, the total system $S \otimes A \otimes O$ under consideration is being present at the q-instant Q of the continuum \mathbb{Q}_{SAO} such that

$$Q(t_0) = |\phi_0\rangle = \sum_i c_i |e_i\rangle |a_0\rangle |O_0, C_0\rangle . \quad (10)$$

The total system containing the measured system, the apparatus and the observer with his memory cells evolves in

time following the Schrodinger equation during the measurement process.

At the end of measurement, at time t_f , similar to (8), (9), we have:

$$Q_i(t_f) = |e_i\rangle |a_i\rangle |O_i, C_i\rangle, \quad (11)$$

$$Q(t_f) = \sum c_i |e_i\rangle |a_i\rangle |O_i, C_i\rangle. \quad (12)$$

So, after the measurement process, similar to the apparatus and the observer, the cells C takes its presences in different q-instants, and at q-instant Q_i , the observer memory cells content is C_i . Note that, due to the time evolution independence of the cells contents in different q-instants, the content of the cells C in one q-instant is not influenced by its contents in other q-instants.

We consider the impact of this on the observer behavior. After measurement, at instant Q_i , the cells content is C_i , but at another instant Q_j , the cells content is replaced by C_j . So at instant Q_j , the observer loses all information of his memory cells at instant Q_i . Due to the time evolution independence of the cells contents at Q_i and Q_j , basing on his memory cells information at Q_j , the observer has no trace or proof that he has ever lived in instant Q_i . By consequence, at instant Q_j , the observer sees the apparatus in position $|a_j\rangle$, but he absolutely *forgets* that he has ever lived in q-instant Q_i and seen the apparatus in position $|a_i\rangle$. In other words, after each measurement, the observer does see different outcomes at different q-instants, but he believes that there is only one outcome, the one that he is currently seeing. \square

So we have proved Fact 2 and solve therefore the problem of definite outcome. How about the probability of an outcome? Objectively, all outcomes are present after the measurement, so the probability of an outcome $|a_i\rangle$ here must be understood as the probability that an outcome $|a_i\rangle$ becomes the one that is *currently* perceived (and illusorily considered as unique) by the observer. In other words, the probability of an outcome $|a_i\rangle$ is the probability that the corresponding instant Q_i is the *current q-instant* in which the observer presents. As we have remarked in *R4* of Section 3, this notion of *current q-instant* is defined with respect to a context. In our case, corresponding to the setting of the measurement process, this context is (Q, E) , where Q is the q-instant under consideration of the total system at time t_0 , and $E = \{Q_i\}$ is the set of orthogonal instants Q_i in which the measured observable F has a definite value. So from *R4* of Section 3, we see that the probability of the outcome $|a_i\rangle$ is the measure of presence of the instant Q_i in instant Q which, from (7), is equal to $|c_i|^2$.

5 Concluding remarks

1. We note that the phenomenon of apparent unique outcome in the measurement process (Fact 2 of Section 4.2) illustrates

also a remark about the definition of *state* in the Instant interpretation in *R1* of Section 3: the state of a physical system is dependent not only on time but also on q-instant. In fact, as we have seen in Section 4.2, the *state* of the total system at the end of measurement is dependent on the q-instants at which the system presents. But, as demonstrated there, the observer is unconscious about this, for him the *state* of a quantum object is always unique at any time instant. The description of state in the Instant interpretation is thus not in contradiction with practical observations.

2. In the Instant interpretation, we consider that, like microscopic objects, a macroscopic object, e.g. an apparatus, also takes its presences in a q-instant continuum which supports the superposition principle. If Q_1 and Q_2 are two q-instants in which the object can present, then it can also present in a q-instant which is a superposition of Q_1 and Q_2 . The question is why can we observe a macroscopic object such as an apparatus in q-instants in which its pointer position is either *up* or *down*, but never in a q-instant in which its pointer is in a superposition of these positions.

This is the problem of *classicality* of macroscopic objects, to which decoherence theory, in particular the environment-induced decoherence, can provide an explanation. In fact, recent development in this domain [7–9, 11, 14–16] has shown that there exists, for macroscopic objects, certain *preferred sets of states*, often referred to as *pointer states* that are robust. These states are determined by the form of the interaction between the system and its environment and are suggested to correspond to the *classical* states of our experience. Thus, for a macroscopic object, one can not observe all of its Hilbert state vector space but only a small subset of it. In the context of Instant interpretation, this means that, while a macroscopic object can present in all q-instants of the continuum, we can observe it only in q-instants that are described by these robust classical states.

In summary, with respect to the measurement problem in Quantum Mechanics, decoherence theory can provide an explanation to the *classicality appearance* of the measurement outcomes, while the Instant interpretation allows to explain the observation of *an unique outcome* at the end of a measurement.

Submitted on July 28, 2008 / Accepted on August 07, 2008

References

1. Bell J. S. On the Einstein-Podolsky-Rosen paradox. *Physics*, 1964, v. 1, 195–200.
2. Greenberger D. M., Horne M. A., Zeilinger A. Going Beyond Bell's Theorem. *Bell's Theorem, Quantum Theory and Conceptions of the Universe*. M. Kafatos (Ed.), Kluwer Academic, 1989, 69–72.
3. Bohm D. A Suggested Interpretation of the Quantum Theory in Terms of "Hidden Variables" I. *Phys. Rev.*, 1952, v. 85, 166–179.

4. Bohm D. A Suggested Interpretation of the Quantum Theory in Terms of "Hidden Variables" II. *Phys. Rev.*, 1952, v. 85, 180–193.
 5. Everett H. "Relative State" Formulation of Quantum Mechanics. *Rev. Mod. Phys.*, 1957, v. 29, 454–462.
 6. DeWitt B. S., Graham N. The Many-Worlds Interpretation of Quantum Mechanics. Princeton Univ. Press, 1973.
 7. Zurek W.H. Pointer basis of quantum apparatus: Into what mixture does the wave packet collapse? *Phys. Rev. D*, 1981, v. 24, 1516–1525.
 8. Zurek W.H. Environment-induced superselection rules. *Phys. Rev. D*, 1982, v. 26, 1862–1880.
 9. Zurek, W.H. Decoherence and the Transition from Quantum to Classical. *Phys. Today*, 1991, v. 44, 36–44.
 10. Wheeler J. A., Zurek W. H. Quantum Theory and Measurement. Princeton University Press, Princeton, NJ, 1983.
 11. Joos E., Zeh H.D. The emergence of classical properties through interaction with the environment. *Zeitschrift für Physik B*, 1985, v. 59, 223–243.
 12. Adler S.L. Why decoherence has not solved the measurement problem: a response to P.W. Anderson. arXiv: quant-ph/0112095.
 13. Bub J. Interpreting the Quantum World. Cambridge University Press, 1997.
 14. Zurek, W.H. Decoherence, einselection and the quantum origins of the classical, *Rev. Mod. Phys.*, 2003, v. 75, 715–775. arXiv: quant-ph/0105127.
 15. Joos E., Zeh H. D., Kiefer C., Giulini D., Kupsch J., Stamatescu I. -O. Decoherence and the appearance of a classical world in quantum theory. Springer, 2003.
 16. Schlosshauer M. Decoherence, the measurement problem and interpretations of quantum mechanics. *Rev. Mod. Phys.*, 2004, v. 76, 1267–1305. arXiv: quant-ph/0312059.
-

Thermoelastic Property of a Semi-Infinite Medium Induced by a Homogeneously Illuminating Laser Radiation

Ibrahim A. Abdallah*, Amin F. Hassan†, Ismail M. Tayel*

*Dept. of Mathematics, †Dept. of Physics, Helwan University, Helwan, 11795, Egypt
E-mail: iaawavelets@yahoo.com

The problem of thermoelasticity, based on the theory of Lord and Shulman with one relaxation time, is used to solve a boundary value problem of one dimensional semi-infinite medium heated by a laser beam having a temporal Dirac distribution. The surface of the medium is taken as traction free. The general solution is obtained using the Laplace transformation. Small time approximation analysis for the stresses, displacement and temperature are performed. The convolution theorem is applied to get the response of the system on temporally Gaussian distributed laser radiation. Results are presented graphically. Concluding that the small time approximation has not affected the finite velocity of the heat conductivity.

1 Introduction

The classical theory (uncoupled) of thermoelasticity based on the conventional heat conduction equation. The conventional heat conduction theory assumes that the thermal disturbances propagate at infinite speeds. This prediction may be suitable for most engineering applications but it is a physically unacceptable situation, especially at a very low temperature near absolute zero or for extremely short-time responses.

Biot [1] formulated the theory of coupled thermoelasticity to eliminate the shortcoming of the classical uncoupled theory. In this theory, the equation of motion is a hyperbolic partial differential equation while the equation of energy is parabolic. Thermal disturbances of a hyperbolic nature have been derived using various approaches. Most of these approaches are based on the general notion of relaxing the heat flux in the classical Fourier heat conduction equation, thereby, introducing a non Fourier effect.

The first theory, known as theory of generalized thermoelasticity with one relaxation time, was introduced by Lord and Shulman [2] for the special case of an isotropic body. The extension of this theory to include the case of anisotropic body was developed by Dhaliwal and Sherief [4].

In view of the experimental evidence available in favor of finiteness of heat propagation speed, generalized thermoelasticity theories are supposed to be more realistic than the conventional theory in dealing with practical problems involving very large heat fluxes and/or short time intervals, like those occurring in laser units and energy channels.

The purpose of the present work is to study the thermoelastic interaction caused by heating a homogeneous and isotropic thermoelastic semi-infinite body induced by a Dirac pulse having a homogeneous infinite cross-section by employing the theory of thermo-elasticity with one relaxation time. The problem is solved by using the Laplace transform technique. Approximate small time analytical solutions to

stress, displacement and temperature are obtained. The convolution theorem is applied to get the spatial and temporal temperature distribution induced by laser radiation having a temporal Gaussian distribution. At the end of this work we present the computed results obtained from the theoretical relations applied on a Cu target.

2 Formulation of the problem

We consider a thermoelastic, homogeneous, isotropic semi-infinite target occupying the region $z \geq 0$, and initially at uniform temperature T_0 . The surface of the target $z = 0$ is heated homogeneously by a laser beam and assumed to be traction free. The Cartesian coordinates (x, y, z) are considered in the solution and z -axis pointing vertically into the medium. The equation of motion in the absence of the body forces has the form

$$\sigma_{ji,j} = \rho \ddot{u}_i, \quad (1)$$

where σ_{ij} is the components of stress tensor, u_i is the components of displacement vector and ρ is the mass density. Due to the Lord and Shalman theory of coupled thermoelasticity [2] (L-S) who considered a wave-type heat equation by postulating a new law of heat conduction equation to replace the Fourier's law

$$\rho c_E \left(\frac{\partial T}{\partial t} + t_0 \frac{\partial^2 T}{\partial t^2} \right) + \gamma T_0 \operatorname{div} \left(\frac{\partial u}{\partial t} + t_0 \frac{\partial^2 u}{\partial t^2} \right) = k \nabla^2 T, \quad (2)$$

where T_0 is a uniform reference temperature, $\gamma = (3\lambda + 2\mu)\alpha_t$, λ , and μ are Lamé's constants. α_t is the linear thermal expansion coefficient, c_E is the specific heat at constant strain and k is the thermal conductivity. The boundary conditions:

$$\sigma_{zz} = 0, \quad z = 0, \quad (3)$$

$$-k \frac{dT}{dz} = A_0 q_0 \delta(t), \quad z = 0, \quad (4)$$

where A_0 is an absorption coefficient of the material, q_0 is the intensity of the laser beam and $\delta(t)$ is the Dirac delta function [5]. The initial conditions:

$$\left. \begin{aligned} T(z, 0) &= T_0 \\ \frac{\partial T}{\partial t} = \frac{\partial^2 T}{\partial t^2} = \frac{\partial w}{\partial t} = \frac{\partial^2 w}{\partial t^2} &= 0, \quad \text{at } t = 0, \quad \forall z \end{aligned} \right\}. \quad (5)$$

Due to the symmetry of the problem and the external applied thermal field, the displacement vector u has the components:

$$u_x = 0, \quad u_y = 0, \quad u_z = w(z, t). \quad (6)$$

From equation (6) the strain components e_{ij} , and the relation of the strain components to the displacement read;

$$\left. \begin{aligned} e_{xx} = e_{yy} = e_{xy} = e_{xz} = e_{yz} &= 0 \\ e_{zz} &= \frac{\partial w}{\partial z} \\ e_{ij} &= \frac{1}{2} (u_{i,j} + u_{j,i}) \end{aligned} \right\}. \quad (7)$$

The volume dilation e takes the form

$$e = e_{xx} + e_{yy} + e_{zz} = \frac{\partial w}{\partial z}. \quad (8)$$

The stress components are given by:

$$\left. \begin{aligned} \sigma_{xx} &= \lambda e - \gamma(T - T_0) \\ \sigma_{yy} &= \lambda e - \gamma(T - T_0) \\ \sigma_{zz} &= 2\mu \frac{\partial w}{\partial z} + \lambda e - \gamma(T - T_0) \end{aligned} \right\}, \quad (9)$$

where

$$\left. \begin{aligned} \sigma_{xy} &= 0 \\ \sigma_{xz} &= 0 \\ \sigma_{yz} &= 0 \end{aligned} \right\}. \quad (10)$$

The equation of motion (1) will be reduces to

$$\sigma_{zz,z} + \sigma_{xz,x} + \sigma_{yz,y} = \rho \ddot{u}_z. \quad (11)$$

Substituting from (9) and (10) into the last equation and using $\theta = T - T_0$ we get,

$$(2\mu + \lambda) \frac{\partial^2 w}{\partial z^2} - \gamma \frac{\partial \theta}{\partial z} = \rho \frac{\partial^2 w}{\partial t^2}, \quad (12)$$

where θ is the temperature change above a reference temperature T_0 . Differentiating (12) with respect to z and using (8), we obtain

$$(2\mu + \lambda) \frac{\partial^2 e}{\partial z^2} - \gamma \frac{\partial^2 \theta}{\partial z^2} = \rho \frac{\partial^2 e}{\partial t^2}. \quad (13)$$

The energy equation can be written in the form:

$$\left. \begin{aligned} \left(\frac{\partial}{\partial t} + t_0 \frac{\partial^2}{\partial t^2} \right) (\rho c_E \theta + \gamma T_0 e) &= k \nabla^2 T \\ \nabla^2 &\equiv \frac{\partial^2}{\partial z^2} \end{aligned} \right\}. \quad (14)$$

For convenience, the following non-dimensional quantities are introduced

$$\left. \begin{aligned} z^* &= c_1 \eta z, \quad w^* = c_1 \eta w, \quad t^* = c_1^2 \eta t \\ t_0^* &= c_1^2 \eta t_0, \quad \sigma_{ij}^* = \frac{\sigma_{ij}}{\mu}, \quad \theta^* = \frac{T - T_0}{T_0} \\ \eta &= \frac{\rho c_E}{k}, \quad c_1^2 = \sigma_{ij}^* = \frac{\lambda + 2\mu}{\rho} \end{aligned} \right\}. \quad (15)$$

Substituting from (15) into (12) we get after dropping the asterisks and adopting straight forward manipulation

$$\left. \begin{aligned} \nabla^2 e - g_1 \nabla^2 \theta &= \frac{\partial^2 e}{\partial t^2} \\ \nabla^2 \theta &= \left(\frac{\partial}{\partial t} + t_0 \frac{\partial^2}{\partial t^2} \right) (\theta + g_2 e) \end{aligned} \right\}, \quad (16)$$

where $g_1 = \frac{\gamma T_0}{(2\mu + \lambda)}$ and $g_2 = \frac{\gamma}{\rho c_E}$.

Substituting from (15) into (9) we get,

$$\left. \begin{aligned} \sigma_{xx} = \sigma_{yy} &= \beta e - \lambda_1 \theta \\ \sigma_{zz} &= \alpha e - \lambda_1 \theta \end{aligned} \right\}, \quad (17)$$

where $\alpha = \frac{\gamma(2\mu + \lambda)}{\mu}$, $\beta = \frac{\lambda}{\mu}$ and $\lambda_1 = \frac{\gamma T_0}{\mu}$. We now introduce the Laplace transform defined by the formula:

$$\bar{f}(z, s) = \int_0^\infty e^{-st} f(z, t) dt. \quad (18)$$

Applying (18) to both sides of equation (16) we get,

$$(\nabla^2 - s^2) \bar{e} - g_1 \nabla^2 \bar{\theta} = 0, \quad (19)$$

$$(\nabla^2 - s(1 + t_0 s)) \bar{\theta} - s(1 + t_0 s) g_2 \bar{e} = 0. \quad (20)$$

Eliminating $\bar{\theta}$ and \bar{e} between equation (19) and (20) we get the following fourth-order differential equations satisfied by \bar{e} and $\bar{\theta}$; respectively

$$(\nabla^4 - A \nabla^2 + C) \bar{e} = 0, \quad (21)$$

$$(\nabla^4 - A \nabla^2 + C) \bar{\theta} = 0, \quad (22)$$

with $A = s^2 + s(1 + t_0 s)(1 + g_1 g_2)$ and $C = s^3(1 + t_0 s)$. One can solve these fourth order ordinary differential equations by using e^{-kz} and finding the roots of the indicial equation

$$k^4 - A k^2 + C = 0, \quad (23)$$

suppose that k_i ($i = 1, 2$) are the positive roots, then the solution of (23) for $z \geq 0$ and $k_i > 0$ are; respectively

$$\bar{e}(z, s) = \sum_{i=1}^2 A_i e^{-k_i z} \tag{24}$$

and

$$\bar{\theta}(z, s) = \sum_{i=1}^2 A'_i e^{-k_i z}, \tag{25}$$

where $A_i = A_i(s)$ and $A'_i = A'_i(s)$ are some parameters depending only on s and k_i are functions of s . Substituting by (24) and (25) into (20) we get the relation,

$$A'_i = \frac{s(1+t_0s)g_2}{k_i^2 - s(1+t_0s)} A_i, \tag{26}$$

while Laplace transform of Equation (8) and integration w.r.t. z we obtain

$$\bar{w}(z, s) = - \sum_{i=1}^2 \frac{A_i}{k_i} e^{-k_i z}. \tag{27}$$

Substituting from Equation (24) and Equation (26) into (17) we get the stresses,

$$\sigma_{xx} = \sigma_{yy} = \sum_{i=1}^2 A_i e^{-k_i z} \times \frac{\beta(k_i^2 - s(1+t_0s)) - s(1+t_0s)\lambda_1 g_2}{k_i^2 - s(1+t_0s)}. \tag{28}$$

$$\sigma_{zz} = \sum_{i=1}^2 A_i e^{-k_i z} \times \frac{\alpha(k_i^2 - s(1+t_0s)) - s(1+t_0s)\lambda_1 g_2}{k_i^2 - s(1+t_0s)}. \tag{29}$$

Therefore it is easy to determine A_i and A'_i for $i = 1, 2$

$$A_1 = \frac{-A_0 q_0 (k_1^2 - s(1+t_0s)) B_1(s)}{g_2 s (1+t_0s) [-k_1 B_2(s) + k_2 B_3(s)]}, \tag{30}$$

$$A_2 = \frac{A_0 q_0 (k_2^2 - s(1+t_0s)) B_1(s)}{g_2 s (1+t_0s) [-k_1 B_2(s) + k_2 B_3(s)]}, \tag{31}$$

$$A'_1 = \frac{-A_0 q_0 B_1(s)}{[-k_1 B_2(s) + k_2 B_3(s)]}, \tag{32}$$

$$A'_2 = \frac{A_0 q_0 B_1(s)}{[-k_1 B_2(s) + k_2 B_3(s)]}, \tag{33}$$

where $B_1(s) = \alpha(k_2^2 - s(1+t_0s))(\alpha + \lambda_1 g_2)$, $B_2(s) = \alpha k_2^2 - s(1+t_0s)(\alpha + \lambda_1 g_2)$, and also $B_3(s) = \alpha k_1^2 - s(1+t_0s)(\alpha + \lambda_1 g_2)$.

3 Small time approximation

We now determine inverse transforms for the case of small values of time (large values of s). This method was used by

Hetnarski [6] to obtain the fundamental solution for the coupled thermelasticity problem and by Sherief [7] to obtain the fundamental solution for generalized thermoelasticity with two relaxation times for point source of heat. k_1 and k_2 are the positive roots of the characteristic equation (23), given by

$$k_1 = \left(\frac{s}{2} \left[s + (1+t_0s)(1+\epsilon) + \sqrt{s^2 + 2s(\epsilon-1)(1+t_0s) + (1+t_0s)^2(1+\epsilon)^2} \right] \right)^{\frac{1}{2}}, \tag{34}$$

$$k_2 = \left(\frac{s}{2} \left[s + (1+t_0s)(1+\epsilon) - \sqrt{s^2 + 2s(\epsilon-1)(1+t_0s) + (1+t_0s)^2(1+\epsilon)^2} \right] \right)^{\frac{1}{2}}, \tag{35}$$

where $\epsilon = g_1 g_2 = \frac{\alpha^2 (3\lambda + 2\mu)^2 T_0}{\rho c_E (2\mu + \lambda)}$. Setting $v = \frac{1}{s}$, equations (34) and (35) can be expressed in the following form

$$k_i = v^{-1} [f_i(v)]^{\frac{1}{2}}, \quad i = 1, 2, \tag{36}$$

where

$$f_1(v) = \frac{1}{2} \left[1 + (v+t_0)(1+\epsilon) + \sqrt{1 + 2(\epsilon-1)(v+t_0) + (v+t_0)^2(1+\epsilon)^2} \right], \tag{37}$$

$$f_2(v) = \frac{1}{2} \left[1 + (v+t_0)(1+\epsilon) - \sqrt{1 + 2(\epsilon-1)(v+t_0) + (v+t_0)^2(1+\epsilon)^2} \right]. \tag{38}$$

Expanding $f_1(v)$ and $f_2(v)$ in the Maclaurin series around $v = 0$ and consider only the first four terms, can be written $f_i(v)$ ($i = 1, 2$) as

$$f_i(v) = a_{i0} + a_{i1}v + a_{i2}v^2 + a_{i3}v^3, \quad i = 1, 2, \tag{39}$$

where the coefficients of the first four terms are given by

$$\left. \begin{aligned} a_{10} &= \frac{1+(1+\epsilon)t_0 + \sqrt{1+2(\epsilon-1)t_0 + (1+\epsilon)^2 t_0^2}}{2} \\ a_{20} &= \frac{1+(1+\epsilon)t_0 - \sqrt{1+2(\epsilon-1)t_0 + (1+\epsilon)^2 t_0^2}}{2} \\ a_{11} &= \frac{1}{2} \left[(1+\epsilon) - \frac{(\epsilon-1)t_0 + (1+\epsilon)^2 t_0}{\sqrt{1+2(\epsilon-1)t_0 + (1+\epsilon)^2 t_0^2}} \right] \\ a_{21} &= \frac{1}{2} \left[(1+\epsilon) + \frac{(\epsilon-1)t_0 + (1+\epsilon)^2 t_0}{\sqrt{1+2(\epsilon-1)t_0 + (1+\epsilon)^2 t_0^2}} \right] \\ a_{12} &= \frac{\epsilon}{[1+2(\epsilon-1)t_0 + (1+\epsilon)^2 t_0^2]^{\frac{3}{2}}} \\ a_{22} &= -\frac{\epsilon}{[1+2(\epsilon-1)t_0 + (1+\epsilon)^2 t_0^2]^{\frac{3}{2}}} \\ a_{13} &= \frac{-\epsilon(-1+\epsilon + (1+\epsilon)^2 t_0)}{[1+2(\epsilon-1)t_0 + (1+\epsilon)^2 t_0^2]^{\frac{3}{2}}} \\ a_{23} &= \frac{\epsilon(-1+\epsilon + (1+\epsilon)^2 t_0)}{[1+2(\epsilon-1)t_0 + (1+\epsilon)^2 t_0^2]^{\frac{3}{2}}} \end{aligned} \right\}. \tag{40}$$

Next, we expand $[f_i(v)]^{\frac{1}{2}}$ in the Maclaurin series around $v = 0$ and retaining the first three terms, we obtain finally the expressions for k_1 and k_2 which can be written in the form

$$k_i = v^{-1} (b_{i0} + b_{i1}v + b_{i2}v^2), \quad i = 1, 2, \quad (41)$$

where

$$b_{i0} = \sqrt{a_{i0}},$$

$$b_{i1} = \frac{a_{i1}}{2\sqrt{a_{i0}}},$$

and

$$b_{i2} = \frac{1}{8a_{i0}^{\frac{3}{2}}(9a_{i2}a_{i0} - a_{i0}^2)}.$$

Consider k_i to be written as

$$k_i = b_{i0}s + b_{i1}, \quad i = 1, 2. \quad (42)$$

Applying Maclaurin series expansion around $v = 0$ of the following expressions;

$$\frac{1}{k_i} A_i, \quad \frac{s(1+t_0s)g_2}{k_i^2 - s(1+t_0s)} A_i, \\ \left[\frac{\beta(k_i^2 - s(1+t_0s)) - s(1+t_0s)\lambda_1g_2}{k_i^2 - s(1+t_0s)} \right] A_i, \\ \left[\frac{\alpha(k_i^2 - s(1+t_0s)) - s(1+t_0s)\lambda_1g_2}{k_i^2 - s(1+t_0s)} \right] A_i,$$

$$i = 1, 2.$$

We find that $\bar{\theta}$, \bar{w} , $\bar{\sigma}_{xx}$, $\bar{\sigma}_{yy}$, and $\bar{\sigma}_{zz}$ can be written in the following form

$$\bar{\theta} = \left(\frac{c_{\theta 0}}{s} + \frac{c_{\theta 1}}{s^2} + \frac{c_{\theta 2}}{s^3} \right) e^{-k_1z} + \left(\frac{c_{\theta 3}}{s} + \frac{c_{\theta 4}}{s^2} + \frac{c_{\theta 5}}{s^3} \right) e^{-k_2z}, \quad (43)$$

$$\bar{w} = \left(\frac{c_{w0}}{s^2} + \frac{c_{w1}}{s^3} + \frac{c_{w2}}{s^4} \right) e^{-k_1z} + \left(\frac{c_{w3}}{s^2} + \frac{c_{w4}}{s^3} + \frac{c_{w5}}{s^4} \right) e^{-k_2z}, \quad (44)$$

$$\bar{\sigma}_{xx} = \bar{\sigma}_{yy} = \left(\frac{c_{\sigma 0}}{s} + \frac{c_{\sigma 1}}{s^2} + \frac{c_{\sigma 2}}{s^3} \right) e^{-k_1z} + \left(\frac{c_{\sigma 3}}{s} + \frac{c_{\sigma 4}}{s^2} + \frac{c_{\sigma 5}}{s^3} \right) e^{-k_2z}, \quad (45)$$

$$\bar{\sigma}_{zz} = \left(\frac{c_{z0}}{s} + \frac{c_{z1}}{s^2} + \frac{c_{z2}}{s^3} \right) e^{-k_1z} + \left(\frac{c_{z3}}{s} + \frac{c_{z4}}{s^2} + \frac{c_{z5}}{s^3} \right) e^{-k_2z}, \quad (46)$$

where

$$\left. \begin{aligned} c_{\theta 0} &= \frac{y_1}{f_0} = 0.00002466 \\ c_{\theta 1} &= \frac{y_2}{f_0} - \frac{f_1 y_1}{f_0^2} = 0.000666 \\ c_{\theta 2} &= \frac{y_3}{f_0} + \frac{f_1^2 y_1}{f_0^3} - \frac{f_2 y_1 + f_1 y_2}{f_0^2} = -0.911471 \\ c_{\theta 3} &= \frac{y_1^*}{f_0} = 0.705 \\ c_{\theta 4} &= \frac{y_2^*}{f_0} - \frac{f_1 y_1^*}{f_0^2} = -1.7696 \\ c_{\theta 5} &= \frac{y_3^*}{f_0} + \frac{f_1^2 y_1^*}{f_0^3} - \frac{f_2 y_1^* + f_1 y_2^*}{f_0^2} = 50.6493 \\ c_{w0} &= \frac{A_1}{R_0} = -0.0007519 \\ c_{w1} &= -\frac{R_1 A_1}{R_0^2} + \frac{A_2}{R_0} = 0.18 \\ c_{w2} &= \frac{R_1^2 A_1}{R_0^3} - \frac{R_2 A_1 + R_1 A_1}{R_0^2} + \frac{A_3}{R_0} = 26.90 \\ c_{w3} &= \frac{A_1^*}{R_0} = 0.000106 \\ c_{w4} &= \frac{-R_1^* A_1^*}{R_0^{*2}} + \frac{A_2^*}{R_0^*} = -0.000493 \\ c_{w5} &= \frac{R_1^{*2} A_1^*}{R_0^{*3}} - \frac{R_2^* A_1^* + R_1^* A_1^*}{R_0^{*2}} + \frac{A_3^*}{R_0^*} = 194.0138 \\ c_{\sigma 0} &= \frac{x_1}{\eta_1} = 0.001511 \\ c_{\sigma 1} &= \frac{x_2}{\eta_1} - \frac{\eta_2 x_1}{\eta_1^2} = -0.03623 \\ c_{\sigma 2} &= \frac{x_1}{\eta_1} - \frac{\eta_2 x_2}{\eta_1^2} - \frac{x_1 \eta_3}{\eta_1^2} = -54.064 \\ c_{\sigma 3} &= \frac{x_1^*}{\eta_1} = -0.002985 \\ c_{\sigma 4} &= \frac{x_2^*}{\eta_1} - \frac{\eta_2 x_1^*}{\eta_1^2} = 0.07314 \\ c_{\sigma 5} &= \frac{x_1^*}{\eta_1} - \frac{\eta_2 x_2^*}{\eta_1^2} - \frac{x_1^* \eta_3}{\eta_1^2} = 53.02 \\ c_{z0} &= \frac{L_1}{\eta_1} = 0.003015 \\ c_{z1} &= \frac{L_2}{\eta_1} - \frac{\eta_2 L_1}{\eta_1^2} = -0.0722 \\ c_{z2} &= \frac{L_1}{\eta_1} - \frac{\eta_2 L_2}{\eta_1^2} - \frac{L_1 \eta_3}{\eta_1^2} = -107.88 \\ c_{z3} &= \frac{L_1^*}{\eta_1} = -0.003 \\ c_{z4} &= \frac{L_2^*}{\eta_1} - \frac{\eta_2 L_1^*}{\eta_1^2} = 0.0722 \\ c_{z5} &= \frac{L_1^*}{\eta_1} - \frac{\eta_2 L_2^*}{\eta_1^2} - \frac{L_1^* \eta_3}{\eta_1^2} = 107.88 \end{aligned} \right\} \quad (47)$$

From equation (39), we obtain

$$e^{-k_1 z} = e^{-(b_{10}s + b_{11})z} = e^{-b_{11}z} e^{-b_{10}sz},$$

and

$$e^{-k_2 z} = e^{-(b_{20}s + b_{21})z} = e^{-b_{21}z} e^{-b_{20}sz}.$$

Applying the inverse Laplace transform for equations (43, 44, 45, 46) we get θ , w , σ_{xx} , σ_{yy} and σ_{zz} in the following form

$$\theta = e^{-b_{11}z} \Theta_1 H(t - b_{10}z) + e^{-b_{21}z} \Theta_2 H(t - b_{20}z), \quad (48)$$

where

$$\Theta_1 = \left[c_{\theta 0} + c_{\theta 1}(t - b_{10}z) + \frac{c_{\theta 2}}{2}(t - b_{10}z)^2 \right],$$

$$\Theta_2 = \left[c_{\theta 3} + c_{\theta 4}(t - b_{20}z) + \frac{c_{\theta 5}}{2}(t - b_{20}z)^2 \right],$$

and also

$$w = e^{-b_{11}z} W_1 H(t - b_{10}z) + e^{-b_{21}z} W_2 H(t - b_{20}z), \quad (49)$$

where

$$W_1 = \left[c_{w0}(t - b_{10}z) + \frac{c_{w1}(t - b_{10}z)^2}{2} + \frac{c_{w2}(t - b_{10}z)^3}{6} \right],$$

$$W_2 = \left[c_{w3}(t - b_{20}z) + \frac{c_{w4}(t - b_{20}z)^2}{2} + \frac{c_{w5}(t - b_{20}z)^3}{6} \right],$$

and also

$$\begin{aligned} \sigma_{xx} = \sigma_{yy} = \\ = e^{-b_{11}z} \Sigma_1 H(t - b_{10}z) + e^{-b_{21}z} \Sigma_2 H(t - b_{20}z), \end{aligned} \quad (50)$$

where

$$\Sigma_1 = \left[c_{\sigma 0} + c_{\sigma 1}(t - b_{10}z) + c_{\sigma 2} \frac{(t - b_{10}z)^2}{2} \right],$$

$$\Sigma_2 = \left[c_{\sigma 3} + c_{\sigma 4}(t - b_{20}z) + c_{\sigma 5} \frac{(t - b_{20}z)^2}{2} \right],$$

and also

$$\sigma_{zz} = e^{-b_{11}z} Z_1 H(t - b_{10}z) + e^{-b_{21}z} Z_2 H(t - b_{20}z), \quad (51)$$

where

$$Z_1 = \left[c_{z0} + c_{z1}(t - b_{10}z) + c_{z2} \frac{(t - b_{10}z)^2}{2} \right],$$

$$Z_2 = \left[c_{z3} + c_{z4}(t - b_{20}z) + c_{z5} \frac{(t - b_{20}z)^2}{2} \right],$$

and $H(t - b_{i0}z)$ is Heavside's unit step functions. By using the convolution theorem $h(t) = \int_0^t f(\tau)g(t - \tau)d\tau$ for (48), (49), (50) and (51) we obtain under the assumption that $f(\tau) = e^{-\frac{(t_b - \tau)^2}{\varphi^2}}$; which represents the time behavior of the

intensity of the laser radiation, where t_b is the time at which $f(\tau)$ has maximum. Here φ is the time at which the intensity of the laser radiation reduces to $\frac{1}{e}$

$$\begin{aligned} \theta = e^{-b_{11}z} \left[\left(c_{\theta 0} + c_{\theta 1}(t - b_{10}z) + c_{\theta 2} \frac{(t - b_{10}z)^2}{2} + \right. \right. \\ \left. \left. + c_{\theta 2} \frac{(t - b_{10}z)^2}{2} + \frac{\varphi^2 c_{\theta 2}}{4} \right) \frac{\sqrt{\pi}}{2} \varphi \operatorname{erf} \left(\frac{t}{\varphi} \right) - c_{\theta 2} \frac{t\varphi}{4} e^{-\frac{t^2}{\varphi^2}} + \right. \\ \left. + (c_{\theta 1} + c_{\theta 2}(t - b_{10}z)) \frac{\varphi^2}{2} \left(1 - e^{-\frac{t^2}{\varphi^2}} \right) \right] + \\ + e^{-b_{21}z} \left[\left(c_{\theta 3} + c_{\theta 4}(t - b_{10}z) + c_{\theta 5} \frac{(t - b_{10}z)^2}{2} + \right. \right. \\ \left. \left. + \frac{\varphi^2 c_{\theta 5}}{4} \right) \frac{\sqrt{\pi}}{2} \varphi \operatorname{erf} \left(\frac{t}{\varphi} \right) - c_{\theta 2} \frac{t\varphi}{4} e^{-\frac{t^2}{\varphi^2}} + \right. \\ \left. + (c_{\theta 4} + c_{\theta 5}(t - b_{10}z)) \frac{\varphi^2}{2} \left(1 - e^{-\frac{t^2}{\varphi^2}} \right) \right], \end{aligned} \quad (52)$$

$$\begin{aligned} w = e^{-b_{11}z} \left[\left(c_{w0}(t - b_{10}z) + \frac{c_{w1}}{2} \left((t - b_{10}z)^2 + \frac{\varphi^2}{2} \right) + \right. \right. \\ \left. \left. + c_{w2} \left(\frac{(t - b_{10}z)^3}{6} + \frac{\varphi^2}{4} \right) \right) \frac{\sqrt{\pi}}{2} \varphi \operatorname{erf} \left(\frac{t}{\varphi} \right) - \right. \\ \left. - \left(c_{w0} + c_{w1}(t - b_{10}z) - \frac{\varphi^2 c_{w2}}{12} (\varphi^2 - (t^2 - \varphi^2)) e^{-\frac{t^2}{\varphi^2}} \right) + \right. \\ \left. + \frac{c_{w2}}{2} (t - b_{10}z)^2 \right) \frac{\varphi^2}{2} \left(1 - e^{-\frac{t^2}{\varphi^2}} \right) - \right. \\ \left. - \frac{1}{4} (c_{w1} + c_{w2}(t - b_{10}z)) t \varphi^2 e^{-\frac{t^2}{\varphi^2}} \right] + \\ + e^{-b_{21}z} \left[\left(c_{w3}(t - b_{20}z) + \frac{c_{w4}}{2} \left((t - b_{10}z)^2 + \frac{\varphi^2}{2} \right) + \right. \right. \\ \left. \left. + c_{w5} \left(\frac{(t - b_{10}z)^3}{6} + \frac{\varphi^2}{4} \right) \right) \frac{\sqrt{\pi}}{2} \varphi \operatorname{erf} \left(\frac{t}{\varphi} \right) - \right. \\ \left. - \left(c_{w3} + c_{w4}(t - b_{10}z) - \frac{\varphi^2 c_{w5}}{12} (\varphi^2 - (t^2 - \varphi^2)) e^{-\frac{t^2}{\varphi^2}} \right) + \right. \\ \left. + \frac{c_{w5}}{2} (t - b_{10}z)^2 \right) \frac{\varphi^2}{2} \left(1 - e^{-\frac{t^2}{\varphi^2}} \right) - \right. \\ \left. - \frac{1}{4} (c_{w4} + c_{w5}(t - b_{10}z)) t \varphi^2 e^{-\frac{t^2}{\varphi^2}} \right], \end{aligned} \quad (53)$$

$$\begin{aligned} \sigma_{zz} = e^{-b_{11}z} \left[\left(c_{z0} + c_{z1}(t - b_{10}z) + \frac{c_{z2}}{2} (t - b_{10}z)^2 + \right. \right. \\ \left. \left. + \frac{\varphi^2 c_{z2}}{4} \right) \frac{\sqrt{\pi}}{2} \varphi \operatorname{erf} \left(\frac{t}{\varphi} \right) - \frac{c_{z2}}{4} t \varphi e^{-\frac{t^2}{\varphi^2}} + \right. \\ \left. + (c_{z1} + c_{z2}(t - b_{10}z)) \frac{\varphi^2}{2} \left(1 - e^{-\frac{t^2}{\varphi^2}} \right) \right] + \\ + e^{-b_{11}z} \left[\left(c_{z3} + c_{z4}(t - b_{10}z) + \frac{c_{z5}}{2} (t - b_{10}z)^2 + \right. \right. \\ \left. \left. + \frac{\varphi^2 c_{z5}}{4} \right) \frac{\sqrt{\pi}}{2} \varphi \operatorname{erf} \left(\frac{t}{\varphi} \right) - \frac{c_{z5}}{4} t \varphi e^{-\frac{t^2}{\varphi^2}} + \right. \\ \left. + (c_{z4} + c_{z5}(t - b_{10}z)) \frac{\varphi^2}{2} \left(1 - e^{-\frac{t^2}{\varphi^2}} \right) \right], \end{aligned} \quad (54)$$

$$\begin{aligned}
 \sigma_{xx} = \sigma_{yy} = e^{-b_{11}z} & \left[\left(c_{\sigma 0} + c_{\sigma 1}(t - b_{10}z) + \right. \right. \\
 & + \frac{c_{\sigma 2}}{2}(t - b_{10}z)^2 + \frac{\varphi^2 c_{\sigma 2}}{4} \left. \right) \frac{\sqrt{\pi}}{2} \operatorname{erf} \left(\frac{t}{\varphi} \right) - \frac{c_{\sigma 2} \varphi}{4} t e^{-\frac{t^2}{\varphi^2}} + \\
 & + (c_{\sigma 1} + c_{\sigma 2}(t - b_{10}z)) \frac{\varphi^2}{2} \left(1 - e^{-\frac{t^2}{\varphi^2}} \right) \left. \right] + \\
 & + e^{-b_{21}z} \left[\left(c_{\sigma 3} + c_{\sigma 4}(t - b_{20}z) + \frac{c_{\sigma 5}}{2}((t - b_{10}z)^2 + \right. \right. \\
 & + \frac{c_{\sigma 5} \varphi^2}{4} \left. \right) \varphi \frac{\sqrt{\pi}}{2} \operatorname{erf} \left(\frac{t}{\varphi} \right) - \frac{\varphi c_{\sigma 5}}{4} t e^{-\frac{t^2}{\varphi^2}} + \\
 & + (c_{\sigma 4} + c_{\sigma 5}(t - b_{10}z)) \frac{\varphi^2}{2} \left(1 - e^{-\frac{t^2}{\varphi^2}} \right) \left. \right].
 \end{aligned} \tag{55}$$

4 Computation and discussions

We have calculated the spatial temperature, displacement and stress θ , w , σ_{xx} , σ_{yy} and σ_{zz} with the time as a parameter for a heated target with a spatial homogeneous laser radiation having a temporally Gaussian distributed intensity with a width of (10E-3 s). We have performed the computation for the physical parameters $T_0 = 293$ K, $\rho = 8954$ Kg/m³,

$$\begin{aligned}
 A &= 0.01, \quad c_E = 383.1 \text{ J/kgK}, \\
 \varphi &= 10^{-3} \text{ s}, \quad \epsilon = g_1 g_2 = 0.01680089, \\
 \alpha_t &= 1.78(10^{-5}) \text{ K}^{-1}, \quad k = 386 \text{ W/mK}, \\
 \lambda &= 7.76(10^{10}) \text{ kg/m sec}^2, \quad \mu = 3.86(10)^{10} \text{ kg/m sec}^2
 \end{aligned}$$

and

$$t_0 = 0.02 \text{ sec}$$

for Cu as a target. We obtain the results displayed in the following figures.

Considering surface absorption the obtained results in Figure 1 show the temperature θ , Figure 2 display the temporal temperature distribution and the temporal behavior of the laser radiation, Figure 3 for the displacement w , Figure 4 for the stress σ_{zz} and Figure 5 for the stresses σ_{xx} and σ_{yy} .

The coupled system of differential equations describing the thermoelasticity treated through the Laplace transform of a temporally Dirac distributed laser radiation illuminating homogeneous a semi-infinite target and absorbed at its irradiated surface. Since the system is linear the response of the system on the Dirac function was convoluted with a temporally Gaussian distributed laser radiation. The theoretical obtained results were applied on the Cu target. Figure 1 illustrates the calculated spatial distribution of the temperature per unit intensity at different values of the time parameter ($t = 0.005, 0.007, 0.01, 0.015, \text{ and } 0.02$). From the curves it is evident that the temperature has a finite velocity expressed through the strong gradient of the temperature which moves deeper in the target as the time increases.

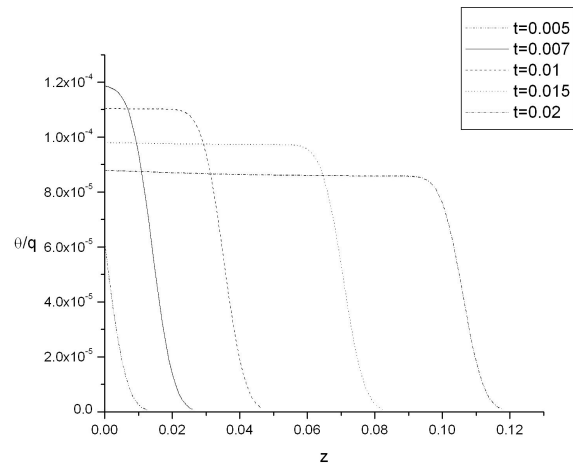


Fig. 1: The temperature distribution θ per unit intensity versus z with the time as a parameter.

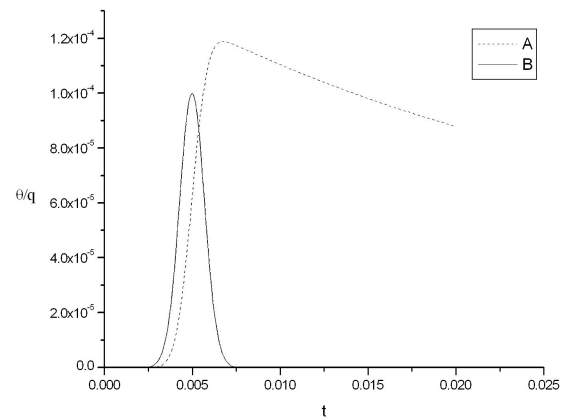


Fig. 2: (A) The temporal temperature distribution θ per unit intensity form the. (B) The temporal behavior of the laser radiation which is assumed to have a Gaussian distribution with width $\varphi = 10^{-3}$ s.

Figure 2 represent the calculated front temporal temperature distribution per unit intensity (curve A); as a result of the temporal behavior of the laser radiation which is assumed to have a Gaussian distribution with a width equals to (10E-3 s) (curve B). From the figure it is evident that the temperature firstly increases with increasing the time this can be attributed to the increased absorbed energy which over compensates the heat losses given by the heat conductivity inside the material. As the absorbed power equals the conducted one inside the material the temperature attains its maximum value. the maximum of the temperature occurs at later time than the maximum of the radiation this is the result of the heat conductivity of Cu and the relatively small gradient of the temperature in the vicinity of $z = 0$ as seen from Figure 1. After the radiation becomes weak enough such that it can not compensate the diffused power inside the material the temperature decreases monotonically with increasing time.

Figure 3 shows the calculated spatial displacement per unit intensity at different times(0.01,0.015 and 0.02). The

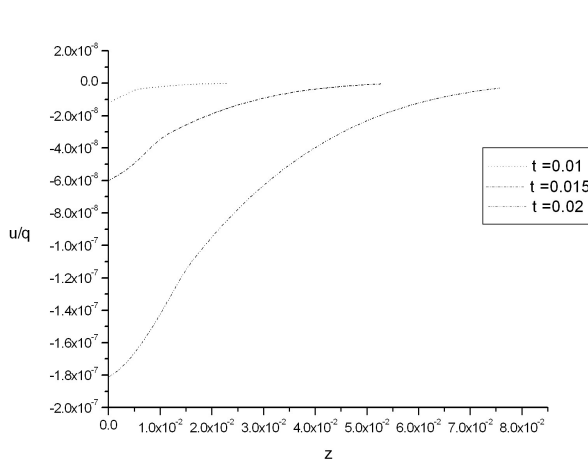


Fig. 3: The displacement distribution u per unit intensity versus z with the time as a parameter.

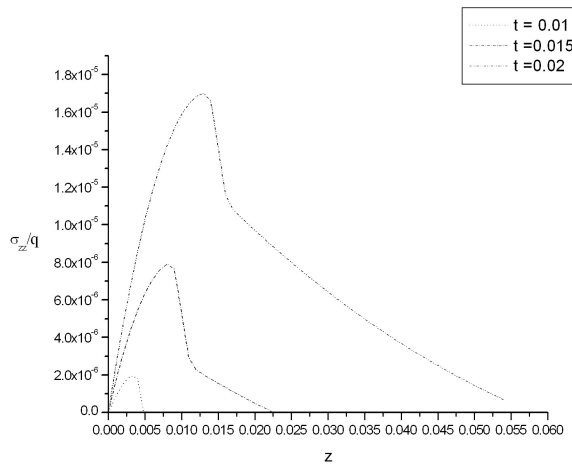


Fig. 4: The stress σ_{zz} distribution per unit intensity versus z with the time as a parameter.

displacement increases monotonically with time. It attains smaller gradient with increasing z . Both effects can be attributed to the temperature behavior. The negative displacement results from the co-ordinate system which is located at the front surface with positive direction of the z -axis pointing down words.

Figure 4 illustrates the spatial distribution of stress σ_{zz} per unit intensity at the times (0.01, 0.015 and 0.02). Since, $\sigma_{zz} = \alpha e - \lambda_1 \theta$, thus from Figure 3 σ_{zz} attains maxima at the locations for which the gradient of the displacement exhibits maxima and this is practically at the same points for which σ_{zz} is maximum. The calculations showed that σ_{xx} and σ_{yy} have the same behavior as σ_{zz} .

5 Results and conclusions

The thermoelasticity problem formulated by a coupled linear system of partial differential equations was discussed. The system was decoupled to provide a fourth order linear differential equations which were solved analytically using Laplace

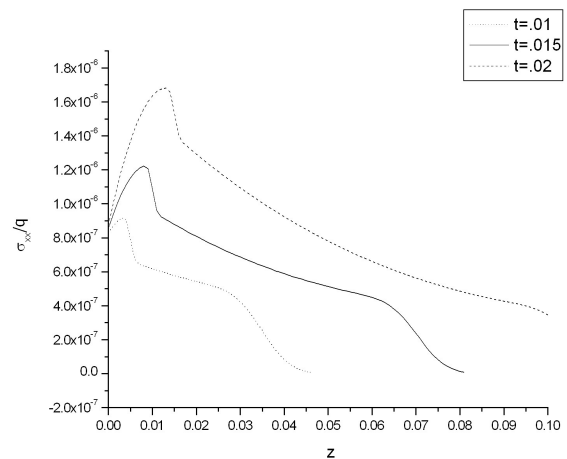


Fig. 5: The stress distribution σ_{xx} and σ_{yy} per unit intensity versus z with the time as a parameter.

transform. The small time approximation analysis was performed for the solution of temperature, displacement and for the stresses; showing that the finite velocity of the temperature described by the D.Es system was not affected by the small time approximation.

Acknowledgements

The authors want to thanks Dr. Ezzat F. Honin for his valuable discussions and comments.

Submitted on June 25, 2008 / Accepted on August 15, 2008

References

1. Biot M. Thermoelasticity and irreversible thermo-dynamics. *J. Appl. Phys.*, 1956, v. 27, 240–253.
2. Lord H. and Shulman Y. A generalized dynamical theory of thermoelasticity. *J. Mech. Phys. Solid.*, 1967, v. 15, 299–309.
3. Bondi H. Negative mass in General Relativity. *Review of Modern Physics*, 1957, v. 29 (3), 423–428.
4. Dhaliwal R. and Sherief H. Generalized thermoelasticity for anisotropic media. *Quatr. Appl. Math.*, 1980, v. 33, 1–8.
5. Hassan A.F., El-Nicklawy M.M., El-Adawi M.K., Nasr E.M., Hemida A.A. and Abd El-Ghaffar O.A. Heating effects induced by a pulsed laser in a semi-infinite target in view of the theory of linear systems. *Optics & Laser Technology*, 1996, v. 28 (5), 337–343.
6. Hetnarski R. Coupled one-dimensional thermal shock problem for small times. *Arch. Mech. Stosow.*, 1961, v. 13, 295–306.
7. Sherief H. and Dhaliwal R. Generalized one-dimensional thermal shock problem for small times. *J. Thermal Stresses.*, 1981, v. 4, 407–420.

Nature of the Excited States of the Even-Even ⁹⁸⁻¹⁰⁸Ru Isotopes

Sohair M. Diab* and Salah A. Eid†

*Faculty of Education, Phys. Dept., Ain Shams University, Cairo, Egypt

†Faculty of Engineering, Phys. Dept., Ain Shams University, Cairo, Egypt

E-mail: mppe2@yahoo.co.uk

The positive and negative parity states of the even-even ⁹⁸⁻¹⁰⁸Ru isotopes are studied within the frame work of the interacting boson approximation model ($IBA - 1$). The calculated levels energy, potential energy surfaces, $V(\beta, \gamma)$, and the electromagnetic transition probabilities, $B(E1)$ and $B(E2)$, show that ruthenium isotopes are transitional nuclei. Staggering effect, $\Delta I = 1$, has been observed between the positive and negative parity states in some of ruthenium isotopes. The electric monopole strength, $X(E0/E2)$, has been calculated. All calculated values are compared with the available experimental and theoretical data where reasonable agreement has obtained.

1 Introduction

The mass region $A = 100$ has been of considerable interest for nuclear structure studies as it shows many interesting features. These nuclei show back bending at high spin and shape transitions from vibrational to γ -soft and rotational characters. Many attempts have been made to explore these structural changes which is due mainly to the n-p interactions.

Experimentally, the nuclear reaction ¹⁰⁰Mo (α, xn) [1] has been used in studying levels energy of ¹⁰⁰Ru. Angular distribution, γ - γ coincidences were measured, half life time has been calculated and changes to the level scheme were proposed. Also, double beta decay rate of ¹⁰⁰Mo to the first excited 0^+ state of ¹⁰⁰Ru has been measured experimentally [2] using γ - γ coincidence technique.

Doppler-shift attenuation measurements following the ¹⁰⁰Ru ($n, n'\gamma$) reaction [3] has been used to measure the life times of the excited states in ¹⁰⁰Ru. Absolute transition rates were extracted and compared with the interacting boson model description. The 2^+ (2240.8 keV) state which decays dominantly to the 2^+ via 1701 keV transition which is almost pure $M1$ in nature considered as a mixed-symmetry state. Again ¹⁰⁰Ru has been studied [4] experimentally and several levels were seen where some new ones are detected below 3.2 MeV.

The excited states of ¹⁰²Ru have been investigated using ⁹⁶Zr (¹⁰B, $p3n$) reaction [5] at a beam of energy 42 MeV and the emitted γ rays were detected. The analysis indicated that the nucleus is a γ -soft and the band crossing as well as staggering effect have been observed.

Theoretically many models have been applied to ruthenium isotopes. Yukawa folded mean field [6] has been applied to ¹⁰⁰Ru nucleus while the microscopic vibrational model has been applied to ¹⁰⁴Ru and some other nuclei with their daughters [7]. The latter model was successful in describing the yrast 0^+ and 2^+ states of most of these nuclei and also some of their half-lives.

The very high-spin states of nuclei near $A \approx 100$ are inves-

tigated by the Cranked Strutinsky method [8] and many very extended shape minima are found in this region. Interacting boson model has been used in studying Ru isotopes using a $U(5)-O(6)$ transitional Hamiltonian with fixed parameters [9, 10] except for the boson number N . The potential arising from a coherent-state analysis indicate that ¹⁰⁴Ru is close to the critical point between spherical and γ -unstable structures.

Hartree-Fock Bogoliubov [11] wave functions have been tested by comparing the theoretically calculated results for ¹⁰⁰Mo and ¹⁰⁰Ru nuclei with the available experimental data. The yrast spectra, reduced $B(E2, 0^+ \rightarrow 2^+)$ transition probabilities, quadrupole moments $Q(2^+)$ and g factors, $g(2^+)$ are computed. A reasonable agreement between the calculated and observed has been obtained.

The microscopic anharmonic vibrator approach (MAVA) [12] has been used in investigating the low-lying collective states in ⁹⁸⁻¹⁰⁸Ru. Analysis for the level energies and electric quadrupole decays of the two-phonon type of states indicated that ¹⁰⁰Ru can be interpreted as being a transitional nucleus between the spherical anharmonic vibrator ⁹⁸Ru and the quasirotational ¹⁰²⁻¹⁰⁶Ru isotopes.

A new empirical approach has been proposed [13] which is based on the connection between transition energies and spin. It allows one to distinguish vibrational from rotational characters in atomic nuclei. The cranked interacting boson model [14] has been used in estimating critical frequencies for the rotation-induced spherical-to-deformed shape transition in $A = 100$ nuclei. The predictions show an agreement with the back bending frequencies deduced from experimental yrast sequences in these nuclei.

The aim of the present work is to use the $IBA - 1$ [15-17] for the following tasks:

- (1) calculating the potential energy surfaces, $V(\beta, \gamma)$, to know the type of deformation exists;
- (2) calculating levels energy, electromagnetic transition rates $B(E1)$ and $B(E2)$;

nucleus	<i>EPS</i>	<i>PAIR</i>	<i>ELL</i>	<i>QQ</i>	<i>OCT</i>	<i>HEX</i>	<i>E2SD(eb)</i>	<i>E2DD(eb)</i>
⁹⁸ Ru	0.6280	0.000	0.0090	-0.0010	0.0000	0.0000	0.1250	-0.3698
¹⁰⁰ Ru	0.5950	0.000	0.0085	-0.0200	0.0000	0.0000	0.1160	-0.3431
¹⁰² Ru	0.5650	0.0000	0.0085	-0.0200	0.0000	0.0000	0.1185	-0.3505
¹⁰⁴ Ru	0.4830	0.0000	0.0085	-0.0200	0.0000	0.0000	0.1195	-0.3535
¹⁰⁶ Ru	0.4560	0.0000	0.0085	-0.0200	0.0000	0.0000	0.1020	-0.3017
¹⁰⁸ Ru	0.4540	0.0000	0.0085	-0.0200	0.0000	0.0000	0.1035	-0.3062

Table 1: Parameters used in IBA-1 Hamiltonian (all in MeV).

- (3) studying the relation between the angular momentum I , the rotational angular frequency $\hbar\omega$ for bending in ruthenium isotopes;
- (4) calculating staggering effect and beat patterns to detect any interactions between the (+ve) and (-ve) parity states; and
- (5) calculating the electric monopole strength $X(E0/E2)$.

2 (IBA-1) model

2.1 Level energies

IBA-1 model was applied to the positive and negative parity states in even-even ⁹⁸⁻¹⁰⁸Ru isotopes. The Hamiltonian employed in the present calculation is:

$$\begin{aligned}
H = & EPS \cdot n_d + PAIR \cdot (P \cdot P) \\
& + \frac{1}{2} ELL \cdot (L \cdot L) + \frac{1}{2} QQ \cdot (Q \cdot Q) \\
& + 5OCT \cdot (T_3 \cdot T_3) + 5HEX \cdot (T_4 \cdot T_4),
\end{aligned} \quad (1)$$

where

$$P \cdot P = \frac{1}{2} \left[\begin{array}{c} \left\{ (s^\dagger s^\dagger)_0^{(0)} - \sqrt{5} (d^\dagger d^\dagger)_0^{(0)} \right\} x \\ \left\{ (ss)_0^{(0)} - \sqrt{5} (\tilde{d}\tilde{d})_0^{(0)} \right\} \end{array} \right]_0, \quad (2)$$

$$L \cdot L = -10 \sqrt{3} \left[(d^\dagger \tilde{d})^{(1)} x (d^\dagger \tilde{d})^{(1)} \right]_0, \quad (3)$$

$$Q \cdot Q = \sqrt{5} \left[\begin{array}{c} \left\{ (S^\dagger \tilde{d} + d^\dagger s)^{(2)} - \frac{\sqrt{7}}{2} (d^\dagger \tilde{d})^{(2)} \right\} x \\ \left\{ (s^\dagger \tilde{d} + \tilde{d}s)^{(2)} - \frac{\sqrt{7}}{2} (d^\dagger \tilde{d})^{(2)} \right\} \end{array} \right]_0, \quad (4)$$

$$T_3 \cdot T_3 = -\sqrt{7} \left[(d^\dagger \tilde{d})^{(2)} x (d^\dagger \tilde{d})^{(2)} \right]_0, \quad (5)$$

$$T_4 \cdot T_4 = 3 \left[(d^\dagger \tilde{d})^{(4)} x (d^\dagger \tilde{d})^{(4)} \right]_0. \quad (6)$$

In the previous formulas, n_d is the number of boson; $P \cdot P$, $L \cdot L$, $Q \cdot Q$, $T_3 \cdot T_3$ and $T_4 \cdot T_4$ represent pairing, angular momentum, quadrupole, octupole and hexadecupole interactions

between the bosons; *EPS* is the boson energy; and *PAIR*, *ELL*, *QQ*, *OCT*, *HEX* is the strengths of the pairing, angular momentum, quadrupole, octupole and hexadecupole interactions.

2.2 Transition rates

The electric quadrupole transition operator employed in this study is:

$$\begin{aligned}
T^{(E2)} = & E2SD \cdot (s^\dagger \tilde{d} + d^\dagger s)^{(2)} + \\
& + \frac{1}{\sqrt{5}} E2DD \cdot (d^\dagger \tilde{d})^{(2)}.
\end{aligned} \quad (7)$$

The reduced electric quadrupole transition rates between $I_i \rightarrow I_f$ states are given by

$$B(E2, I_i - I_f) = \frac{[\langle I_f || T^{(E2)} || I_i \rangle]^2}{2I_i + 1}. \quad (8)$$

3 Results and discussion

3.1 The potential energy surfaces

The potential energy surfaces [18], $V(\beta, \gamma)$, as a function of the deformation parameters β and γ are calculated using:

$$\begin{aligned}
E_{N_\pi N_\nu}(\beta, \gamma) = & \langle N_\pi N_\nu; \beta \gamma | H_{\pi\nu} | N_\pi N_\nu; \beta \gamma \rangle = \\
= & \zeta_d (N_\nu N_\pi) \beta^2 (1 + \beta^2) + \beta^2 (1 + \beta^2)^{-2} \times \\
& \times \{ k N_\nu N_\pi [4 - (\bar{X}_\pi \bar{X}_\nu) \beta \cos 3\gamma] \} + \\
& + \left\{ [\bar{X}_\pi \bar{X}_\nu \beta^2] + N_\nu (N_\nu - 1) \left(\frac{1}{10} c_0 + \frac{1}{7} c_2 \right) \beta^2 \right\},
\end{aligned} \quad (9)$$

where

$$\bar{X}_\rho = \left(\frac{2}{7} \right)^{0.5} X_\rho \quad \rho = \pi \text{ or } \nu. \quad (10)$$

The calculated potential energy surfaces, $V(\beta, \gamma)$, are presented in Fig. 1. It shows that ⁹⁸Ru is a vibrational — like nucleus while ¹⁰⁰⁻¹⁰⁴Ru are γ -soft where the two wells on the oblate and prolate sides are equal. ^{106,108}Ru are rotational - like where they are prolate deformed.

$I_i^+ I_f^+$	^{98}Ru	^{100}Ru	^{102}Ru	^{104}Ru	^{106}Ru	^{108}Ru
0 ₁ Exp*. 2 ₁	0.392(12)	0.490(5)	0.630(10)	0.820(12)	0.770(20)	1.010(15)
0 ₁ Theor. 2 ₁	0.3930	0.4853	0.6279	0.8274	0.7737	1.0110
2 ₁ 0 ₁	0.0786	0.0970	0.1256	0.1655	0.1547	0.2022
2 ₂ 0 ₁	0.0000	0.0006	0.0012	0.0027	0.0032	0.0040
2 ₂ 0 ₂	0.0226	0.0405	0.0548	0.0826	0.0870	0.1257
2 ₃ 0 ₁	0.0000	0.0000	0.0000	0.0002	0.0006	0.0017
2 ₃ 0 ₂	0.0658	0.0759	0.0993	0.1135	0.0853	0.0830
2 ₃ 0 ₃	0.0093	0.0087	0.0121	0.0207	0.0264	0.0402
2 ₄ 0 ₃	0.0041	0.0066	0.0121	0.0286	0.0448	0.0795
2 ₄ 0 ₄	0.0565	0.0588	0.0712	0.0786	0.0530	0.0448
4 ₁ 2 ₁	0.1260	0.1683	0.2257	0.3071	0.2912	0.3791
4 ₁ 2 ₂	0.0092	0.0142	0.0190	0.0271	0.0267	0.0360
4 ₁ 2 ₃	0.0269	0.0319	0.0424	0.0498	0.0384	0.0386
6 ₁ 4 ₁	0.1420	0.2039	0.2838	0.3897	0.3681	0.4747
6 ₁ 4 ₂	0.0172	0.0179	0.0228	0.0285	0.0256	0.0323
6 ₁ 4 ₃	0.0208	0.0242	0.0333	0.0382	0.0292	0.0300
8 ₁ 6 ₁	0.1264	0.2032	0.2998	0.4208	0.4012	0.5194
8 ₁ 6 ₂	0.0247	0.0183	0.0223	0.0256	0.0217	0.0265
8 ₁ 6 ₃	0.0113	0.0157	0.0239	0.0286	0.0228	0.0247
10 ₁ 8 ₁	0.0791	0.1678	0.2768	0.4081	0.3997	0.5264
10 ₁ 8 ₂	0.0319	0.0175	0.0207	0.0224	0.0183	0.0217

*Ref. 19.

Table 2: Values of the theoretical reduced transition probability, $B(E2)$ (in $e^2 b^2$).

$I_i^+ I_f^+$	^{98}Ru	^{100}Ru	^{102}Ru	^{104}Ru	^{106}Ru	^{108}Ru
1 ₁ 0 ₁	0.0000	0.0030	0.0050	0.0104	0.0176	0.0261
1 ₁ 0 ₂	0.1084	0.1280	0.1285	0.1280	0.1258	0.1227
3 ₁ 2 ₁	0.1055	0.1211	0.1219	0.1306	0.1432	0.1564
3 ₁ 2 ₂	0.0470	0.0415	0.0471	0.0544	0.0618	0.0712
3 ₁ 2 ₃	0.0013	0.0002	0.0000	—	0.7737	—
3 ₂ 2 ₁	0.0158	0.0024	0.0018	0.0029	0.0067	0.0130
3 ₂ 2 ₂	0.0347	0.0197	0.0136	0.0102	0.0104	0.0121
3 ₂ 2 ₃	0.1600	0.2126	0.2119	0.1943	0.1660	0.1352
5 ₁ 4 ₁	0.2261	0.2533	0.2533	0.2605	0.2737	0.2881
5 ₁ 4 ₂	0.0608	0.0480	0.0563	0.0648	0.0714	0.0784
5 ₁ 4 ₃	0.0020	0.0006	—	—	0.7737	—
7 ₁ 6 ₁	0.3657	0.3950	0.3912	0.3970	0.4083	0.4213
7 ₁ 6 ₂	0.0609	0.0446	0.0551	0.0641	0.0701	0.0757
9 ₁ 8 ₁	0.5276	0.5439	0.5367	0.5386	0.5465	0.5568
9 ₁ 8 ₂	0.0425	0.0342	0.0472	0.0574	0.0640	0.0695
11 ₁ 10 ₁	0.7143	0.6983	0.6872	0.6845	0.6882	0.6951

Table 3: Values of the theoretical reduced transition probability, $B(E1)$ (in $\mu e^2 b$).

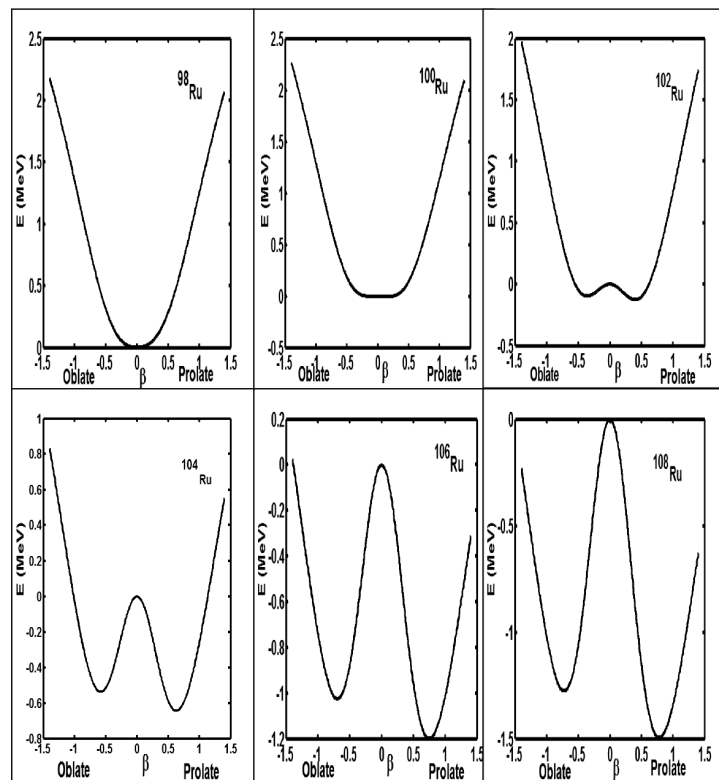


Fig. 1: Potential energy surfaces for $^{98-108}\text{Ru}$ nuclei.

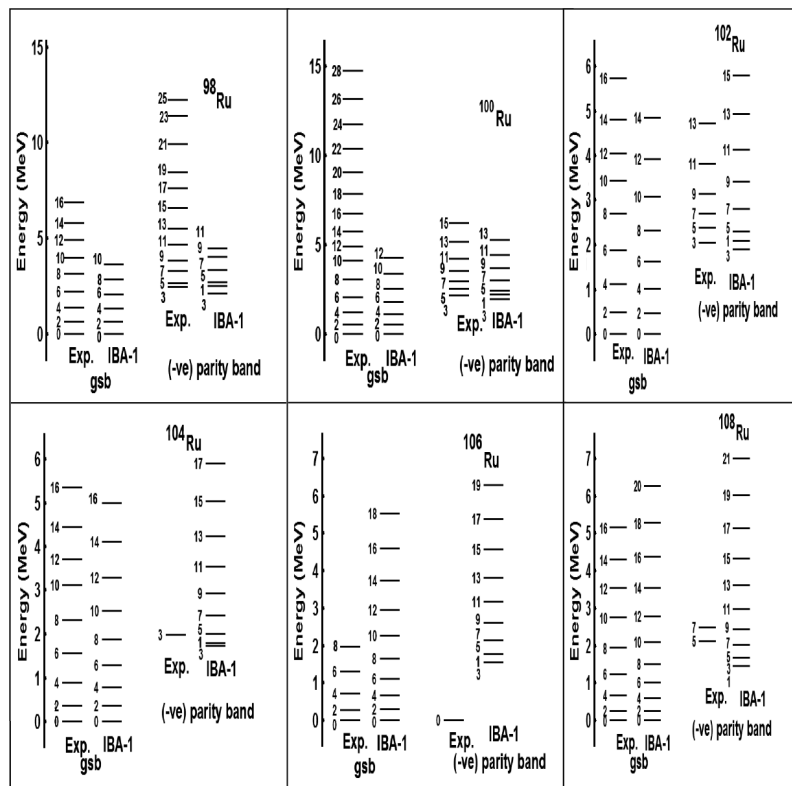


Fig. 2: Comparison between exp. [21–26] and theoretical (IBA-1) energy levels.

I_i^+	I_f^+	I_{if}^+	^{98}Ru	^{100}Ru	^{102}Ru	^{104}Ru	^{106}Ru	^{108}Ru
0 ₂	0 ₁	2 ₁	0.011	0.027	0.057	0.166	0.213	0.227
0 ₃	0 ₁	2 ₁	0.250	0.347	1.333	0.894	1.076	1.328
0 ₃	0 ₁	2 ₂	0.001	0.009	0.005	0.010	0.086	0.112
0 ₃	0 ₁	2 ₃	1.000	0.042	0.026	0.024	0.043	0.130
0 ₃	0 ₂	2 ₁	—	0.086	0.500	0.421	0.184	0.171
0 ₃	0 ₂	2 ₂	—	0.002	0.002	0.004	0.014	0.014
0 ₃	0 ₂	2 ₃	—	0.010	0.010	0.011	0.007	0.016
0 ₄	0 ₁	2 ₂	1.600	0.010	0.046	—	—	—
0 ₄	0 ₁	2 ₃	0.024	0.010	0.003	—	—	—
0 ₄	0 ₁	2 ₄	0.363	0.113	0.003	—	—	—
0 ₄	0 ₂	2 ₂	1.200	0.030	0.097	—	—	—
0 ₄	0 ₂	2 ₃	0.018	0.034	0.070	0.114	0.476	0.808
0 ₄	0 ₂	2 ₄	0.272	0.340	0.142	1.035	3.696	2.082
0 ₄	0 ₃	2 ₁	0.111	0.454	—	—	0.558	0.458
0 ₄	0 ₃	2 ₂	0.600	0.010	0.010	—	0.002	0.611
0 ₄	0 ₃	2 ₃	0.009	0.011	0.007	—	0.074	0.058
0 ₄	0 ₃	2 ₄	0.136	0.113	0.015	—	0.575	0.150

Table 4. Theoretical $X_{if} (E0/E2)$ in Ru isotopes.

3.2 Energy spectra

The energy of the positive and negative parity states of ruthenium series of isotopes are calculated using computer code PHINT [20]. A comparison between the experimental spectra [21–26] and our calculations, using values of the model parameters given in Table 1 for the ground state band are illustrated in Fig. 2. The agreement between the calculated levels energy and their correspondence experimental values for all nuclei are slightly higher especially for the higher excited states. We believe this is due to the change of the projection of the angular momentum which is due mainly to band crossing.

Unfortunately there is no enough measurements of electromagnetic transition rates $B(E1)$ or $B(E2)$ for these series of nuclei. The only measured $B(E2, 0_1^+ \rightarrow 2_1^+)$'s are presented, in Table 2 for comparison with the calculated values. The parameters $E2SD$ and $E2DD$ are used in the computer code NPBEM [20] for calculating the electromagnetic transition rates after normalization to the available experimental values and displayed in Table 1.

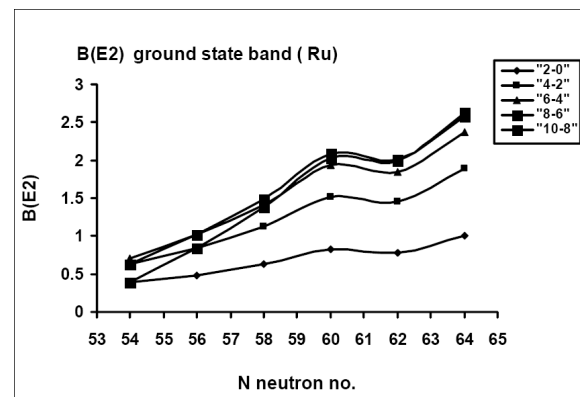
No new parameters are introduced for calculating electromagnetic transition rates $B(E1)$ and $B(E2)$ of intraband and interband. Some of the calculated values are presented in Fig. 3 and show bending at $N = 60, 62$ which means there is an interaction between the $(+ve)$ and $(-ve)$ parity states of the ground state band.

The moment of inertia I and angular frequency $\hbar\omega$ are calculated using equations (11, 12):

$$\frac{2I}{\hbar^2} = \frac{4I - 2}{\Delta E(I \rightarrow I - 2)}, \quad (11)$$

$$(\hbar\omega)^2 = (I^2 - I + 1) \left[\frac{\Delta E(I \rightarrow I - 2)}{(2I - 1)} \right]^2. \quad (12)$$

The plots in Fig. 4 show back bending at angular momentum $I^+ = 10$ for $^{98-108}\text{Ru}$ except ^{106}Ru where there is no experimental data available. It means, there is a crossing between the $(+ve)$ and $(-ve)$ parity states in the ground state band which confirmed by calculating staggering effect to these series of nuclei and the bending observed in Fig. 3.

Fig. 3: The calculated $B(E2)$'s for the ground state band.

3.3 Electric monopole transitions

The electric monopole transitions, $E0$, are normally occurring between two states of the same spin and parity by transferring energy and zero unit of angular momentum. The strength of the electric monopole transition, $X_{if} (E0/E2)$, [27] can be calculated using equations (13, 14) and presented

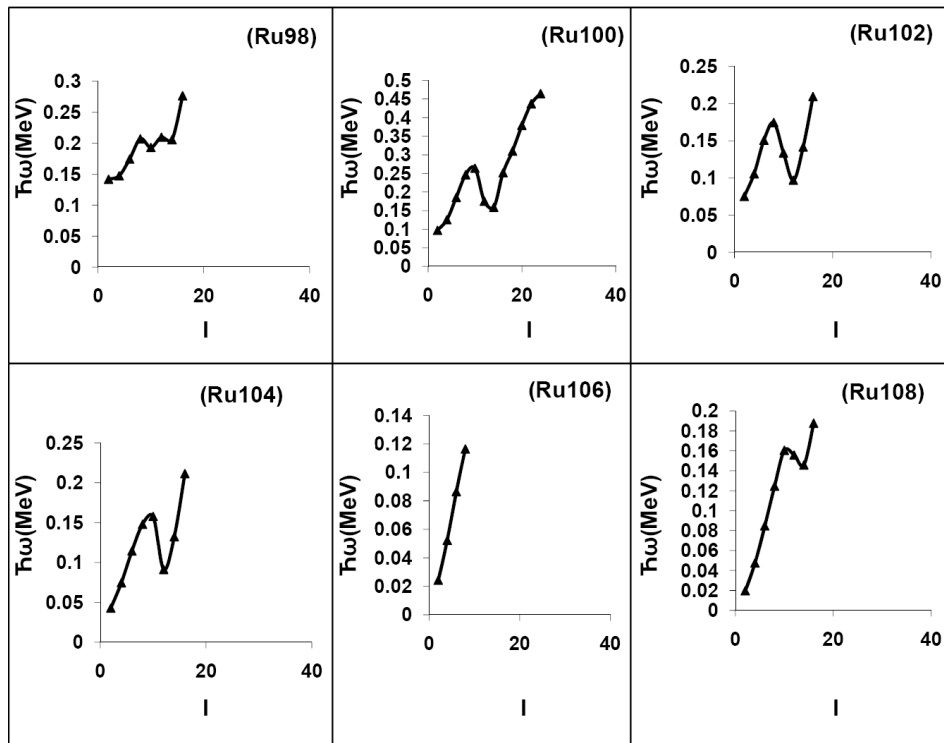


Fig. 4: Angular momentum I as a function of $(\hbar\omega)$.

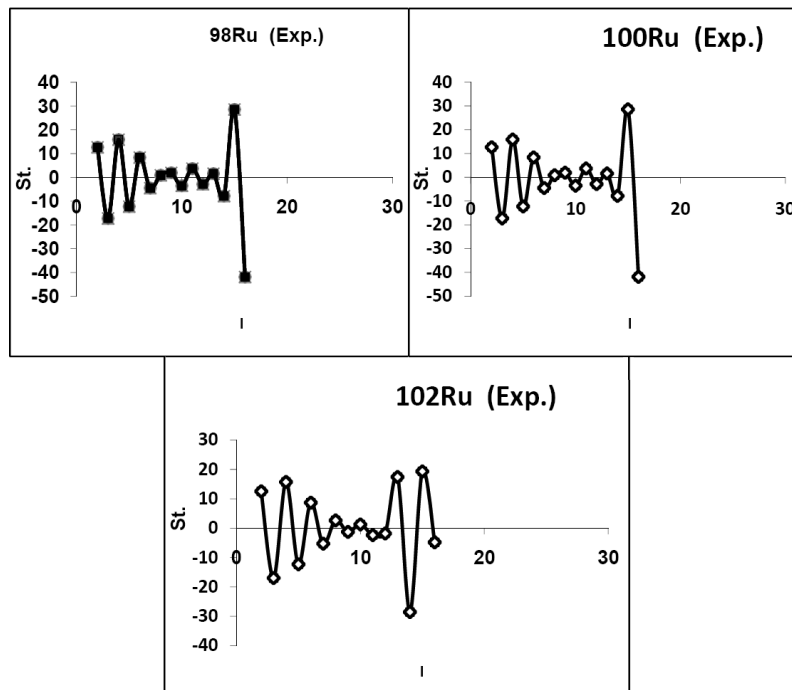


Fig. 5: $\Delta I = 1$, staggering patterns for $^{98-102}\text{Ru}$ isotopes.

in Table 4

$$X_{if'f}(E0/E2) = \frac{B(E0, I_i - I_f)}{B(E2, I_i - I_f)}, \quad (13)$$

$$X_{if'f}(E0/E2) = (2.54 \times 10^9) A^{3/4} \times \frac{E_\gamma^5(\text{MeV})}{\Omega_{KL}} \alpha(E2) \frac{T_e(E0, I_i - I_f)}{T_e(E2, I_i - I_f)}. \quad (14)$$

3.4 The staggering

The presence of $(+ve)$ and $(-ve)$ parity states has encouraged us to study staggering effect [28–30] for $^{98-108}\text{Ru}$ series of isotopes using staggering function equations (15, 16) with the help of the available experimental data [21–26].

$$\text{Stag}(I) = 6\Delta E(I) - 4\Delta E(I-1) - 4\Delta E(I+1) + \Delta E(I+2) + \Delta E(I-2), \quad (15)$$

with

$$\Delta E(I) = E(I+1) - E(I). \quad (16)$$

The calculated staggering patterns are illustrated in Fig. 5 and show an interaction between the $(+ve)$ and $(-ve)$ parity states for the ground state of $^{98-102}\text{Ru}$ nuclei.

3.5 Conclusions

IBA-1 model has been applied successfully to $^{98-108}\text{Ru}$ isotopes and we have got:

1. The levels energy are successfully reproduced;
2. The potential energy surfaces are calculated and show vibrational-like to ^{98}Ru , γ -soft to $^{100-104}\text{Ru}$ and rotational characters to $^{106-108}\text{Ru}$ isotopes where they are mainly prolate deformed nuclei;
3. Electromagnetic transition rates $B(E1)$ and $B(E2)$ are calculated;
4. Bending for $^{98-108}\text{Ru}$ has been observed at angular momentum $I^+ = 10$ except for ^{106}Ru , where there is no experimental data are available;
5. Electromagnetic transition rates $B(E1)$ and $B(E2)$ are calculated;
6. Strength of the electric monopole transitions $X_{if'f}(E0/E2)$ are calculated; and
7. Staggering effect has been calculated and beat patterns are obtained which show an interaction between the $(-ve)$ and $(+ve)$ parity states for $^{98-102}\text{Ru}$.

Submitted on August 23, 2008 / Accepted on August 29, 2008

References

1. Maazek J., Honusek M., Spalek A., Bielicik J., Slivova J. and Pasternak A. A. *Acta Physica Polonica B*, 1998, v. 29, 433.

2. Braecheleer L. L., Hornish M., Barabash A. and Umatov V. *Phys. Rev.*, 2001, v. 86, 3510.
3. Genilloud L., Brown T. B., Corminboeuf F., Garrett P. E., Hannant C. D., Jolie J., Warr N. and Yates S. W. *Nucl. Phys. A*, 2001, v. 683, 287.
4. Horodyski-Matsushigue L. H., Rodrigues C. L., Sampaio F. C. and Lewin T. B. *Nucl. Phys. A*, 2002, v. 709, 73.
5. Lalkovski S. L., Rainovski G., Starosta K., Carpenter M. P., Fossan D. B., Finnigan S., Ilieva S., Joshi P., Koike T., Paul E. S., Pietralla N., Vaman C. and Wadsworth R. *Phys. Rev. C*, 2005, v. 71, 034318.
6. Nerlo-Pomorska B., Pomorski K. and Bartel J. *Phys. Rev. C*, 2006, v. 74, 034327.
7. Raina P. K. and Dhiman R. K. *Phys. Rev. C*, 2001, v. 64, 024310.
8. Chasman R. R. *Phys. Rev. C*, 2001, v. 64, 024311.
9. Frank A., Alonso C. E. and Arias J. M. *Phys. Rev. C*, 2001, v. 65, 014301.
10. Cejnar P., Jolie J. and Kern J. *Phys. Rev. C*, 2001, v. 63, 047304.
11. Chaturvedi K., Dixit B. M. and Rath P. K. *Phys. Rev. C*, 2003, v. 67, 064317.
12. Kotila J., Suhonen J. and Delion D. S. *Phys. Rev. C*, 2003, v. 68, 054322.
13. Regan P. H., Beausang C. W., Zamfir N. V., Casten R. F., Zhang J., Meyer D. A. and Ressler J. J. *Phys. Rev. Lett.*, 2003, v. 90, 152502.
14. Cejnar P. and Jolie J. *Phys. Rev. C*, 2004, v. 69, 011301.
15. Arima A. and Iachello F. *Ann. Phys. (N.Y.)*, 1976, v. 99, 253.
16. Arima A. and Iachello F. *Ann. Phys. (N.Y.)*, 1978, v. 111, 201.
17. Arima A. and Iachello F. *Ann. Phys. (N.Y.)*, 1979, v. 123, 468.
18. Ginocchio J. N. and Kirson M. W. *Nucl. Phys. A*, 1980, v. 350, 31.
19. Raman S., de Nestor C. W., JR. and Tikkanen P. *Atomic Data and Nucl. Data Tab.*, 2001, v. 78, 128.
20. Scholten O. *The program package PHINT (1980) version, internal report KVI-63, Gronigen: Keryfysisch Versneller Institut.*
21. Singh B. and Zhiqiang H. U *Nucl. Data Sheets*, 2003, v. 98, 335.
22. Singh B. *Nucl. Data Sheets*, 1997, v. 81, 1997.
23. Frenne D. D. and Jacobs E. *Nucl. Data Sheets*, 1998, v. 83, 535.
24. Blachot J. *Nucl. Data Sheets*, 1991, v. 64, 1.
25. Frenne D. D. and Jacobs E. *Nucl. Data Sheets*, 1994, v. 72, 1.
26. Blachot J. *Nucl. Data Sheets*, 2000, v. 91, 135.
27. Rasmussen J. O. Theory of $E0$ transitions of spheroidal nuclei. *Nucl. Phys.*, 1960, v. 19, 85.
28. Minkov N., Yotov P., Drenska S. and Scheid W. *J. Phys. G*, 2006, v. 32, 497.
29. Bonatsos D., Daskaloyannis C., Drenska S. B., Karoussos N., Minkov N., Raychev P. P. and Roussev R. P. *Phys. Rev. C*, 2000, v. 62, 024301.
30. Minkov N., Drenska S. B., Raychev P. P., Roussev R. P. and Bonatsos D. *Phys. Rev. C*, 2001, v. 63, 044305.

Progress in Physics is an American scientific journal on advanced studies in physics, registered with the Library of Congress (DC, USA): ISSN 1555-5534 (print version) and ISSN 1555-5615 (online version). The journal is peer reviewed and listed in the abstracting and indexing coverage of: Mathematical Reviews of the AMS (USA), DOAJ of Lund University (Sweden), Zentralblatt MATH (Germany), Scientific Commons of the University of St. Gallen (Switzerland), Open-J-Gate (India), Referential Journal of VINITI (Russia), etc. *Progress in Physics* is an open-access journal published and distributed in accordance with the Budapest Open Initiative: this means that the electronic copies of both full-size version of the journal and the individual papers published therein will always be accessed for reading, download, and copying for any user free of charge. The journal is issued quarterly (four volumes per year).

Electronic version of this journal:
<http://www.ptep-online.com>

Editorial board:

Dmitri Rabounski (Editor-in-Chief)
Florentin Smarandache
Larissa Borissova
Stephen J. Crothers

Postal address for correspondence:

Department of Mathematics and Science
University of New Mexico
200 College Road, Gallup, NM 87301, USA

Printed in the United States of America

